NIST Special Publication 250-91

Calibration of Cryogenic Resistance Thermometers between 0.65 K and 165 K on the International Temperature Scale of 1990

Weston L. Tew

This publication is available free of charge from:
http://dx.doi.org/10.6028/NIST.SP.250-91

National Institute of Standards and Technology
U.S. Department of Commerce

NIST Special Publication 250-91

Calibration of Cryogenic Resistance Thermometers between 0.65 K and 165 K on the International Temperature Scale of 1990

Weston L. Tew
Sensor Science Division
Physical Measurement Laboratory

This publication is available free of charge from:
http://dx.doi.org/10.6028/NIST.SP.250-91

March 2015

U.S. Department of Commerce
Penny Pritzker, Secretary

National Institute of Standards and Technology
Willie E. May, Acting Under Secretary of Commerce for Standards and Technology and Acting Director

National Institute of Standards and Technology Special Publication 250-91
Natl. Inst. Stand. Technol. Spec. Publ. 250-91, 109 pages (March 2015)
CODEN: NSPUE2

This publication is available free of charge from:
http://dx.doi.org/10.6028/NIST.SP.250-91

Table of Contents

List of Figures

List of Tables

ABSTRACT

Calibrations of cryogenic resistance thermometers at NIST are performed by comparison to standard thermometers on the International Temperature Scale of 1990 (ITS-90). The NIST Low Temperature Calibration Facility (LTCF) can accommodate most capsule and miniature type resistance thermometers suitable for use in vacuum within the range 0.65 K to 83.8 K, with special tests possible as high as 165 K. All calibrations are traceable to the ITS-90 through standard check thermometers owned and maintained by NIST. The ITS-90 defines temperatures from 0.65 K upward via standard interpolating instruments, fixed points, and interpolation equations. NIST has performed realizations of the ITS-90 in the range 0.65 K to 24.5561 K and maintains standard Rhodium-Iron Resistance Thermometers (RIRTs) to represent the results of those realizations. Realizations of the ITS-90 over the range 13.8033 K to 273.16 K have been performed at NIST and are maintained on a set of capsule-type Standard Platinum Resistance Thermometers (SPRTs). Together, these check thermometers form the basis for maintenance and dissemination of the ITS-90 at NIST over the range 0.65 K to 83.8 K. The techniques for performing calibrations for a variety of resistance thermometers and the associated calibration uncertainties are described.

Keywords: Low Temperature; Cryogenic; Thermometry; ITS-90; Calibration; Resistance Thermometers;

1 Cryogenic Resistance Thermometry

1.1 Introduction

The practical measurement of temperatures T below ≈77 K is a highly specialized subject which utilizes a large variety of thermometers depending on the exact application. Resistance thermometers are one class of devices commonly used in cryogenic systems which includes both standard and industrial types. Most of the materials employed in cryogenic resistance thermometers do not exhibit a high degree of interchangeability and rarely can a measurement of the resistance R near 300 K yield accurate predictions of the R versus T characteristic at low temperatures. In most cases this necessitates individual calibrations for almost all such thermometers. This document describes techniques and services at the National Institute of Standards and Technology (NIST) for accomplishing such calibrations on the International Temperature Scale of 1990 (ITS-90) [1]. Temperatures on the ITS-90 are defined down to a lower limit of 0.65 K. The services described herein are primarily in the range 0.65 K to 83.8 K, but some special test capability as high as 165 K is available.

The term ‘cryogenic’ refers to the application of low temperatures in science and engineering. It is distinct from ordinary or conventional ‘refrigeration’ methods in both the technology and the lower temperatures achieved. The exact dividing line in temperature between these two disciplines is not well defined and depends on the perspective of a given science or industry sector, with opinions ranging between ≈73 K and ≈120 K. From the practical thermometer calibration standpoint, T≈165 K is a rough dividing line. Below this point vacuum methods are usually required while above this point the more convenient alcohol-bath immersion methods are preferable. This document primarily treats calibrations in vacuum over the range $0.65\ \text{K} \leq T \leq 165\ \text{K}$, which is roughly the same range covered in the most recent review by Rubin [2].

There are many excellent reviews of cryogenic thermometry going back in time as far as 1962 [3], with later reviews from Rubin [2,4,5], Sparks [6], Courts *et. al.* [7], Yeager and Courts [8], and most recently by Ekin [9]. These reviews include a great deal of information on various practical thermometers appropriate for large-scale industrial applications. Some also include descriptions of the development of reference grade resistance thermometers which are used to maintain temperature scales at the national metrology institutes such as NIST. In contrast to those reviews, the intent in this chapter is to only briefly introduce some basic concepts and describe a few types of resistance thermometers which can be calibrated at NIST. These include thermometers commonly used today in two categories: a.) standard reference thermometers with the highest stability and b.) certain industrial thermometers which also exhibit good stability.

Cryogenic Resistance Thermometers (RTs) are commercially available in many material and style variations. The general features are: a.) a temperature-sensitive material made from fine wire, single crystal, poly-crystalline, or composite samples; b.) a protective sheath, normally less than 5.7 mm in diameter, and sealed with He gas; c.) a two, three, or four-wire connection with insulated lead wires. The temperature-sensitive material is generally distinguished according to

the sign of its temperature-coefficient of resistance (TCR) $\alpha(T)$. The instantaneous TCR is normally defined as:

$$\alpha(T) \equiv \frac{1}{R_0}\frac{dR(T)}{dT} \qquad 1.1$$

where R is the thermometer resistance at temperature T with a normalization resistance $R_0=R(T_0)$ referred to a reference temperature T_0. The temperature T_0 is chosen for convenience, usually 273.15 K or 273.16 K for materials which are predominately linear in T. For highly non-linear materials the normalization is usually omitted (i.e. $R_0 \rightarrow 1$). Materials for which $\alpha(T)>0$ are referred to as positive temperature coefficient (PTC), and those for which $\alpha(T)<0$ are referred to as negative temperature coefficient (NTC).

PTC resistance thermometers are normally made from fine metal wire such as Pt, Rh-Fe alloys and Pt-Co alloys. These thermometers are usually low resistance, $R(273.16\ \mathrm{K}) \leq 100\ \Omega$. In contrast, NTC materials can have relatively high resistances in the *l*-He range with $R \gtrsim 10^4\ \Omega$ being fairly common in n-type germanium, and $R \gtrsim 10^3\ \Omega$ for zirconium oxy-nitride and ruthenium oxide. NTC materials are also highly non-linear, having an approximately exponential $R(T)$ characteristic.

A more general parameterization of the temperature coefficient is sometimes used when comparing PTC and NTC materials. This is the logarithmic sensitivity or

$$S_R(T) \equiv \frac{d\ln(R(T))}{d\ln(T)} = \frac{T}{R(T)}\frac{dR(T)}{dT}, \qquad 1.2$$

also referred to as the 'specific sensitivity'[10]. S_R is a bulk material property independent of device geometry. Knowledge of S_R for a given thermometer allows prediction of the relative thermometric resolution, ε_T , of a measurement system given the system's relative resolution in resistance, ε_R ,or voltage, ε_V via $\varepsilon_T = \varepsilon_R/S_R$. It is simple to show that $T\alpha(T) = S_R W(T)$ where $W(T) \equiv R(T)/R_0$ is the resistance ratio. In the ideal case of a purely linear $R(T)$ characteristic, $\alpha = T_0^{-1}$ and $S_R=1$ for all values of T so that a system with 1 μΩ/Ω resolution achieves a thermometric resolution of 1 μK/K. In the real case of high-purity metals and dilute alloys, $W(T)$ is very linear for ambient ($T \approx 300$ K) temperatures such that $S_R \approx T_0\alpha(T_0) \approx 1$, but departs from this special case both at lower and higher temperatures as nonlinearities become more pronounced. The $W(T)$ characteristics for a selection of PTC thermometers is shown in Figure 1.1 and the S_R characteristics for this same selection is shown in Figure 1.2

For an ideal (i.e. intrinsic) semiconductor $R(T)=R_\infty e^{\beta/T}$ where R_∞ is the high-temperature limit and β is a parameter related to the band gap. In this case $S_R = -\beta/T$ and some composite NTC materials such as NiMn oxides or bismuth-ruthenates will approximate this dependence over limited temperature intervals. In most cases, however, real NTC materials in the cryogenic range will exhibit a milder temperature dependence such that $S_R \sim -\gamma(\beta/T)^\gamma$ where $\frac{1}{2} < \gamma < 1$. The general feature is that of increasing sensitivity with decreasing temperature. For all practical purposes, S_R can be calculated from calibration data. Typical values for $R(T)$ are shown in Figure 1.3 and

values of $|S_R|$ are plotted in Figure 1.4 for a sample of thermometer types discussed in this chapter.

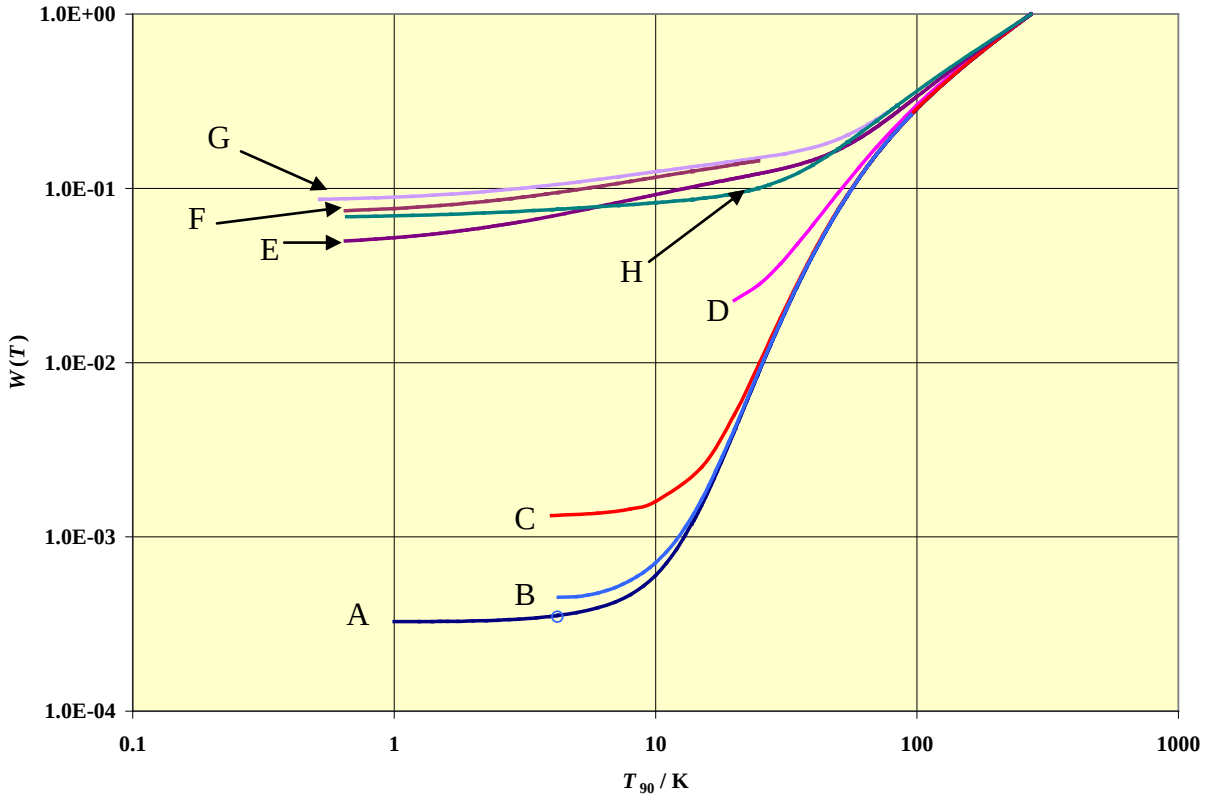

Figure 1.1 The resistance ratio $W(T)$ characteristics for a selection of PTC resistance thermometers (data from NIST unless otherwise noted): A.) Standard Platinum Resistance Thermometer (SPRT) reference function 13.8 K to 273.16 K [1] and a closely matching SPRT, s/n 1812279[11] from 1 K to 13.8 K; B.) a miniature capsule PRT; C.) A 99.99 % pure sample of Pt from 4 K to 273.15 K[12] and similar to wire grades used in aerospace sensors; D) An industrial PRT from 20 K to 273.15 K matching the $\bar{\alpha}_{100}$ =0.00385 specification[13] ; E.) a standard capsule Rhodium-Iron Resistance Thermometer (RIRT) using 50 μm wire,0.65 K to 273.16 K; F.) a Ceramic-Encapsulated RIRT using 38 μm wire**;** G.) a thin-film RIRT from 0.52 K to 273.16 K; H.) a Pt-0.5% Co standard capsule thermometer from 0.65 K to 273.16 K.

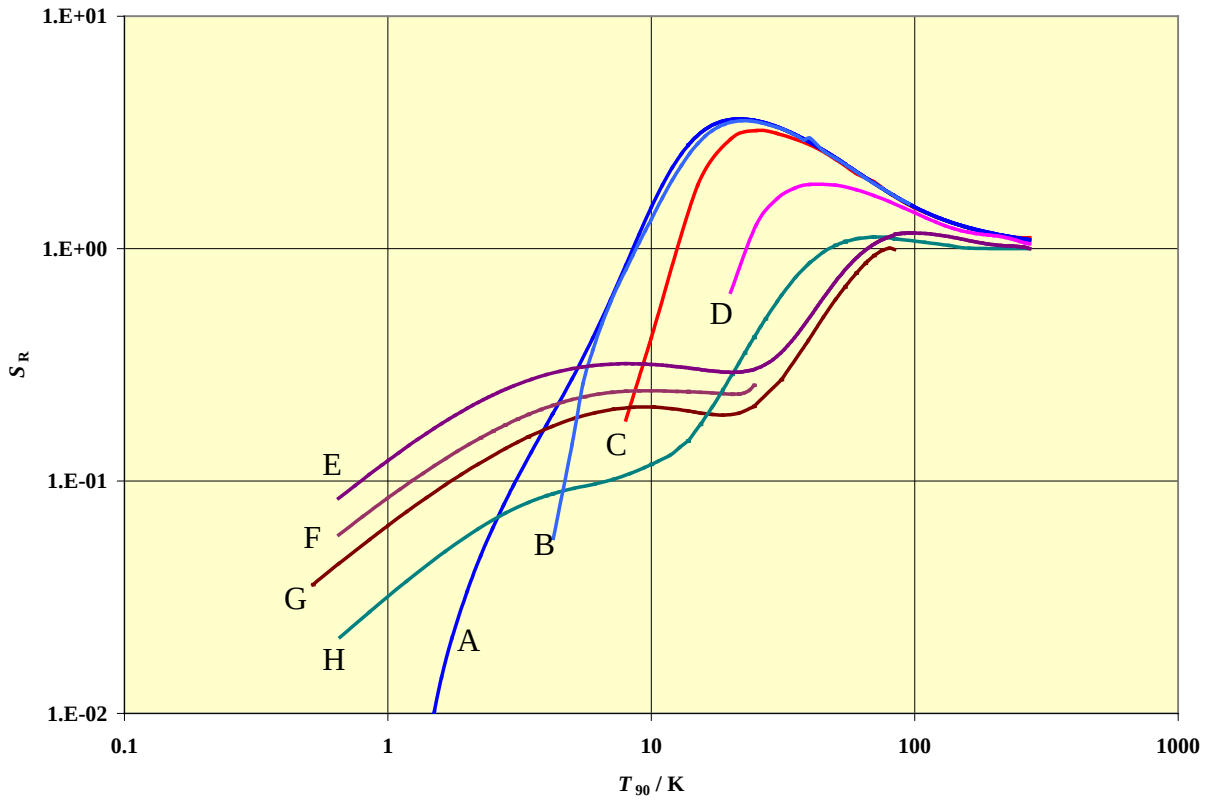

Figure 1.2 The logarithmic sensitivities of several types of PTC cryogenic resistance thermometers. See Figure 1.1 for curve identifications.

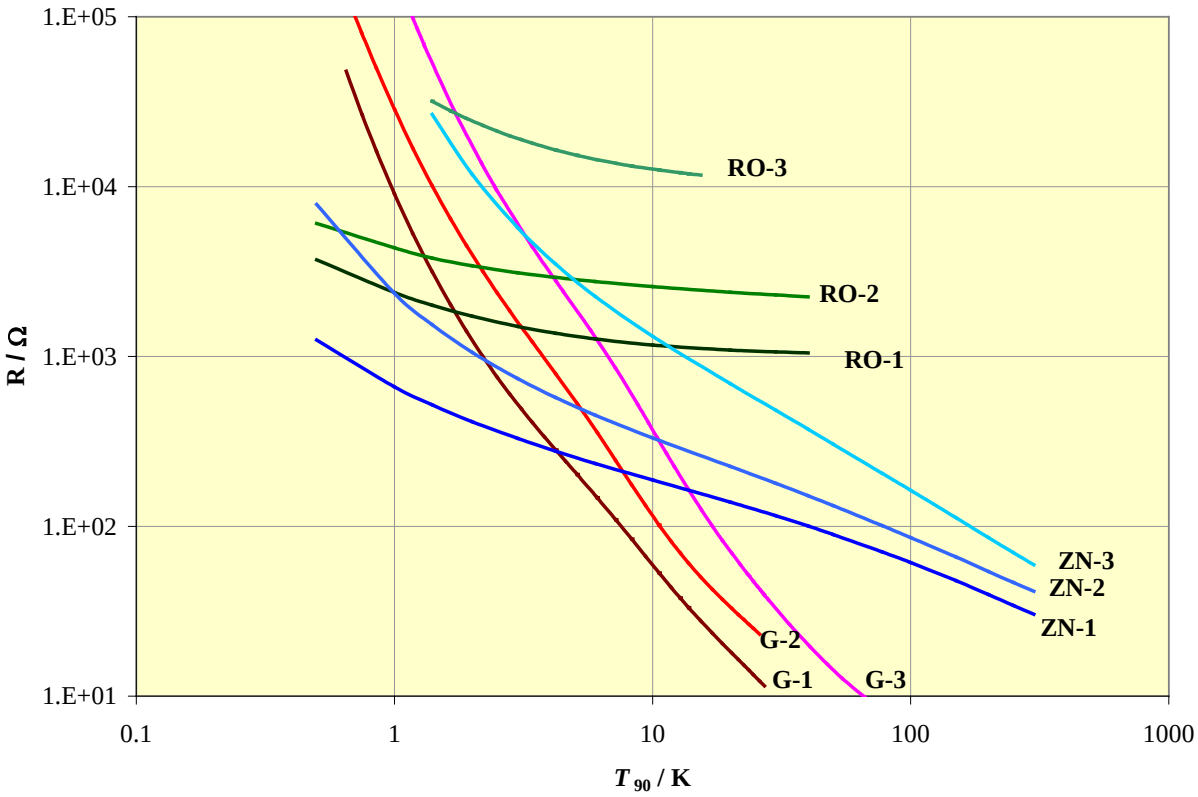

Figure 1.3. The characteristic Resistance versus Temperature curves for three types each of NTC thermometers. G-1, GeRT 250 Ω at 4.2 K; G-2, GeRT 800 Ω at 4.2 K; G-3, GeRT 2.8 kΩ at 4.2 K; RO-1, Ruthenium Oxide Resistance Thermometer (RORT) 1 kΩ at 300 K; RO-2, RORT 2.2 kΩ at 300 K; RO-1, RORT 10 kΩ at 300 K; ZN-1, Zirconium oxy-Nitride Resistance Thermometer (ZNRT) model CX-1010; ZN-2, ZNRT model CX-1030; ZN-3, ZNRT model CX-1050 [13].

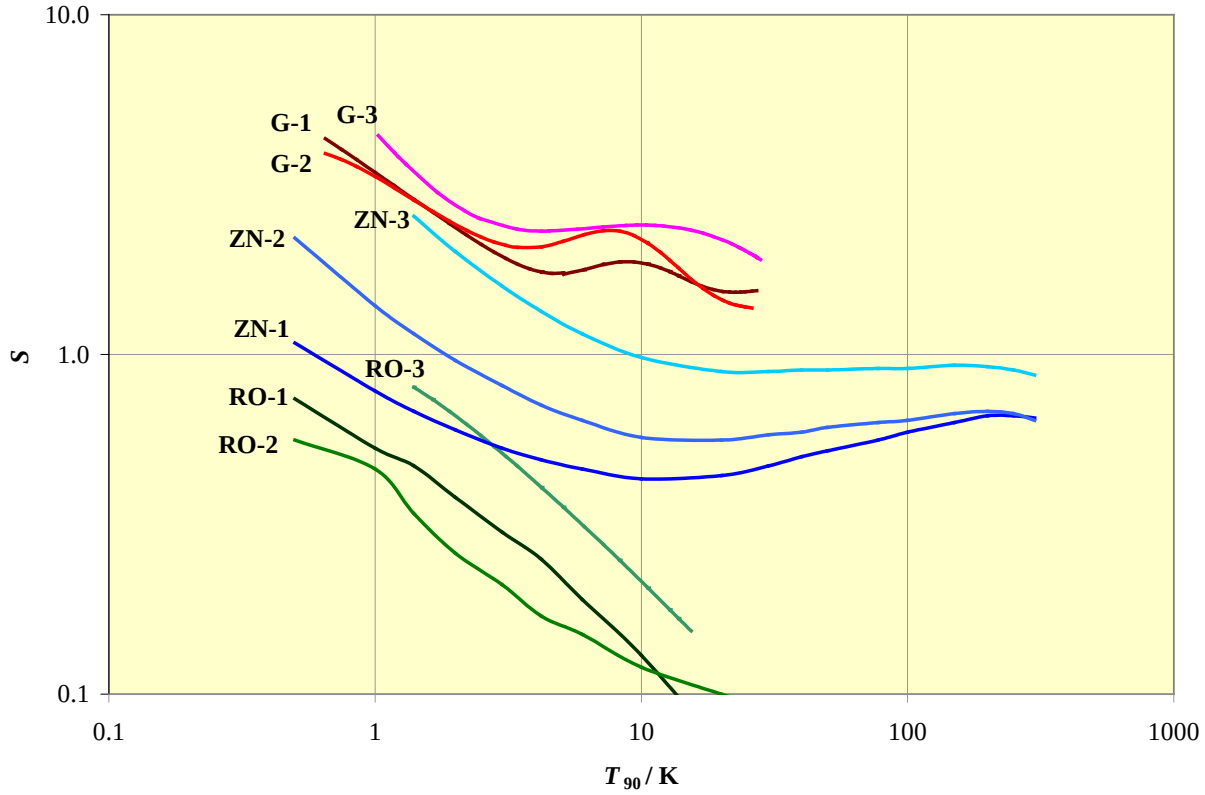

Figure 1.4. The absolute magnitude logarithmic sensitivities $|S|$ versus temperature curves for three varieties of three NTC thermometers. G-1, GeRT 250 Ω at 4.2 K; G-2, GeRT 800 Ω at 4.2 K; G-3, GeRT 2.8 kΩ at 4.2 K; RO-1, Ruthenium Oxide Resistance Thermometer (RORT) 1 kΩ at 300 K; RO-2, RORT 2.2 kΩ at 300 K; RO-1, RORT 10 kΩ at 300 K; ZN-1, Zirconium oxy-Nitride Resistance Thermometer (ZNRT) model CX-1010; ZN-2, ZNRT model CX-1030; ZN-3, ZNRT model CX-1050 [13] .

1.2 Resistance Measurement

Four-wire measurements of the thermometer resistance can be performed in either of two modes, a.) constant current I, or b.) constant voltage V excitations. In constant current mode the open-circuit voltage across the device is measured under a fixed current excitation. In constant voltage mode the current through the device is measured under a fixed voltage excitation. For PTC materials constant current excitation is always used, with currents usually in the range 0.1 mA to 1.0 mA. For SPRTs at T<25 K, currents are normally increased to the 5 mA to 10 mA range. In the case of NTC materials, either measurement mode may be used depending on the self-heating present, design of the thermometer package, and other factors. In practice, a constant voltage calibration is usually preferred with a typical range of voltage excitations of 1 mV to 10 mV. Individual measurements may still be performed in constant current mode, providing that the currents are adjusted for every new calibration point to the appropriate voltage level.

Further distinctions in the four-wire resistance measurements are made regarding direct current (DC) or alternating current (AC) excitations. The choice is normally made from signal-to-noise considerations, which in turn are affected by the sensitivity of the thermometer. For the same excitation level and integration time, AC excitation will generally result in a higher signal-to-noise ratio ε_V^{-1} than would be achievable using DC excitations. For PTC materials, AC excitation is generally preferred in order to maximize the noise-equivalent temperature resolution as these materials generally exhibit only modest temperature coefficients, typically (0.05 to 0.5) Ω/K, or logarithmic sensitivities of $0.1 < S_R < 2$. For NTC materials, the much higher sensitivities at lower temperatures permit the use of DC measurement systems with higher noise, (i.e. lower signal-to-noise ratio) and still yield acceptable thermometric resolutions. At ultra-low temperatures ($T \lesssim 1$ K) low power dissipation becomes paramount. In this case AC excitation may be preferred in order to achieve the highest signal-to-noise ratio while using the lowest excitation levels. Considerations regarding AC versus DC excitation sometimes come into play due to Peltier effects at semiconductor-metal contacts for temperatures ≳35 K, and these are discussed briefly in section 1.5.4.

AC resistance measurement systems are constructed from bridge-type networks with linear voltage dividers. The most accurate of these are based on inductive voltage dividers (IVDs) [14] but precision AC resistive dividers are more common and simpler to construct [15]. The newest type of AC resistance meter now commercially available is a purely digital design based on a precision analog-to-digital converter (ADC), square-wave excitation currents, and a substitution topology [16]. In all cases, AC carrier frequencies are in the lower audio to sub-audio range in order to minimize errors due to parasitic reactance in the cables and interconnecting networks. Commercial versions of these instruments are available [17-19]. The IVD-based instruments are designed to determine resistance ratios with the lowest possible uncertainty in conjunction with standard reference resistors. At NIST, AC bridges using IVDs with uncertainties of 0.1 μΩ/Ω are used for PTC thermometers and NTC thermometers where R<129 Ω and I >0.1 mA. Further descriptions are given in Chapter 5, section 4.

DC resistance measurement systems are constructed from direct current comparators (DCC) [20] or from ordinary resistance ratio voltage dividers in conjunction with precision ADCs and

standard reference resistors. The most accurate systems make the use of current reversals in order to cancel the effects of voltage bias offsets and thermal voltages. Commercial DCC instruments optimized for thermometry are available [21]. The distinction between these bi-polar DC measurement systems and low-frequency AC measurement systems becomes blurred in some cases, particularly for reversal rates ≈ 1 Hz, above which one could consider the system to be an AC square wave excitation for most practical purposes.

Commercial digital multi-meters (DMMs) with 6.5 or more digits on a 100 mV range can be combined with a programmable bi-polar current source and stable reference resistors to form a DC measurement system suitable for most cryogenic thermometry applications. In well-designed systems, relative uncertainties of ≈ 1 μΩ/Ω are possible when excitation voltages are ≳ 30 mV. Commercial instruments which combine these components into an integrated system are also available [22].

All of these resistance measurement circuits will in some way detect a signal voltage of $V_R=IR(T)$ in the presence of some equivalent input voltage noise V_{ne} associated with the excitation and detection circuitry. In addition, the finite bit depth of digital instruments produces an effective quantization noise V_q . The relative voltage resolution limit ε_V is then given by

$$\varepsilon_v = \frac{\left(V_{ne}^2 + V_q^2\right)^{1/2}}{V_R}. \qquad 1.3$$

Since the thermometric resolution is $\varepsilon_T = \varepsilon_V / S_V$, this could in principle be improved (i.e. decreased) to arbitrary precision by simply increasing the excitation current or voltage. In practice there are inevitable limitations to this approach due to power dissipation. In a few cases other limitations exist due to low frequency or "one-over-f" noise [23] or non-linearity effects.

1.3 Self-heating Effects

The upper limit on excitation levels is tied to the power dissipation $P_R=I^2R(T)=V^2/R(T)$ in the thermometer. The dissipation causes an elevated internal temperature difference ΔT_{sh} relative to the environment being sampled, commonly referred to as "self-heating". The self-heating coefficient [24] is defined by $\eta = \Delta T_{sh} / P_R$ and often expressed in units of $mK \cdot \mu W^{-1}$. Alternative terminology is found in the literature, such as the "thermal resistance" [25] and "thermal impedance"[26] whose definitions are equivalent to the self heating coefficient used here. In other cases, the "heat-transfer coefficient"[27] h, is used in this same context, but this is the inverse of the self-heating coefficient used here (i.e. $h=\eta^{-1}$). In the thermistor literature, the term "dissipation constant" is used, which is also the inverse of the self-heating coefficient.

In general, η depends on details of heat transport mechanisms through the sensor package and on the installation medium. In practice the observed η is a combination of the associated series and parallel thermal impedances such that a complete description of the net effect is complicated. Fortunately, it is possible to directly measure the self-heating effect in practice and experimental

values for η are readily obtained providing the measurement system has adequate resolution. Measurements at two or more currents $I_2 > I_1$ allow a simple calculation using

$$\eta \cong \frac{R(I_2) - R(I_1)}{\left(I_2^2 - I_1^2\right)R} \frac{\mathrm{d}T}{\mathrm{d}R} \qquad 1.4$$

The measurement of η requires that the excitation levels are high enough to resolve the self-heating in the presence of temperature control fluctuations and measurement system noise. A good rule of thumb is to set excitation levels such that the observed self heating is 5 to 10 times the statistical precision of each measurement, providing that the self-heating remains linear in P_R. The use of equation 1.4 presumes that the joule heating contribution from the portion of the current lead wires outside of the four-terminal junction is negligible. This is normally a safe assumption for most thermometers, with certain types of germanium resistance thermometers being a possible exception. In those special cases, η as defined here would be considered an "effective" self-heating coefficient, whose values would be larger than the true coefficient which would include the extra joule heating contributions in the denominator of eqn. 1.4.

The assumption is normally made that η is a constant independent of P_R and primarily a property of the thermometer package construction and materials. This will be approximately true as long as the power levels are sufficiently small, the thermometer is properly installed, and $\Delta T_{\mathrm{sh}} << T$. When any of these conditions are not met, ΔT_{sh} will no longer be linear in P_R and the measured value of η will depend on P_R and possibly also on the details of the thermal coupling which are external to the thermometer [28]. Under these conditions the indicated temperatures will be in error and measured values for η will lack reproducibility.

An extreme form of self-heating nonlinearity can exist in some NTC devices (e.g. bulk semiconductors, thermistors, etc.) when current biased into a 'super-heated' region where the *I*-*V* curve exhibits negative dynamic resistance. In this case the device no longer functions as a thermometer, but instead more as a heat-transfer or gas flow-sensor [29]. In contrast, when NTC devices are voltage biased above some threshold value, a thermal runaway condition can be created by ever increasing values of $V^2/R(T)$ resulting in a failure or "burn-out" of the thermometer. Users are advised to take precautions and consult manufacturers for their recommended maximum excitation voltages when using NTC resistance thermometers.

The measurement of self heating of cryogenic resistance thermometers can be used to evaluate the efficacy of the thermometer installation and/or the integrity of the thermometer's sheath and hermetic seals. A standard capsule thermometer with insufficient thermal coupling to its environment will indicate a higher than normal self heating. A thermometer with a damaged seal which allows the He exchange gas to leak out of or into the sheath will also indicate higher than normal self heating under vacuum, but the effect may be somewhat reversible when the vacuum chamber is backfilled with He exchange gas. For many other thermometer designs, however, this gas-pressure-dependent self-heating is not observed because the dominant thermal coupling to the external environment is via the lead wires (see section 1.4) [25].

The third law of thermodynamics requires that all heat transport coefficients such as $h=\eta^{-1}\rightarrow 0$ as $T\rightarrow 0$. Hence, at low temperatures η exhibits divergent behavior or $\eta \sim T^{-n}$ where typically $0.5 \leq n \leq 3$ in the temperature ranges of interest here. The larger values of n are observed at the lowest temperatures. Self-heating exponents as large as n=4 have been observed for certain types of Ge thermometers well below 1 K [26]. The various exponents are associated with different heat transport mechanisms (e.g. thermal diffusion mediated by different gas molecules, solid-state particles or excitations across varying geometric boundaries, etc.) each of which will dominate in a different temperature region [30].

There are a few notable exceptions to the rule that η increases with decreasing T. Most notable are those cases where, in narrow regions of temperature, a phase change occurs in the thermometer fill gas. Such a case is observed in capsule RIRTs and PCRTs with ^{4}He fill gas near 1.3 K where a depressed λ-point transition occurs in the condensed He film and η drops precipitously [31]. (see section 1.6.1) Other exceptions may occur in certain small capsule germanium and platinum thermometers in the region between 45 K and 60 K if air has contaminated the He fill gas. As the air gradually condenses with lowering temperature, the decreasing vapor pressure of the condensed air produces fewer collisions between the remaining gas-phase air molecules and the He gas atoms. The He fill gas can then more effectively transfer heat out of the device, so η decreases with decreasing T until the vapor pressure of the remaining condensed air is negligible [27]. In cases where significant air is present, the observed η may appear hysteretic or otherwise lack reproducibility in this temperature range.

In practice a distinction is made between “internal” self heating (due to heat transfer within the sensor package) and “external self heating (due to heat transfer external to the sensor package) [32]. The respective self-heating coefficients for these are denoted, η_{int} and η_{ext} . A capsule thermometer will exhibit negligible external self heating when the sheath is directly installed in an ice bath (not recommended practice) , liquid nitrogen, or in liquid helium near 4 K, but these nearly ideal cases are difficult to emulate in other more practical vacuum or fixed-point cell installations. Ideally, installation techniques should be designed to minimize η_{ext}. In practice, however, some degree of external self-heating is inevitable in vacuum installations. The two effects normally act as series thermal impedances such that the total observed self-heating coefficient is the linear sum $\eta = \eta_{\text{int}} + \eta_{\text{ext}}$. The mechanisms responsible for η_{int} are solely a function of the thermometer package design and materials, while η_{ext} is in general installation dependent. In certain types of fixed-point cell or vacuum comparison installations, η_{ext} can be significant and variable in which case the measured η will lack reproducibility from one installation to the next. Variability of $\pm$ 50% in the observed η value between different installations can be expected in some cases.

It has been customary at NIST to obtain calibration data for cryogenic resistance thermometers using two or more excitation currents for each calibration point. NIST calibration reports for cryogenic thermometers have contained this information in some form since 1996. In some cases calibration results are reported at both currents, in other cases results may be reported in terms of the zero-power resistance $R(I=0)$ as derived by

$$R(I=0) = \frac{R(I_1)I_2^2 - R(I_2)I_1^2}{I_2^2 - I_1^2}. \qquad 1.5$$

Calibrations in terms of $R(I=0)$ are preferable for achieving the highest reproducibility possible for a given thermometer type. By using $R(I=0)$ it is possible to account for both η_{int} and η_{ext} even when η_{ext} is significant and variable. The main caveat is that for temperatures $T \lesssim 4$ K, the excitation levels must be sufficiently low for the self heating to be purely quadratic in the current, or linear in power.

An alternative approach to the self-heating problem is to treat it as an uncertainty component in combination with other measurement uncertainties [28]. The excitation level may then be chosen as an optimization between the competing effects of signal-to-noise ratio and self heating. The optimum excitation power is then that which produces self-heating approximately equal to the rms thermometric uncertainty due to all other sources which are independent of the excitation level. For most NTC materials, the net result is an optimized excitation which slowly decreases with decreasing temperature. This is a useful technique for finite-excitation calibrations. If actual measurements of $\eta(T)$ are to be made, however, the measurement currents used during the calibration will always be larger than these optimized excitation values.

Values of $\eta(T)$ are plotted in figure 1.5 for a sample of cryogenic resistance thermometer types over the range 0.65 K to 84 K as measured in vacuum. The values are representative of these specific types and particular packages only. Other thermometers of the same model should exhibit similar values but differences should be expected depending on the exact installation and certain construction and design variations.

In those cases where the results are given for a finite excitation level(s), tables are included in each NIST calibration report with experimental values of the self heating for that specified calibration current and or the as-measured self-heating coefficient (see section 5.6 and Appendix A). Self-heating effects for specific types of resistance thermometers are discussed further in later sections of this chapter. Additional aspects of self heating are discussed in chapter 6 on calibration uncertainties.

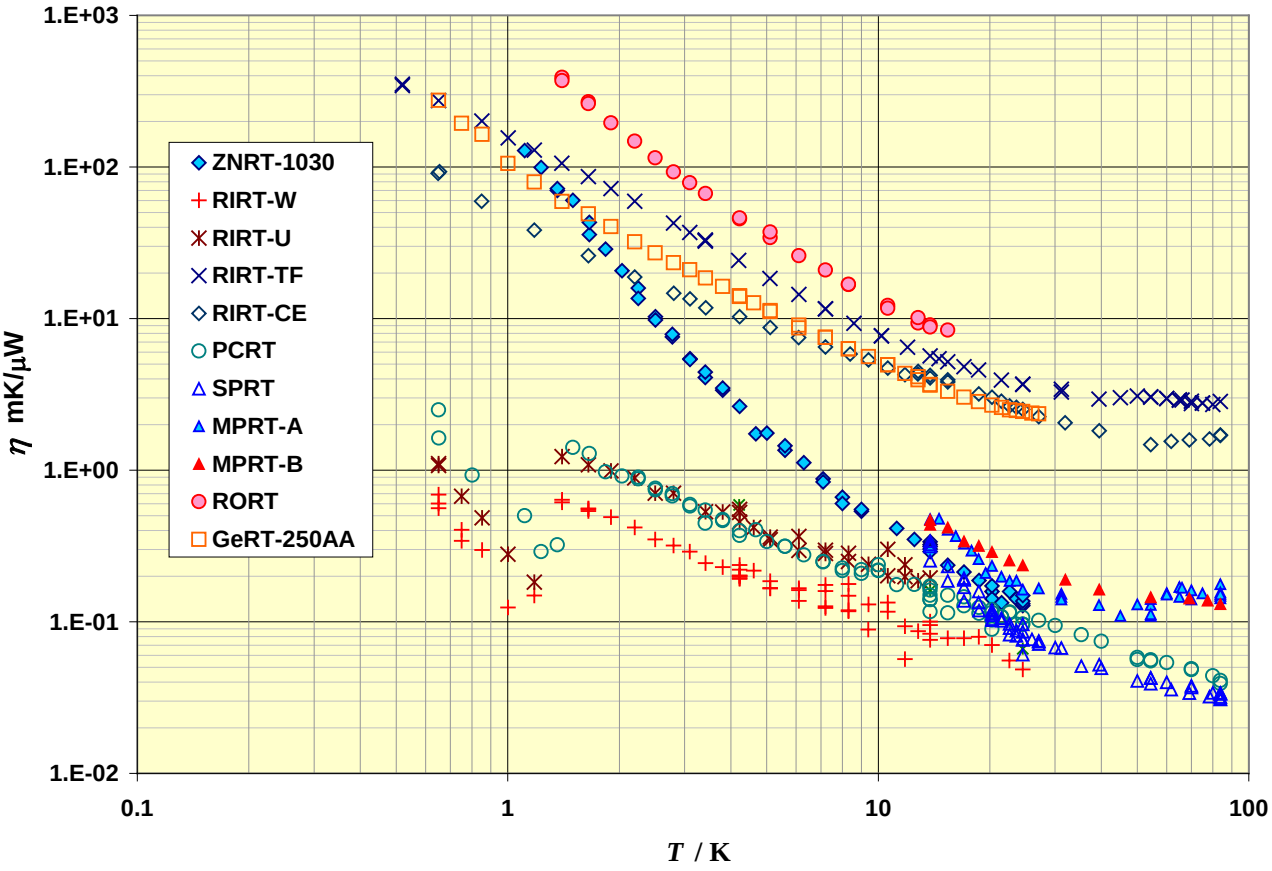

Figure 1.5. The self-heating coefficient $\eta(T)$ over the range 0.5 K to 84 K for a sample of cryogenic resistance thermometers as measured under vacuum: ZNRT-1030 , Lakeshore model CX-1030-AA; RIRT-W and -U, Tinsley model 5187-W and -U; RIRT-TF, Lakeshore model RF-100-AA; RIRT-CE, Lakeshore model RF-800 ;PCRT, Chino model R-800-4; SPRT, Leeds & Northrup model 8164; MPRT-A and -B, Minco model S1059; RORT, custom 10 kΩ TFCR bonded to copper strip; GeRT-250AA, Lakeshore model GR-200-A-250.

1.4 Thermometer Packaging and Installation

Hermetic packaging of the sensor is an important component of cryogenic thermometer design. The details of the packaging technologies are usually proprietary, but the basic function is to protect the sensor as well as to facilitate installation with minimum adverse effect on achieving good thermal contact. The proper installation of the thermometer is equally important, particularly in vacuum systems.

The sensor materials used in cryogenic resistance thermometers are almost always sensitive to any applied mechanical stress. Inadvertent mechanical stress is practically unavoidable when two dissimilar materials are mechanically coupled and cooled, due to the differential thermal contraction between the materials. Thermal contraction stresses in thermometers produce mechanical strains in the sensor element which in turn can lead to hysteretic behavior [33] or time-dependent behavior (e.g. drift) [34], the exact mix and degree of which depend on the specific sensor material. Time-dependent drift in the resistance will eventually stabilize if it is a purely stress-induced effect, but the stabilization time can be anywhere from hours to weeks depending on the details of the sensor material's microstructure. For this reason it is generally necessary to mechanically decouple the sensor element from the protective sheath. Manufacturers will usually take this into account in the normal practice for good thermometer package designs, but exceptions to this practice also exist. Users should be aware that unstable thermometers occasionally show up in the mix of commercial devices and often either poor package design or package construction flaws are the root cause. NIST may choose to reject thermometers for calibration if drift behavior is present (see section 2.4).

The necessity of mechanical decoupling (i.e. strain-free construction) imposes limits on the heat transfer characteristics of practical thermometer designs. The usual approach is to thermally couple the sensor to the exterior sheath via either the He exchange gas or via fine internal lead wires (e.g. Au bonding wire) of relatively high thermal conductivity. These design considerations ultimately determine the magnitude of the internal self-heating coefficient η_{int}, the stability of the resistance under thermal cycling, and (in part) the long term stability.

The degree of hermeticity achieved in various sensor packages is variable from one design and fabrication process to the next, and may slowly degrade over time and with thermal cycling. For those thermometers with exchange-gas-mediated self heating, the integrity of the hermetic seal is especially critical, but all thermometer sensor materials can degrade over time when exposed to moisture and oxygen through leaks in the package. As was described in section 1.3, routine monitoring of the self-heating coefficient under vacuum can help detect leaks in package seals. In addition, careful measurements of η_{int} between 40 K and 70 K can be used to detect the presence of air contamination since the thermal conductivity of N_2 gas is approximately 10 times smaller than that of He at 70 K. In some cases, however, air contamination may not necessarily be an indication of a leak, but simply a factory defect. Such cases are known to exist in both miniature and standard capsule type thermometers and usually do not present a serious limitation for calibration or use so long as there is still some He present. Slow contamination of hermetic capsules with hydrogen which outgases from the construction materials is also possible. The

effects of such contamination would rarely be observable, however, except in cases below ≈40 K where there is no He fill gas present.

Installation techniques vary from one application to the next and according to package designs. An installation technique which is adequate for one type of sensor may be inadequate for another. The ultimate goal of installation techniques is to reduce η_{ext} to a manageable level or otherwise bound the magnitude of any associated effects. While a detailed discussion of these subjects is beyond our limited scope here, an excellent practical guide for commercial sensors is readily available [35]. Useful discussions of the technical issues are also found in Chapter 5 of the text by Ekin [9]. Users are advised to refer to the literature and consult the thermometer manufacturer for the recommended installation practice.

At NIST, all cryogenic capsule-type resistance thermometers are installed in a vacuum comparison block via close-fitting cylindrical thermowells with a thermal contact grease applied to fill in any gaps between the inner thermowell and thermometer sheath surfaces (see section 5.2). The grease is a carbon-based composition and may include small particles of copper for certain installations. Provisions for surface-mounted sensor packages are made using a variety of single screw-thread anchoring holes. Lead wires are thermally anchored to the isothermal zone near the wire terminations.

1.4.1 Thermal Response Time

Thermal response time τ_{tr} is a dynamic characteristic of all thermometers and is usually defined as the time for the resistance (or voltage) reading to change by some nominal fraction (often 0.63 ≅1−1/*e*) of the final equilibrium reading in response to an imposed step change in temperature. For calibration purposes, τ_{tr} is a useful parameter for estimating the degree of thermal equilibrium which can be expected for a given thermometer after some thermal perturbation has taken place. Some manufacturers give nominal values for τ_{tr} at specified temperatures, while others may not specify an exact temperature (usually implying the values are for $T \approx 273$ K to 297 K). The techniques used to define and measure τ_{tr} will vary from one manufacturer to the next and the terminology is likewise variable. Terminology such as “sensor time constant”, “thermal time constant”, and “thermal delay time” are found in the literature and are nominally equivalent. A standard test method exists [36] but this is not well suited to capsule designs.

For standard capsule-type resistance thermometers typical values for τ_{tr} are in the 4 s to 7 s range near 273 K. Observed values of τ_{tr} are usually only weakly temperature dependent in the region near 273 K, but large decreases in τ_{tr} should be expected to occur as temperature is lowered from ≈ 100 K down to 4 K as the specific heat capacity decreases rapidly with decreasing temperature over that range. For temperatures $\lesssim 1$ K, τ_{tr} will usually increase with further decreases in temperature.

In practice the observed thermal response time is a function of the thermometer mass, the package materials, the package design, and the installation method. Hence, the observed τ_{tr} is actually a superposition of several internal and external thermal time constants and quantitative modeling is extraordinarily cumbersome. Rough estimates can be calculated based on simple thermal analogs of lumped-parameter *RC* time constants if the dominant self-heating and heat capacitance values are known. A simple two-time-constant model roughly approximates one dimensional heat flow in an installed thermometer as shown in Figure 1.6.

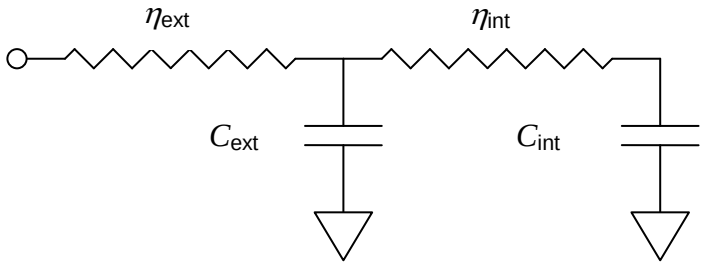

Figure 1.6. A simple two-time-constant lumped-parameter model for estimating the observed thermal response time.

The parameters are divided according to internal and external thermal resistances η_{int} and η_{ext}, and heat capacities C_{int} and C_{ext}, resulting in the two time constants. These are the internal response time τ_{int} and the external response time τ_{ext} as approximated by

$$\tau_{int} \simeq (\eta_{int} + \eta_{ext}) C_{int} \qquad 1.6a$$

$$\tau_{ext} \simeq \eta_{ext} C_{ext} \ . \qquad 1.6b$$

In this approximation of the model, the internal heat capacitance couples to both internal and external thermal resistances while the external heat capacity couples only to the external thermal resistance. The ideal response of a simple two stage system is such that the effective thermal response time is slightly less than the sum $\tau_{int} + \tau_{ext}$. In practice, however, this approximation will typically underestimate the observed τ_{tr} by factors of ≈2. A significant limitation exists due to the uncertainty in η_{ext}, since only $\eta_{int} + \eta_{ext}$ can be directly measured.

While this simple one-dimensional two-stage model is of limited predictive value in the absolute sense, it can still be useful for estimating the relative temperature dependence of τ_{tr} via the known temperature dependence of η_{int}, η_{ext}, C_{int} and C_{ext}. For the purposes of estimating thermal equilibrium uncertainties, the approximation $\tau_{tr} \approx 2(\tau_{int} + \tau_{ext})$ is used. (see section 6.1.3)

The best method for direct measurements of τ_{tr} are through use of a stirred bath (e.g. water or *l*-N_2) where the heat capacity of the bath fluid is so large that the introduction of the thermometer under test is a negligible perturbation. Direct measurements of τ_{tr} in a vacuum comparison system, however, are complicated by the fact that at temperatures ≲50 K, the thermal diffusion

time constant of the comparison block can be comparable to τ_{tr} (see section 5.3, Figure 5.5). In this case one is measuring the composite response of the thermometer + comparison block and it is not possible to extract τ_{tr} from the measurement.

1.5 Resistance Thermometer Types

This section describes a few of the most common types of PTC and NTC cryogenic resistance thermometers that are known to exhibit good or exceptional stability. In this chapter we will somewhat loosely quote limits of 'stability' as ± X mK, meaning reproducibility is typically achieved within a coverage factor of $2 \leq k \leq 3$.

1.5.1 Platinum

Platinum resistance thermometers (PRTs) come in a variety of grades and packages, some of which are more suitable for cryogenic service than others. The highest purity platinum wire, sometimes referred to as "reference grade" platinum, is used in standard platinum resistance thermometers (SPRTs). Most SPRTs are sufficiently pure to qualify as defining instruments on the ITS-90 and these qualification criteria are given in chapter 3. Other grades of purity can be found in PRTs designed for aerospace applications. Industrial types are of a lower purity and are generally less useful below ≈30 K. Historically, PRT grades have been distinguished via the 0 °C to 100 °C average TCR, $\bar{\alpha}_{100}$, and much of the commercial and engineering literature still utilize this parameter today (e.g. 'alpha value', or just 'α'). The range of values typically exhibited in the various grades of wire-based PRTs are $0.00385 \leq \bar{\alpha}_{100} \leq 0.003928$. However, the more modern parameterization is to simply specify resistance ratios W at certain fixed-point temperatures.

For $T \gtrsim 30$ K, PRTs exhibit the highest degree of uniformity/interchangeability of all resistance thermometers and SPRTs in particular are unsurpassed in this respect. A typical magnitude of interchangeability is $\Delta W(T) \approx 10^{-4}$, which is equivalent to ≈53 mK at 30 K for an SPRT. At 13.8 K, however, a deviation of this size is equivalent to ≈420 mK due to the diminishing sensitivity as temperature is lowered. At $T \lesssim 30$ K, the $W(T)$ of Pt specimens are observed to be increasingly sample dependent (i.e. less interchangeable) as temperature is lowered (see figure 1.1). A figure of merit which illustrates this behavior is the so-called "residual resistance ratio", X_{RR}, normally defined as

$$X_{RR} = \frac{R(273.15\,\mathrm{K})}{R(4.22\,\mathrm{K})} = \frac{0.99996}{W(4.22\,\mathrm{K})}, \qquad 1.7$$

where W(4.22 K) is the measured resistance ratio at the normal boiling point of liquid ^{4}He as normalized to the WTP (273.16 K) resistance. The parameter X_{RR} can be used to characterize the degree of chemical purity and lattice defects in a nominally pure metal, and in PRTs values range from ≈100 to 3000 depending on the grade of the wire and the degree of strain. The distributions of values of X_{RR} and $\bar{\alpha}_{100}$ are inversely correlated, as is the case with X_{RR} and $\Delta W(T)$ values [37]. The characteristic variations from one sample to the next, however, are more readily observed in the X_{RR} distribution.

1.5.1.1 Standard capsule types

SPRTs are made from carefully annealed reference grade wire specimens which are mounted in a strain-free fashion and fabricated into capsules sealed with a He fill gas. The wire is normally either 76 μm or 100 μm diameter and the capsule outer diameters typically are in the 5 to 5.7 mm range, depending on the exact model. The original helical coil design is from Meyers [38] and some modern designs still employ some of his design concepts. Other variations in the winding methods are more recently conceived. Examples of commercial designs are shown in Figure 1.7. Sheath materials may be platinum, glass, or Ni alloys. In most cases the wire elements are trimmed such that $R_0=R(273.16\ \mathrm{K}) = 25.5\ \Omega$, which yields $\alpha R_0=0.1\ \Omega\cdot\mathrm{K}^{-1}$.

SPRTs are defining instruments of the ITS-90 and their specification criteria and specified interpolation equations are discussed in chapter 3. Capsule-type SPRTs can be used from 13.8 K upwards to a limit as high as 505 K depending on the particular construction. The reproducibility of well annealed capsule SPRTs can be within ± 0.1 mK at 273 K. They are, however, extremely sensitive to mechanical shock and must be handled with great care. Unlike long-stem SPRTs, capsule types cannot be re-annealed, so cumulative strains from mechanical shocks permanently build up in the wire and increase the R_0 value.

SPRTs usually exhibit X_{RR} values in the range 1900 to 3000, although some specimens with lower values may still meet ITS-90 reference grade criteria (see chapter 3). The ITS-90 reference function [1] was derived [40] based on a particular SPRT from the National Physical Laboratory (NPL) of the United Kingdom, serial number 217894, with X_{RR} =2872[41]. At NIST, certain capsule SPRTs are maintained with values of X_{RR} as high as 3245. The X_{RR} values for annealed reference grade Pt wire of 500 μm diameter are even larger than those for SPRTs. For example, the Pt wire used for SRM-1967 standard thermocouple material [42] exhibited values in the range $3407\leq X_{\mathrm{RR}} \leq 3678$. While SPRT wire is derived from material comparable to that of SRM 1967, the achievable X_{RR} values for wire of diameters <100 μm will always be lower due to the exposure to impurities and the formation of lattice defects during the wire drawing process.

It should be noted that X_{RR} as defined via eqn. 1.7 at the normal ^{4}He boiling point is not truly the 'residual' resistance for specimens of very high purity such as SPRTs. In those cases the residual resistance at $T\approx 1$ K can be as much as ~8% higher [11]. Nonetheless, the usefulness of X_{RR} as defined at 4.2 K is that it is a sensitive indicator of both the chemical purity and the degree of physical strain in the wire. It also can provide a parameter useful for approximate interpolation schemes [43]. NIST does not normally report values of X_{RR} for calibrations of capsule SPRTs, but this information can be provided as a special test (see chapter 2) if the customer so requests.

SPRTs exhibit $S_R\gtrsim 1$ over the entire range from 13.8 K to 273.16 K (see figure 1.2). Despite this advantage, use of SPRTs below ≈20 K requires special instrumentation capable of resolving small signal voltages. For example, at 13.8 K, S_R=2.79, but an SPRT will have a resistance of only $R(13.8\ \mathrm{K})\approx 0.03\ \Omega$. A practical upper limit in excitation current is ≈10 mA for most cryogenic systems, yielding a signal voltage of 300 μV. In order to resolve 0.1 mK, or

$\varepsilon_T \cong 7\ \mu K \cdot K^{-1}$, a voltage noise of V_{ne}=6 nV or less is necessary. So while it is possible to use SPRTs even below 13.8 K, there are alternative thermometers which are much less demanding on the instrumentation and which exhibit comparable or better stability.

The self heating of 25.5 Ω capsule SPRTs is difficult to measure below ≈25 K due to the very low resistance and diminishing sensitivity. Consequently, any observed values for $\eta(T)$, such as those plotted in Fig. 1.5 , will lack reproducibility below that temperature. For T>25 K, SPRTs will exhibit $\eta \sim T^{-0.7}$ indicative of a heat-transfer mediated by the He exchange gas [44]. Typical values for η are 0.3 mK/μW to 0.4 mK/μW at T=83.8 K for standard capsule SPRTs.

Standard capsule SPRTs are calibrated at NIST over their full range of use. Calibration data are always presented in terms of the resistance ratio $W(T)$ normalized to R(273.16 K) unless otherwise specified by the customer. The methods for obtaining calibration data below 83.8 K at NIST are described in chapter 5 of this document. At temperatures of 83.8 K and above, calibration points are performed via immersion fixed-point cells as maintained in a separate facility, the NIST SPRT Calibration Laboratory. Those services are discussed in a separate document [45]. Capsule SPRTs which have been pre-calibrated at NIST over the range 13.8 K to 429 K are available for purchase as a standard reference material (SRM) designated as SRM 1750 [37].

1.5.1.2 Miniature capsule types

A miniature type of capsule PRT, which we refer to as MPRTs, uses reference grade wire of slightly smaller diameters than normally used in standard capsule types. These are commercially available with R(273.16 K) = 25 Ω or 100 Ω made from 50 μm and 25 μm diameter wire respectively [46]. The 100 Ω variety is much more common. They are encapsulated in a miniature copper capsule package approximately 3 mm in diameter and can usually achieve reproducibilities of ± 1 mK. MPRTs generally exhibit X_{RR} values in the range 1600 to 2500.

Values for the self-heating coefficient will typically be factors of 3 to 10 times larger than those of standard capsule SPRTs at the same temperature. It is not uncommon for MPRTs to be contaminated with air in the helium fill gas. This produces unusual behavior in η in the range of 40 K to 65 K as the air condenses or sublimes, depending on the direction of the temperature change (see discussion, section 1.3). Two examples are shown (MPRT-A and MPRT-B) in Fig. 1.5 with apparently differing degrees of air contamination. This is not necessarily a serious defect, but it will effectively limit an MPRTs reproducibility in this range as far as finite current calibrations are concerned. Similar phenomena have been observed with certain older types of GeRTs [27] (see section 1.5.4).

MPRTs have the same range of use as do the standard capsule types and may be calibrated at NIST from 13.8 K to 505 K. They are calibrated in the same manner as are SPRTs except that lower excitation currents are used due to their larger values of both R and η. Further information describing their design and performance is found in the article by Lucas [47].

1.5.1.3 Other types of platinum thermometers

The most common type of PRT is the industrial type ('IPRT') where the average TCR of $\bar{\alpha}_{100}$ = 0.00385 is specified by international standards [48-49]. The standard curve extends to a lower limit of 73.15 K (–200 °C) but the nominal interchangeability tolerance for even the best tolerance grade is only ±0.47 K at that temperature. Individual unit calibrations are possible to improve the interpolation accuracy, and extend the range downward in temperature, but they are generally not worth the effort below 20 K due to diminishing sensitivity. Certain wire-wound IRPTs will exhibit stability of ±5 mK at 20 K when adequately protected from moisture intrusion. While not very useful below 20 K, IPRTs can be calibrated over higher temperature ranges up to ≈550 °C at NIST in the Industrial Thermometer Laboratory. Those services are discussed in a separate document [50].

Thin film PRTs are usually made to match the industrial specification or sometimes match an even lower $\bar{\alpha}_{100}$ specification,(e.g. 0.00377) [51], but many of these are not recommended for use below –70 °C due to large hysteresis effects. One manufacturer has recently added a standard film PRT product which conforms to the IEC 60751 specification over the full lower range down to 77 K with a class B tolerance [51].

Special designs of PRTs are available for aerospace applications which are made from wire of intermediate purity to that of the reference and industrial grades, typically $0.00391 \leq \bar{\alpha}_{100} \leq 0.00392$. The values of X_{RR} typically are in the range 500 to 1000 [43]. The wire diameters vary considerably, typically from 8 μm to 80 μm and values for R_0 can be as high as 8 kΩ. These are routinely used at temperatures as low as 20 K and exhibit better interchangeability (e.g. $\Delta W(T) \approx 3 \times 10^{-3}$) at the lower temperatures than do the industrial types [52]. Most of these types are presently not calibrated at NIST due to their exceptional size and or their intended use in liquid hydrogen service. In some cases they may be tested and or partially calibrated at NIST in cryogenic liquid baths at 4.2 K, 77.3 K, and or 87.3 K via a special test arrangement. See chapter 2 for more information on this option.

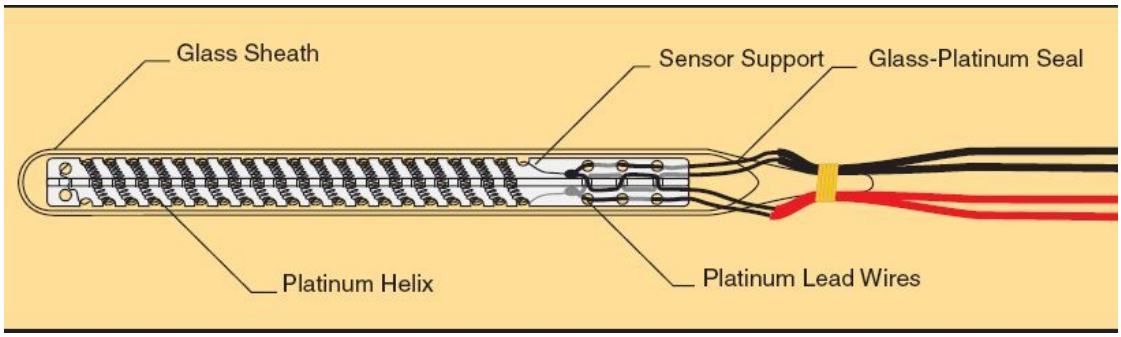

Figure 1.7a A standard capsule SPRT design utilizing a helical coil of Pt wire in a sealed glass sheath (Credit: Fluke Calibration, Inc.).

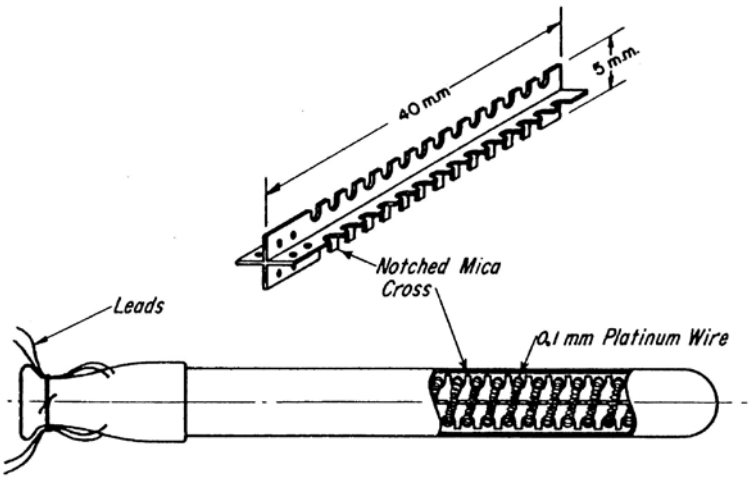

Figure 1.7b A standard capsule SPRT design utilizing a helical coil of Pt wire in a sealed Pt sheath.

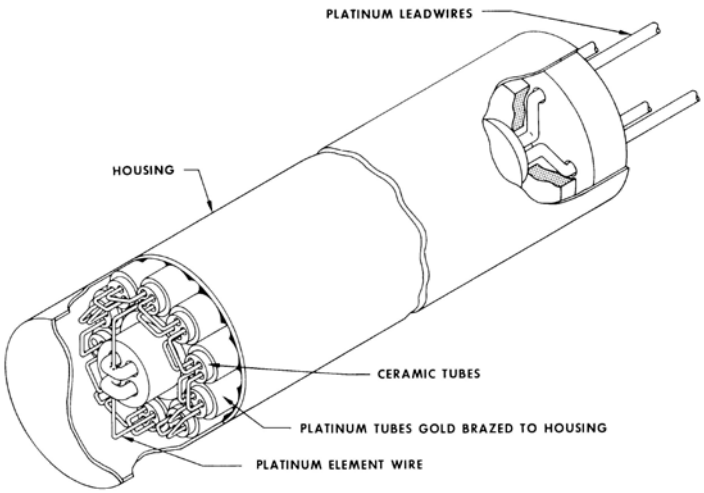

Figure 1.7c A standard capsule SPRT design utilizing a 'birdcage' design for the Pt wire in a sealed Ni-alloy sheath (Credit: Goodrich Aerospace).

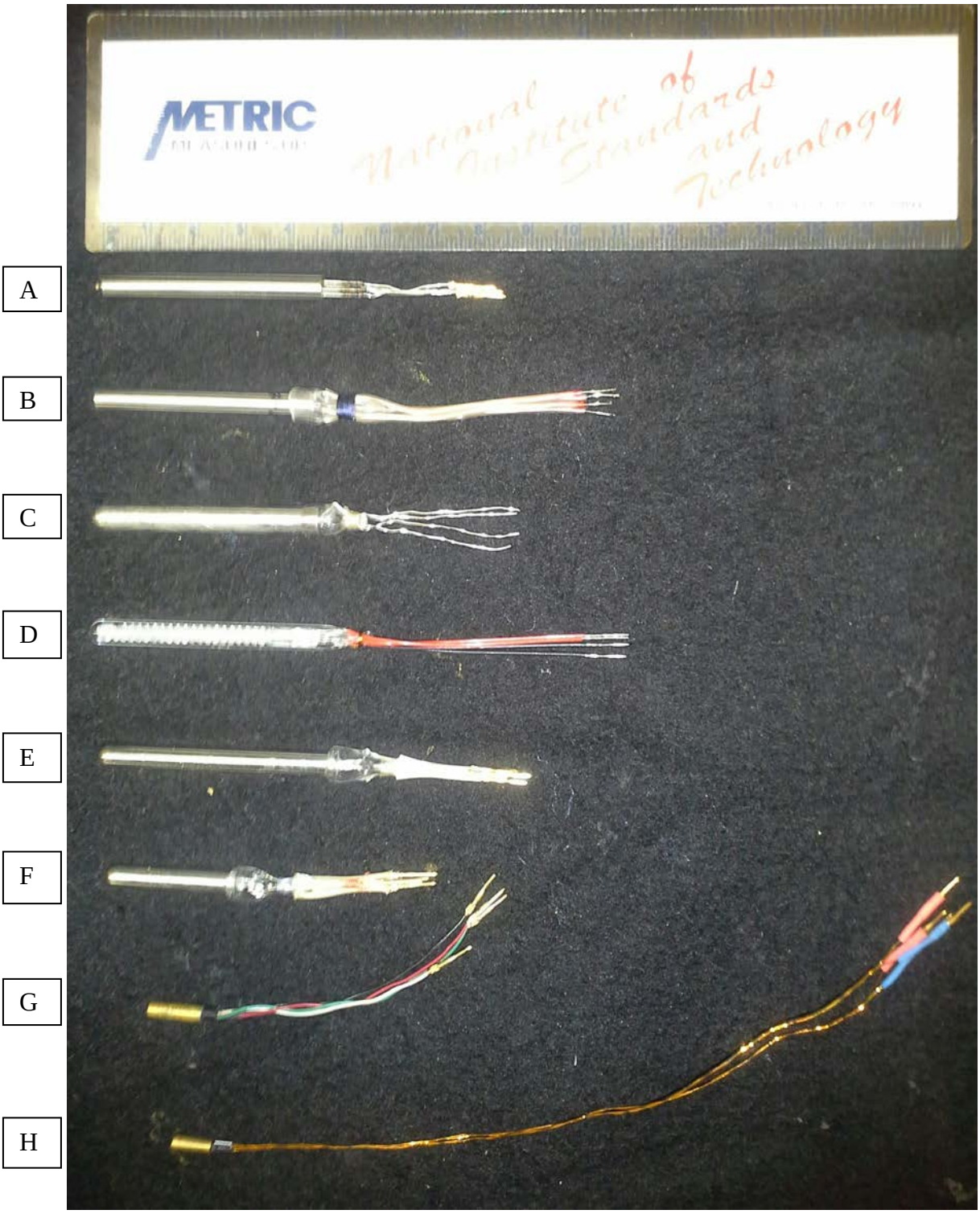

Figure 1.8 Various commercial designs of capsule type SPRTs, RIRTs, PCRTs, and GeRTs: A. 5.7 OD SPRT with inconel outer sheath [39, 53]; B. 5 mm OD SPRT or PCRT with platinum sheath [54] ; C.5.5 mm OD platinum sheath SPRT [55] ; D. 5.7 mm OD glass sheath SPRT [56]; E. 5 mm OD SPRT or 100 Ω RIRT [57] ; F. 5 mm OD 50 Ω RIRT with platinum sheath [57] ; G 3.6 mm OD GeRT ; H. 3 mm OD GeRT, also similar packages are used for MPRTs , thin-film RIRTs, ZNRTs, and other common NTC devices.

1.5.2 Rhodium-Iron

Rhodium-iron resistance thermometers (RIRTs) are made from a dilute magnetic alloy of 99.5 % Rh and 0.5 % Fe [57]. The Rh-Fe system is in a special class of binary alloys exhibiting anomalous positive TCRs at low temperatures [58-59]. The 0.5% Fe composition alloy is an optimal composition for calibration purposes which minimizes non-linearity while retaining adequate sensitivity. As shown in Figure 1.1, the resistance characteristic is nearly linear down to ~50 K where the sensitivity begins to decrease until reaching an inflection point near 26 K. The resistance remains predominately linear in T even below 1 K and $S_R \approx 0.05$ to 0.08 at T=0.65 K. This is still sufficient to resolve ≈0.013 mK with 1 μΩ/Ω even at this lower bound of the ITS-90.

The 0.5 % Fe alloy wire has had limited production with all of the commercial thermometers in use up to the year 2000 containing wire from a single supplier [60].The alloy is drawn down from bars to wire diameters of 50 μm and 37 μm for constructing the resistance elements in two common commercial sensor designs. Despite the common origin, there are significant variations in resistance characteristics of the wire, with $0.06 \leq W(4.2\text{ K}) \leq 0.09$. While some efforts to create a standardized reference function have been made, [52] no such internationally recognized function currently exists for this material. A summary of research on RIRTs prior to 1990 has been published by the CCT [61].

All RIRT calibrations at NIST are reported in 1990 Ohms [62]. Additional information on RIRT calibrations at NIST are given in section 2.1 and in chapter 5.

1.5.2.1 Standard Capsule Types

The first commercial design is the standard 5 mm diameter He-filled capsule similar in construction to certain capsule-type SPRTs. The 50 μm diameter wire is wound in a strain-free fashion within four glass insulators and sealed with a ~30 kPa He atmosphere inside the platinum outer sheath of the capsule (see Figure 1.9). These were commercially available up until circa 2001 from one source [63] but (as of this writing) are no longer available and the supply of 50 μm wire has been exhausted [64]. Two sizes were produced: type "W", approximately 5.5 cm long with $R_0 \approx 100\ \Omega$ and; type "U", approximately 3 cm long and $R_0 \approx 50 \pm 5\ \Omega$. Substantial inventories of these thermometers still exist within the NMIs and various secondary calibration facilities throughout the world. These thermometers (along with certain varieties of Ge RTs) are indispensable for the most accurate dissemination of the ITS-90 below ~20 K.

The self-heating characteristics of RIRTs are unusual in the immediate region of $T \approx 1.3$ K where a depressed superfluid transition occurs in the condensed He film [31]. As illustrated in figure 1.5, typical values are η=0.2 mK/μW for the type W capsule at 4.2 K where the ^{4}He exists as an unsaturated normal-state film on the bulb's inner surfaces and as temperature is lowered η diverges as $\sim T^{-1}$. As temperature is further lowered, η increases until $T \approx 1.3$ K where the film becomes a superfluid allowing the film to flow at a rate limited only by its critical velocity [65]. This superfluid film flow allows an efficient heat transport process to exist where the film evaporates from heated surfaces of the wire and recondenses on the inner surfaces of the sheath

with the film flow preserving mass conservation. The onset of this mechanism of superfluid film flow and evaporation/condensation produces a decrease in η by a factor of 5 to 6. As temperature is lowered still further, the heat transport is limited by the thermal-boundary-layer impedance between the film and metal surfaces and η diverges as $\sim T^{-3}$.

The 5 mm standard capsule-type RIRTs are highly stable when properly handled. Experience at NIST indicates that over a 10 year time period (~20 thermal cycles) the resistances of reference RIRTs are as stable as the best e-H_2 triple point cells, exhibiting reproducibility within the limit of statistical precision or ±20 μK at 13.803 K. Comparison of some RIRTs maintained at NIST for over 30 years have indicated relative stability (no relative changes) at the ±100 μK level for $T \leq 25$ K.

When roughly handled or shipped by air freight, small resistance shifts $\Delta R_0 \sim 100$ μΩ can occur which can be detected through monitoring the resistance value at the water triple point. The consequences of such shifts, however, are not always straightforward to interpret for all temperatures. Since RIRTs calibrations are not customarily normalized in the way SPRT calibrations are, a resistance shift δR at 273.16 K would imply a shift in the calibration over the entire range by an amount $\delta T = \delta R/(\mathrm{d}R/\mathrm{d}T)$. This scaling can be observed over the higher ranges of temperature but at the lowest ranges, particularly below 4 K, the effects of such resistance shifts are unnoticeable. This relative immunity to lattice strain at low temperature is consistent with the model where the spin-fluctuation resistivity is dominant at low temperatures and independent of the lattice state [59].

Other sources of RIRT production are in Russia [66] and China [67] although these sources have been limited in unit volumes and the thermometers are not widely available. These are wire-wound devices using variations on the basic capsule design trimmed to $R_0 \approx 100$ Ω. Less is known about the source material or stability characteristics of these thermometers compared to the commercial types discussed above and below. Limited experience with the Russian RIRTs at NIST indicates that they can exhibit instability of ≲0.2 mK at 273 K when carefully handled under a single thermal cycle. The stability at lower temperatures would then be expected to be somewhat better still. Experience elsewhere [68] indicates their stability is ± 3 mK over the range 5 K to 300 K. The resistance characteristics of a single sample of the Russian type are shown in figures 1.1 and 1.2 and are similar to that of the 37 μm commercial wire discussed below.

1.5.2.2 Miniature and Thin-film Types

The second commercial type of wire-wound RIRT is made from 37 μm wire in a ceramic four-bore tube and trimmed to $R_0 \approx 27$ Ω [69]. The alumina ceramic is 3.2 mm in outer diameter and 5 mm in length, resembling some industrial PRTs in appearance and design. To differentiate these RIRTs from the larger capsule type described above, we adopt Besley's terminology [70] and refer to this ceramic-based design as "ceramic-encapsulated" (CE) RIRTs. As of 2005, these continue to be produced commercially using 37 μm wire [64] but from a new source [69].

The stability of CE-RIRTs is very good under thermal cycling and reasonably good under physical handling. Besley [70] has studied the stability of a set of three of these and found stability under 20 thermal cycles between 20 K and 288 K to be in the range 20 μΩ to 50 μΩ as measured at 20 K (thermometric shifts of only 0.5 mK to 1.3 mK). When the lead wires are handled for soldering and unsoldering, however, larger shifts are observed. In this case resistance changes were as large as 600 μΩ as measured at 20 K (a thermometric shift of ≈15 mK). In this case there is an apparent weakness in the strain relief provided in the ceramic package construction and some forces are transmitted to the resistance element inside the ceramic body. Experience at NIST has shown that resistance shifts from handling lead wires of ≈200 μΩ at the triple point of water ($\Delta T \approx 2$ mK) may be expected.

The self-heating characteristics of CE-RIRTs are highly variable with observed values for $\eta(T)$ in different devices differing by factors of 10 or more at the same temperature [67]. These self-heating variations are presumably due to variations in the construction and use of glass-powder filling agents. The example shown for $\eta(T)$ of a CE RIRT in Figure 1.5 represents a nominal characteristic, but other devices of the same model may exhibit self-heating of considerably larger or smaller degrees.

Thin film RIRTs were commercially available in miniature (3 mm diameter) hermetic packages up until 2010. These are patterned films sputtered onto alumina substrates and trimmed to R_0=100 Ω. The composition of the alloy element is evidently somewhat different from that of the wire as can be seen by differences in both $W(T)$ and $S_R(T)$ in figures 1.1 and 1.2 . The self-heating characteristics are approximately 50 to 100 times greater than that of the standard capsule types for T>1.3 K (see Fig. 1.5, "RIRT-TF"). No superfluid transition is observed in $\eta(T)$ because the self-heating is dominated by solid conduction through the case and η diverges as $\sim T^{-1.2}$.

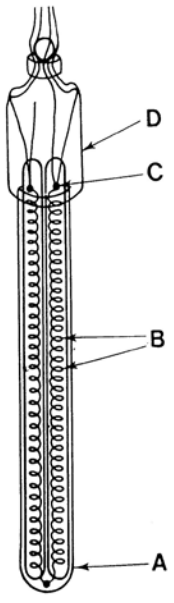

Figure 1.9 A standard capsule RIRT: A. platinum sheath; B. rhodium-iron alloy elements; C. 4-wire junction to Pt-Rh alloy lead wires; D. hermetic glass seal header. (Credit: Rusby, 1972[57]).

1.5.3 Platinum-Cobalt

Platinum-cobalt resistance thermometers (PCRTs) are another type of dilute magnetic alloy with a low temperature anomaly similar to that of RIRTs [71]. The same 0.5 % atomic concentration is used for the Co impurity to achieve the low temperature spin-fluctuation-mediated resistivity [72]. These are commercially available from a single source in Japan [73]. Two package types are available, one is a standard 5 mm diameter platinum-sheathed capsule design of R_0=100 Ω and the other is a 2 mm diameter copper-alloy-sheathed industrial design also of R_0=100 Ω. The standard capsule design utilizes a strain-free coil quartz cross-frame design and is filled with He gas.

A typical resistance ratio and S_R characteristic are shown in figures 1.1 and 1.2 respectively. Like the RIRT, the resistance characteristic is very linear down to ≈50 K where the sensitivity also begins to decrease until reaching a minimum near 12 K. The minimum TCR is α(12 K)=0.00092 K^{-1} but, as in the case of RIRTs, the TCR improves significantly at lower temperatures reaching α(0.65 K)=0.0022 K^{-1}. While these values are considerably lower than those exhibited by RIRTs, S_R values are higher in PCRTs for $T \gtrsim 19$ K. Shiratori and Mitsui[71] have proposed a reference function for PCRTs over the range 3 K to 27 K. That function, derived from examples available in the 1970s, does not appear to match the characteristics of contemporary material.

An early version of the industrial design has been tested for stability under thermal cycling [71]. The results of that study indicated stability within ±10 mK when cycled between 4.2 K and 300 K. Similar stability was found in a later study [74] of five industrial PCRTs cycled 21 times. Relatively little is known regarding the stability and or reproducibility of the capsule-type PCRTs as currently commercially produced, but stability would generally be expected to exceed (i.e. smaller irreproducibility) that of the industrial design. The very first prototypes produced exhibited stability of ±1 mK when thermally cycled 20 times [71]. Limited experience at NIST suggests that the contemporary thermometers should be stable to within 0.5 mK at 13.8 K for any one thermal cycle. Cycling effects usually produce only positive changes in the resistance so the cumulative effects of many thermal cycles could be much larger. On the other hand, the principal mechanisms which produce these resistance shifts could be self limiting and some empirical evidence from PCRT use at NIST supports this scenario. As is the case for RIRTs, small resistance shifts due to lattice strains are expected to have negligible effects on the calibration at temperatures $\lesssim$4 K.

The self-heating characteristics of the industrial-type PCRTs have been measured by Sakurai and Besley [74] for a sample of five devices in the range 1 K to 27 K. Their results indicate moderately high self-heating effects in the liquid He temperature range or η(1 K)≈100 mK/μW. The self heating characteristics for the standard capsule design are approximately 100 times lower and similar to those of the standard capsule RIRTs. The standard capsules also exhibit the same unusual dip in $\eta(T)$ at T≈1.3 K as seen in RIRTs, again due to the depressed superfluid transition in the unsaturated He film (see Fig. 1.5).

PCRTs are calibrated at NIST using the same point spacing and currents as are used for capsule RIRTs. Also like RIRTS, all calibration data are in ohms. The standard ranges are 0.65 K to 24.6 K and 0.65 K to 84 K. Additional information on PCRT calibrations at NIST is given in section 2.1 and in chapter 5.

1.5.4 n-type Germanium

Germanium Resistance Thermometers (GeRTs) are NTC devices made from specimens of doped single-crystal semiconductors. Early versions were in use by circa 1960. Since that time a significant amount of technological refinement has taken place [76-79] resulting in improved device characteristics. Various commercial versions are available, most of which are based on bulk crystals cut from wafers of high-purity boules [80]. The doping (typically with arsenic) is n-type and the concentration determines the resistivity and hence the usable temperature range. The crystals are typically packaged in miniature capsules (see Figure 1.10) in one of three common sizes: 4 mm ; 3 mm; and 2.3 mm diameters. Other package variations, such as 'bobbin' types, are commercially available [35]. A much newer variation of the GeRT is based on Ge film-GaAs heterostructures [81], but current commercial availability of those devices is limited. A summary of research and development activities on GeRTs up to 1990 has been prepared by the CCT Working Group 2 [82].

GeRTs are among the highest-sensitivity types of all resistance thermometers, but at the expense of limiting the practical range of use for any one device. The bulk crystal types are generally used at temperatures below 30 K, although selected models may be used up to ≈100 K with certain precautions. Ge films are useable to 300 K or higher for certain models [81], but there is comparatively little practical information available concerning their use in the higher ranges. A bulk GeRT will typically change in resistance by more than 4 decades from 0.65 K to 30 K. (see Fig. 1.3) They are differentiated by the device resistance at 4.2 K, which can be in the range $20\ \Omega \leq R(4.2\ \mathrm{K}) \leq 3000\ \Omega$. Units with similar values of R(4.2 K), however, will normally not be interchangeable over other regions of the calibration unless a special selection process is employed. The smallest R(4.2 K) devices are most suitable for use down into the ≳20 mK range, while the largest R(4.2 K) devices are most suited for use up to ≈100 K. The sensitivities at 4.2 K may likewise vary over $1\ \Omega/\mathrm{K} \leq \mathrm{d}R/\mathrm{d}T(4.2\ \mathrm{K}) \leq 2000\ \Omega/\mathrm{K}$ with the highest resistance devices exhibiting the highest sensitivities. The logarithmic sensitivities are generally in the range $0.3 \leq S(4.2\ \mathrm{K}) \leq 3$, with most devices exhibiting $S(4.2\ \mathrm{K}) \approx 2$ (see Fig. 1.4).

GeRT capsule packages are backfilled with He gas or sometimes with He/air gas mixtures in older devices. Unlike larger wire-based sensors, however, this exchange gas usually has relatively little effect on the self-heating coefficient below ≈40 K [27,44]. For most modern designs now in use, the self-heating below 40 K is mediated by solid conduction through the lead wiring and base-mounting materials. Self-heating coefficients are typically $\eta \approx 100\ \mathrm{mK}/\mu\mathrm{W}$ at T=1 K and diverge as $\sim T^{-n}$ ($1.2<n<2$) in that region, but significant variations exist according to the exact model [28]. The proper installation of these devices is therefore critical in this low temperature region. The wire leads must be bonded to metal surfaces at the same temperature as the reference thermometer in order to assure proper equilibration. These installation techniques are described in detail elsewhere [9],[35].

GeRT calibrations are normally performed at NIST using bi-polar DC excitation currents I such that the sensor excitation voltage $V = IR(T)$ is in the range 1 mV$\leq V \leq$ 10 mV. The calibration can be specified to a constant excitation voltage in this range depending on the observed self-heating and customer preference. The optimum excitation voltage is a trade-off between higher signal-to-noise ratio versus larger self-heating and this is often in the 2 mV to 4 mV range. In this case the observed resistance values will be corrected for self-heating to the values appropriate for the specified excitation. For certain lower resistance devices in the upper temperature range (e.g. R<100 Ω and T> 20 K), NIST can also provide AC excitation resistance data as necessary.

GeRTs are known to exhibit a large Peltier effect at the interface between the current lead wire and the Ge crystal which is generally observed at temperatures above ≈35 K [83]. When the Seebeck coefficient, s, is sufficiently large between the bond wires and the Ge crystal, the excitation current drives heat through the sensor element of thermal conductivity λ, and electrical resistivity ρ. The resulting thermal gradient across the sensor length l produces errors in the measured potential, again due the finite Seebeck coefficient, at the junction of the potential leads. This gives rise to differences in the resistance as measured via AC versus DC excitation, with the DC resistance in error by a relative amount $s^2T/\lambda\rho$. The AC resistance is always lower and free from the Peltier-induced error for excitation frequencies $f >> f_0$, where the characteristic frequency is $f_0 = \alpha_d/l^2$ and α_d is the thermal diffusivity of the Ge crystal [84]. The observed resistance difference $\Delta R_{acdc} = R_{dc} - R_{ac}$, increases with temperature leading to an increasingly negative thermometric error with increasing T. A typical magnitude for the effect in modern GeRTs is $\Delta R_{acdc}/R_{dc}$ =350 μΩ/Ω (≈25 mK) at 84 K and 30 Hz. As long as the calibration is all DC excitation, however, the effect is already included as a part of the calibration and would only be of consequence if AC excitations were later used by the customer rather than DC excitations. The effect is not observable for T<30 K, but NIST will normally evaluate the magnitude of the effect at f=30 Hz or 90 Hz for a special test calibration when the calibration range exceeds 30 K.

When pre-screened during manufacturing for obvious instabilities, GeRTs are normally highly stable over many thermal cycles. Most units will reproduce to better than ±0.5 mK at 4.2 K. There is a large volume of technical literature which describes stability testing results for a variety of GeRT designs [85-88].

The standard calibration range for GeRTs at NIST is 0.65 K to 24.56 K. A GeRT of R(4.2 K)≈250 Ω is best suited for calibration over this range, but resistances in the range 100 Ω≤ R(4.2 K) ≤1000 Ω will usually yield acceptable results. GeRTs outside of this resistance range may only be calibrated according to a special test arrangement over a customer-specified temperature range in consultation with NIST staff (see section 2.2). Larger resistances will generally require a higher temperature for the lower limit of the calibration. GeRTs are calibrated at NIST using a slightly modified spacing of calibration points compared to those used for RIRTs and PCRTs, with several additional calibration points in the region between 0.65 K and 2 K (see chapter 5). Calibration data are reported in ohms at the specified excitation voltage or excitation currents.

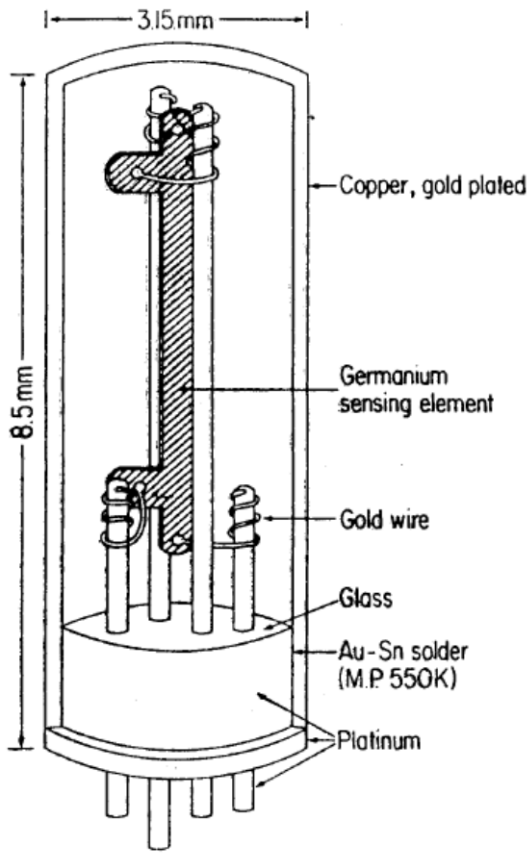

Figure 1.10 A cross-section of a typical GeRT in a cylindrical hermetic package. (Credit: Blakemore, 1972 [76]).

1.5.5 Other NTC Thermometers

There are many other semi-conducting NTC thermometers suitable for cryogenic applications. Some of these exhibit sufficient stability to justify calibrations at NIST. As is the case with GeRTs, calibrations would be reported in ohms at a specified excitation voltage. We include some brief descriptions below of selected types of commercially available devices. We omit carbon (a.k.a. 'radio resistors') despite their past popularity as these are generally not sufficiently stable to warrant the costs of high-accuracy calibrations.

1.5.5.1 Zirconium oxy-nitride

Thin-films of zirconium nitride and zirconium oxide are now commercially produced and fabricated into thermometers under the trademark name Cernox™ [89]. For the present purposes we refer to these devices as Zirconium-oxy-Nitride Resistance Thermometers (ZNRTs). These are NTC devices capable of being calibrated over temperature ranges as large as 0.3 K to 420 K. Their principle application is in high-magnetic field and moderate ionizing radiation

environments. Their sensitivities are less than that of GeRTs (see Fig. 1.4) but still more than adequate to achieve 0.1 mK resolution in the liquid-He range. ZNRTs are not interchangeable, but will exhibit a broad range of resistance characteristics for any given model.

ZNRTs will typically exhibit stability under thermal cycling of ±1 mK or better in the liquid helium temperature range [90-91]. Calibration shifts near ambient temperatures are larger, typically 0.1 K to 0.2 K, for $T \approx 300$ K. The resistance normally increases over many cycles, resulting in gradual negative thermometric shifts. Evidence suggests that units exposed to 25 or more thermal cycles will achieve better subsequent stability for $T > 20$ K than will un-cycled units (i.e. the thermal aging process is somewhat self-limiting) [90]. The manufacturer gives more conservative long-term specifications, however, of ±25 mK for $T \leq 77$ K over 200 thermal cycles [92].

There are a variety of packages available for ZNRTs. Among these are the 3 mm diameter miniature copper capsule as used for GeRTs and other cryogenic thermometers. The self-heating characteristics of ZNRTs depends on the package design, installation methods, and calibration medium (e.g. liquid vs. vacuum) [25]. Reported values at $T = 2$ K are in the range $40 \text{ mK}/\mu\text{W} \leq \eta(2 \text{ K}) \leq 1200 \text{ mK}/\mu\text{W}$ [28]. Values obtained at NIST for miniature capsule packages (i.e. type "AA") are $\eta(2 \text{ K}) \approx 20 \text{ mK}/\mu\text{W}$.

Calibrations of ZNRTs at NIST are considered special tests (see section 2.2) but in many cases they can be treated in a manner similar to GeRTs. In the case of ZNRTs, however, calibration data can be provided as high as the package specification allows (e.g. ≈420 K in some cases). As in the case of IPRTs described in 1.5.1.2, any required calibrations points above ≈165 K would be performed in the NIST Industrial Thermometer Laboratory [50].

1.5.5.2 Ruthenium Oxide

Thick films of ruthenium oxide (RuO_2) and bismuth ruthenate ($Bi_2Ru_2O_7$) have long been used to produce surface mount resistor components (i.e. "chip resistors") for printed circuit boards with very low TCRs at $T \approx 300$ K [93]. These components become useful NTC thermometers at temperatures <~20 K [94] and a large variety of commercial compositions are readily available [95]. When used as thermometers, we refer to these devices as Ruthenium-Oxide Resistance Thermometers (RORTs). Since their compositions are variable, however, the more generic terminology Thick-Film Chip Resistor (TFCR) is also found in the literature [2]. These devices are popular due to their very low magneto-resistance, small size, and low cost. The bare chip devices will usually consist of a rectangular film (e.g.'0603' ≈1.5 mm×0.75 mm, etc.) with two terminals on a 0.5 mm thick alumina substrate. The compositions and resistance values of the resistive films vary, but devices within the range $1 \text{ k}\Omega \leq R(300 \text{ K}) \leq 10 \text{ k}\Omega$ are usually those adapted for thermometry. Some types are optimized for wide-range of use, others are optimized for interchangeability, while others are optimized for low magneto-resistance. The sensitivities are generally low for $T > 10$ K and typically $-0.4 \leq S(4 \text{ K}) \leq -0.2$.

RORTs will exhibit hysteresis effects and abrupt resistance shifts under thermal cycling, presumably due to stress-induced micro-cracks. The cracking process appears to be self-limiting, therefore it is now customary for these devices to be thermally cycled many times before calibration to stabilize the measured resistance [96]. Customers should verify with their supplier that their RORTs have been stabilized prior to sending them to NIST for calibration.

Commercial packages are available which serve to protect the chips from moisture and other environmental degradation and provide convenient lead wire connections and or heat sinking capacity [97]. Customers sometimes provide their own custom-designed package for these devices which may not include a protective sheath (i.e. 'bare chip') , in which case it is necessary to consult with NIST staff regarding adaptation of these packages to NIST equipment. Adequate thermal coupling of the substrate to the package exterior surface is necessary to achieve reasonably low values of self-heating. Values of $\eta(4.2\ \mathrm{K}) \approx 50\ \mathrm{mK/\mu W}$ are typical with a temperature dependence of $\sim T^{-2}$ in the liquid He range. Calibrations of RORTs are considered a special test (see section 2.2) and work must be planned in close consultation with the NIST staff. In many cases it is possible to provide calibrations over a range 0.65 K to ≈20 K, with a few additional higher temperature calibration points if required.

2 Description of Cryogenic Resistance Thermometer Calibration Services

NIST provides regular calibration services for cryogenic resistance thermometers for temperatures ranging between 0.65 K and 83.8 K on the ITS-90.[99] These calibrations are performed within the NIST Low Temperature Calibration Facility (LTCF) as described in this document. Special test and calibration services of certain types of resistance thermometers can also be arranged over extended temperature ranges as high as 165 K within the LTCF. In the case of certain varieties of capsule SPRTs, calibrations are possible up to 505 K in conjunction with the fixed-point calibration methods available in the NIST PRT Calibration Laboratory [100,45]. In addition, calibration ranges for other suitable resistance thermometers may be extended to 823 K in combination with other related services offered by the NIST Industrial Thermometer Calibration Laboratory as described elsewhere [50].

General information and policies on NIST calibration services can be found at the following world-wide-web address:
http://www.nist.gov/calibrations/policy.cfm.
Ordering information specific to US domestic customers can be found at:
http://www.nist.gov/calibrations/domestic.cfm. Similar ordering information specific to non-US customers is located at:
http://www.nist.gov/calibrations/foreign.cfm . The current fees and calibration service ID for resistance thermometry standard service ID numbers and pricing can be found at:
http://www.nist.gov/calibrations//resistance_thermometry.cfm .

2.1 Regular Catalog Services

The regular calibration services available within the LTCF are found in tables 2.1 and 2.2 below. The service ID is used to identify the calibration or test. All calibration data for services listed in Table 2.1 are reported in ohms and measurements are performed entirely within the NIST LTCF using data derived from comparisons with NIST reference thermometers. Calibrations of capsule SPRTs shown in Table 2.2 are performed within both the NIST LTCF and SPRT calibration laboratory using data derived from fixed-point methods for $T \geq 83.8$ K and from comparisons with NIST reference thermometers for $T \leq 83.8$ K. Customers may specify a particular excitation current or voltage for the calibration including ‘zero-power’ values for the resistance. Further details concerning the calibration procedures are given in Chapter 5.

These standard catalog services represent calibrations at the smallest practical uncertainty given the typical characteristics of these thermometers. The interpolation uncertainty associated with use of the thermometer between calibration points is kept to a level comparable to the calibration uncertainty for any given point. In the case of the thermometers listed in Table 2.1, there are no reference functions or standard specifications, so a relatively large number of calibration points are required. A comparison calibration of RIRTs or PCRTs, over the temperature range from 0.65 K to 24.6 K will normally require 25 calibration points. Extended range RIRT or PCRT calibrations, for temperatures up to 83.8 K, will require approximately 35 calibration points. Calibrations of GeRTs over the range 0.65 K to 24.6 K will normally require 30 calibration

points. The specific temperatures used by NIST for calibration purposes are given in chapter 5. The calibration uncertainties of these standard service IDs are discussed in chapter 6.

The services listed in table 2.2 for capsule SPRTs apply equally well to MPRTs. In both cases the thermometers are calibrated according to the requirements of the ITS-90 defined subrange. The number of points required for the calibration depends on the subrange as is discussed in Chapter 3. Both SPRT and MPRT data are normally reported as resistance ratios.

Table 2.1 Regular SP-250 Catalog Services for Cryogenic Resistance Thermometer Calibrations performed entirely within the NIST LTCF.

Service ID No.	Description
33140C	Rhodium-Iron or Platinum-Cobalt Resistance Thermometers (0.65 K to 24.6 K)
33141C	Rhodium-Iron or Platinum-Cobalt Resistance Thermometers (0.65 K to 84 K)
33142C	n-type Germanium Resistance Thermometers (0.65 K to 24.6 K)
33355S	Special Tests of Cryogenic Resistance Thermometers

Table 2.2 Regular SP-250 Catalog Services for capsule-type SPRT Calibrations performed jointly between the NIST LTCF and SPRT Calibration Laboratory.

Service ID No.	Description
33010C	Capsule SPRT (13.8 K to 30 °C) H_2 to Ga
33020C	Capsule SPRT (13.8 K to 157 °C) H_2 to In
33030C	Capsule SPRT (13.8 K to 232 °C) H_2 to Sn
33031C	Capsule SPRT (24.5 K to 30 °C) Ne to Ga
33032C	Capsule SPRT (24.5 K to 157 °C) Ne to In
33033C	Capsule SPRT (24.5 K to 232 °C) Ne to Sn
33040C	Capsule SPRT (54 K to 30 °C) O_2 to Ga
33050C	Capsule SPRT (54 K to 157 °C) O_2 to In
33060C	Capsule SPRT (54 K to 232 °C) O_2 to Sn

2.2 Special Tests

The large variety of sensor types used in cryogenic thermometry preclude the use of standard service IDs for every possible type and range combination. The service ID 33355S “Special Test of Cryogenic Resistance Thermometers” is intended to cover some of those possibilities not included as regular services. This may involve use of a more limited range of temperatures or a more expanded range. Special tests may include an interpolation table and fitting function when explicitly requested by the customer and when such an analysis is appropriate for the given number of points specified for the test. Special tests may also include calibration of RT types not listed in Tables 2.1 and 2.2, such as those discussed in section 1.5.5. Special tests which consist of residual resistance (i.e. X_{RR}) measurements are also possible. Special tests are performed on an “at-cost” basis and under prior arrangement with NIST. In all cases, it is necessary for the customer to discuss the request with NIST calibration staff before the viability of the test and or calibration can be determined.

Tests which include temperatures in the extended range from 84 K to 165 K may be arranged for within the LTCF for appropriate thermometer types, with higher uncertainties than those achievable for $T \leq 83.8$ K (see chapter 6). For temperatures above 165 K, the vacuum block method becomes very cumbersome and a stirred alcohol bath is more practical. In cases where customers have requirements above 165 K, those points will be measured in the NIST Industrial Thermometer Calibration Laboratory [112]. In those cases capsule type thermometers will be adapted for use in liquid-immersion baths via glass protection tubes.

Special tests in liquid cryogenic baths are also possible for three specific cases: liquid helium (4.2 K); liquid nitrogen (77.3 K); and liquid argon (87.3 K). This option may be appropriate for those customers with large immersion-type sensors or those with a relatively large number of identical sensors types. Certain dimensional and count limitations will still exist and customers must consult with NIST staff to determine which variations are viable.

Stability testing or thermal stabilization of thermometers are intensive long-term projects and may also be possible as special tests. While NIST has this capability and has undertaken similar projects in the past [98], work of this nature may sometimes be beyond the scope of calibration services and would be better handled under a contract basis. Extensive consultation with NIST calibration staff and management would be necessary in those cases.

2.3 Procedures for submitting a thermometer for calibration

Calibrations of cryogenic RTs at NIST are only performed by "batch" on a once per year basis. Customers are advised to consult NIST staff well in advance of their anticipated delivery time requirement. There is no exact schedule for when these calibrations are performed, but usually work begins in the 4th quarter of the calendar year and proceeds during the winter months. An absolute minimum turnaround of 60 days should be expected between the time the thermometer and purchase order are received at NIST and the return of the thermometer and issue of the calibration report. Longer turn-around times may be expected depending on the amount of work assigned to a given batch calibration run, the range of temperatures required, and the timing of the customer's shipments. As always, consultation of the NIST calibration staff is advised in order to minimize the time which a thermometer remains at NIST during a calibration. As of 2006, low temperature calibrations which require the use of liquid helium are not performed during August and September due to supply shortages which typically exist during those months. Additional restrictions may occur in the future which further constrain testing schedules subject to the availability of liquid helium.

All thermometers submitted for tests at NIST should have a unique serial number permanently etched into the capsule sheath. If no serial number is visible or otherwise supplied by the customer, then NIST will assign a number to the device for book-keeping and reporting purposes. NIST will not etch or otherwise mark the thermometer but will tag a lead wire with the assigned number when the unit is returned to the customer. Some manufacturers will print serial numbers onto the thermometer sheath using ink. All such methods are prone to failure due to dissolution of all such inks in the carbon-based grease normally used for installation of the thermometers at NIST and elsewhere. Customers submitting such thermometers are advised to

consider this risk. NIST will also tag the thermometer's lead wire in the event that a manufacturer's serial number dissolves or otherwise becomes illegible. In the event that a thermometer's identity becomes in doubt due to dissolution of the manufacturer's markings, use of the triple point of water resistance can often remove any ambiguity providing that such records are available. NIST will also assign other numbers such as a test folder number and NIST-ID number for book-keeping purposes during the calibration. These numbers can be cross-referenced with the serial number.

The customer should include the following information on the purchase order:

1) NIST Calibration service ID and description
2) Thermometer model number, serial number, and manufacturer
3) Special test conditions (if any) and handling instructions (if any)
4) Nominal value of either R_0 or R(4.2 K) in ohms.
5) Special instructions (if any) regarding the Report of Calibration (e.g. different customer name or different mailing address)
6) Name, address, and telephone number of customer's Procurement Officer
7) Name, address, and telephone number of customer's Technical Contact
8) Customer identification number; i.e., social security number (EIN) for individuals; tax identification number (TIN) for organizations; or agency location code (ALC) for government customers
9) Return shipping address and Return shipping method and account number
10) Shipping insurance requirement (if any).

For shipment, the thermometer should be softly supported within a well-fitting hardshell case, but not be free to rattle. This necessitates the use of packing material that does not become compacted. The thermometer case should be softly packed inside a shipping container. The shipping container must be sufficiently rigid and strong that it will not appreciably deform under the treatment usually given by common carriers. Styro-foam is not sufficiently rigid to be used as an outside container. Similarly, mailing tubes are unacceptable. Thermometers will not be returned in containers that are obviously unsuitable, such as those closed by nailing. Suitable containers will be provided when a thermometer shipping container is not satisfactory for re-use.

2.4 Acceptance Tests, Calibration Status, and Acceptance Criteria

Once a thermometer arrives at NIST it is visually inspected and the leads tested for continuity and possible shorts to the sheath or to other leads. In most cases an initial check at the triple point of water will be performed to enable some overall assessment of the thermometer's repeatability, reproducibility, self-heating, and stability over the calibration's thermal cycle. Once these initial tests are passed, the thermometer will be considered accepted for test and the customer duly notified with an anticipated completion date via a NIST Acceptance Form (NIST-64, Test Record, Acceptance).

The calibration information is then entered into the NIST Calibration Support System (CSS) database. Authorized customers may access certain NIST web pages on the CSS through Customer Access portals. This allows the customers to check the status of their calibration or other test from the Internet via a web browser. The web address is given on the NIST-64 along with a unique username/password required for access. The customer/user will be provided status information concerning that specific calibration only. NIST does not provide proprietary information via internet connections, and all customer access is password secured. The status of a calibration or test is available on the web site for 60 days after the service is completed.

NIST will install connector pins at the terminations of the thermometer's lead wires to facilitate connection to NIST equipment. These connector pins may be crimped and/or soldered to the leads. They are generally left connected to the leads when the thermometer is returned to the customer unless otherwise requested. Mating socket connections can be made available to those customers who wish to continue to use this type of connection.

A thermometer may be rejected if any of the following conditions are found: 1.) evidence of a leak in the hermetic seal; 2.) evidence of moisture intrusion; 3.) crimped, crushed, cracked, or otherwise damaged sheath or header; 4.) internal shorts or open circuit leads; and 5.) an instability or drift at 273.16 K which significantly exceeds what would be expected for a particular type thermometer. In addition, all thermometer terminals should be isolated from the sheath. Sensor packages with one side of the resistive element tied to the sheath are not suitable for high-accuracy calibrations and these will likewise be rejected**.** A minimum handling fee applies to a rejected thermometer.

Four-terminal packages are greatly preferred. Any thermometer with fewer than four terminals (i.e. two or three terminal types) will be converted to four-wire termination via external solder joints in a way which is most readily compatible with the NIST cryostat wiring and connections. After the calibration is completed, the thermometer will be returned to the customer with this adaptation in place and a note regarding the use of the adaptation will occur in the calibration report. It will normally not be practical to calibrate sensor packages with excessively long (> 1 m) lead wires. In such cases NIST will request permission from the customer to cut down the leads to a more manageable length. If this is not possible, then the thermometer will be rejected.

3 Overview of the ITS-90 below 273.16 K

The ITS-90 is a set of practical definitions for the realization of temperatures which approximate thermodynamic temperature. The scale is defined through fixed point temperatures of pure elemental or molecular substances together with standard interpolating instruments and interpolation equations [1]. The notation shown in Table 3.1 for the ITS-90 fixed points is used throughout this document. A graphical synopsis showing all defined ranges and sub-ranges between 273.16 K and 0.65 K is shown in Figure 3.1

Table 3.1 The fixed points of the ITS-90 used for realization purposes for $T \leq 273.16$ K.

Notation	Descriptive Name	T_{90} / K
^{3}He VP	helium-3 vapor pressure	0.65 K to 3.0 K
^{4}He VP	helium-4 vapor pressure	1.25 K to 5.0 K
e-H_2 TP	equilibrium-hydrogen triple point	13.8033
e-H_2 VP_1	point of liquid equilibrium-hydrogen under a saturated vapor pressure near 33.3213 kPa	17.036
e-H_2 VP_2	point of liquid equilibrium-hydrogen under a saturated vapor pressure near 101.292 kPa	20.2714
Ne TP	neon triple point	24.5561
O_2 TP	oxygen triple point	54.3584
Ar TP	argon triple point	83.8058
Hg TP	mercury triple point	234.3156
WTP	water triple point	273.16

3.1 SPRT Definitions: 13.8 K to 273.16 K

While the overall range of use for SPRTs as defined on the ITS-90 is from 13.8033 K to 1234.93 K, we restrict this discussion to temperatures below the triple point of water (273.16 K) and likewise restrict the treatment to ‘capsule-type’ SPRTs only. The ITS-90 specifies eleven different SPRT subranges in all, but for the purposes of the NIST LTCF, we only need consider the lowest four subranges. These four subranges are identified with a subscript notation of 1 to 4 consistent with that used in the NIST Technical Note 1265 [99]. The temperature ranges and required fixed points are shown in figure 3.1.

Calibration of an SPRT is accomplished through use of ITS-90 defined fixed points. There are eight defined fixed points within the restricted SPRT temperature range. Each one of the four calibration subranges includes the WTP plus some combination of one or more other fixed points. The required fixed points for each of the four calibration subranges 1 through 4 are given in table 3.2.

Table 3.2. Subranges for the SPRT definitions of the ITS-90 below 273.16 K.

Subrange Number	Temperatures Covered	Fixed Points Used
1	13.8033 K ≤ T_{90} ≤ 273.16 K	e-H_2 TP, e-H_2 VP1, e-H_2 VP2, Ne TP, O_2 TP, Ar TP, Hg TP, TPW
2	24.5561 K ≤ T_{90} ≤ 273.16 K	e-H_2 TP, Ne TP, O_2 TP, Ar TP, Hg TP, TPW
3	54.3584 K ≤ T_{90} ≤ 273.16 K	O_2 TP, Ar TP, Hg TP, TPW
4	83.8058 K ≤ T_{90} ≤ 273.16 K	Ar TP, Hg TP, TPW

Interpolation of temperature on the ITS-90, through the use of SPRTs, is accomplished by three basic steps: a) calibration of the SPRT for a particular subrange; b) measurement of the SPRT's resistance at some unknown temperature, T_{90}, within the specified range; and c) calculation of the temperature through use of the ITS-90 defined equations appropriate for the range of calibration. All ITS-90 defined equations for SPRTs are expressed in terms of the SPRT resistance ratio, $W(T_{90})$, defined as

$$W(T_{90}) \equiv \frac{R(T_{90})}{R(T_{\mathrm{WTP}})} \tag{3.1}$$

where $R(T_{90})$ is the SPRT resistance at the unknown temperature T_{90} and $R(T_{\mathrm{WTP}})$ is the SPRT resistance at the water triple point (WTP).

The ITS-90 specifies a minimum criterion and a maximum criterion for SPRTs used below 933.473 K, at least one of which must be met in order for the SPRT to be suitable as a defining instrument of the scale. These criteria are given in terms of the measured $W(T_{90})$ value at the triple point of mercury (HgTP) and the melting point of gallium (GaMP). These criteria are

$$W(T_{\mathrm{Ga\,MP}}) \geq 1.11807, \tag{3.2a}$$

and

$$W(T_{\mathrm{HgTP}}) \leq 0.844235. \tag{3.2b}$$

These criteria are essentially specifications for the minimum purity of the platinum element in the SPRT and are effectively equivalent (i.e. redundant).

When using SPRTs, accurate calculation of temperature on the ITS-90 requires a detailed understanding of the equations used for the calibration subrange of interest. There are essentially two types of functions that are used for interpolation of temperature within any given calibration subrange. These are reference functions and deviation functions, all of which are described below.

3.1.1 Reference Function

The ITS-90 specifies two reference functions which cover the overall SPRT temperature range and which we refer to as the 'lower-range reference function' and the 'upper-range reference

function'. One reference function spans the range 13.8033 K to 273.16 K (lower range) and the other reference function spans the range 273.15 K to 1234.93 K (upper range). For the purposes of this document, we treat only the lower-range reference function, and from this point forward will refer to this function simply as "the SPRT reference function" with the understanding that the temperature range is restricted to $T_{90} \leq 273.16$ K. The SPRT reference function, $W_r(T_{90})$, is an idealized representation which is designed to closely approximate any real SPRT resistance ratio, $W(T_{90})$. Figure 3.2 is a plot of the SPRT reference function over this temperature range.

The SPRT reference function is given by the following equation,

$$\ln\left[W_r(T_{90})\right] \equiv A_0 + \sum_{i=1}^{12} A_i \left[\frac{\ln\left(T_{90}/273.16\ \text{K}\right)+1.5}{1.5}\right]^i \qquad 13.8033\ \text{K} \leq T_{90} \leq 273.16\ \text{K}, \quad (3.3)$$

where the values for the A_i are given in table 3.3. An approximate inverse function, which expresses T_{90} as a function of W_r , is given by the equation

$$T_{90}(W_r) \cong 273.16\left[B_0 + \sum_{j=1}^{15} B_j \left\{\frac{\left[W_r(T_{90})\right]^{1/6} - 0.65}{0.35}\right\}^j\right] \quad 13.8033\ \text{K} \leq T_{90} \leq 273.16\ \text{K}, \quad (3.4)$$

where the B_j are also given in table 3.3.

It is important to remember that temperature is defined on the ITS-90 through the reference functions, not through their respective inverse functions. The inverse functions are, however, very close approximations. The difference between an interpolated temperature when using the reference functions and when using their approximate inverse functions is less than 0.1 mK over the entire SPRT range of use. This difference is shown as a function of temperature in figure 3.3 for the range below 273.16 K.

3.1.2 Deviation Functions

The extent to which a real SPRT does not perfectly conform to the ideal representation given by the reference function is referred to as the deviation, or deviation function, which is defined as the difference between the observed resistance ratio and the reference function or

$$\Delta W(T_{90}) \equiv W(T_{90}) - W_r(T_{90}). \quad (3.5)$$

The SPRT deviation is that part of its resistance-temperature relationship which is considered unique to each SPRT and the specified deviation function is solved as part of the calibration process. The form of the deviation depends on which of the different calibration subranges is being used. In all cases there are one or more unspecified coefficients in the deviation function which are uniquely determined for a given SPRT from the fixed point calibration data. The equations specific to the lowest four SPRT subranges (1 to 4) are given here. There are seven others defined for higher temperature use which are described elsewhere [99].

3.1.2.1 Calibration Subrange 13.8033 K to 273.16 K (SPRT subrange 1).

The SPRT resistance is measured at the equilibrium hydrogen triple point (e-H2TP), the equilibrium hydrogen vapor pressure point (e-H2VP1) near 33.32 kPa (T90≅17.035 K),), the equilibrium hydrogen vapor pressure point (e-H2VP2) near 101.29 kPa (T90≅20.27 K), the neon triple point (NeTP), the oxygen triple point (O2TP), the argon triple point (ArTP), the mercury triple point (HgTP) and the WTP. The deviation function for this calibration subrange is given by

$$\Delta W_1(T_{90}) \equiv a_1\left[W(T_{90})-1\right] + b_1\left[W(T_{90})-1\right]^2 + \sum_{i=1}^{5} c_i \left\{\ln\left[W(T_{90})\right]\right\}^{i+2}. \qquad (3.6)$$

The coefficients a_1 , b_1, c_1, c_2, c_3, c_4, and c_5 are determined by solving a system of seven simultaneous equations using the fixed point calibration data. These data must include the results of seven ratio measurements of $W(T_{\mathrm{H2TP}})$, $W(T_{\mathrm{H2VP1}})$, $W(T_{\mathrm{H2VP2}})$, $W(T_{\mathrm{NeTP}})$, $W(T_{\mathrm{O2TP}})$, $W(T_{\mathrm{ArTP}})$ and $W(T_{\mathrm{HgTP}})$ for the SPRT. This subrange covers the entire span of the lower range reference function and is the most complex of all the SPRT calibration subranges.

3.1.2.2 Calibration Subrange 24.5561 K to 273.16 K (SPRT subrange 2).

The SPRT resistance is measured at the equilibrium hydrogen triple point (e-H_2TP), the neon triple point (NeTP), the oxygen triple point (O_2TP), the argon triple point (ArTP), the mercury triple point (HgTP) and the WTP. The deviation function for this calibration subrange is given by

$$\Delta W_2(T_{90}) \equiv a_2\left[W(T_{90})-1\right] + b_2\left[W(T_{90})-1\right]^2 + \sum_{i=1}^{3} c_i \left\{\ln\left[W(T_{90})\right]\right\}^{i}. \qquad (3.7)$$

The coefficients a_2, b_2, c_1, c_2, and c_3 are determined by solving a system of five simultaneous equations using the fixed point calibration data. These data must include the results of five ratio measurements of $W(T_{\mathrm{H2TP}})$, $W(T_{\mathrm{NeTP}})$, $W(T_{\mathrm{O2TP}})$, $W(T_{\mathrm{ArTP}})$ and $W(T_{\mathrm{HgTP}})$ for the SPRT. This subrange has the peculiar property of requiring an extra fixed point (H_2TP) which lies outside of its nominal calibration range.

3.1.2.3 Calibration Subrange 54.3584 K to 273.16 K (SPRT subrange 3).

The SPRT resistance is measured at the oxygen triple point (O_2TP), the argon triple point (ArTP), the mercury triple point (HgTP) and the WTP. The deviation function for this calibration subrange is given by

$$\Delta W_3(T_{90}) \equiv a_3\left[W(T_{90})-1\right] + b_3\left[W(T_{90})-1\right]^2 + c_1 \left\{\ln\left[W(T_{90})\right]\right\}^{2}. \qquad (3.8)$$

The coefficients a_3, b_3, and c_1 are determined by solving a system of three simultaneous equations using the fixed point calibration data. These data must include the results of the three ratio measurements of $W(T_{O2TP})$, $W(T_{ArTP})$ and $W(T_{HgTP})$ for the SPRT.

3.1.2.4 Calibration Subrange 83.8058 K to 273.16 K (SPRT subrange 4).

The SPRT resistance is measured at the argon triple point (ArTP), the mercury triple point (HgTP), and the WTP. The deviation function for this calibration subrange is given by

$$\Delta W_4(T_{90}) \equiv a_4[W(T_{90})-1] + b_4[W(T_{90})-1]\ln[W(T_{90})]. \qquad (3.9)$$

The coefficients a_4 and b_4 are determined by solving a system of two simultaneous equations using the fixed point calibration data. These data must include the results of the two ratio measurements of $W(T_{HgTP})$ and $W(T_{ArTP})$ for the SPRT.

Table 3.3. Coefficients for the ITS-90 reference function and inverse function for $T \leq 273.16$ K

Reference Function Coefficients for $T_{90} \leq 273.16$ K		Approximate Inverse Function Coefficients for $T_{90} \leq 273.16$ K	
A_0	–2.135 347 29	B_0	0.183 324 722
A_1	3.183 247 20	B_1	0.240 975 303
A_2	–1.801 435 97	B_2	0.209 108 771
A_3	0.717 272 04	B_3	0.190 439 972
A_4	0.503 440 27	B_4	0.142 648 498
A_5	–0.618 933 95	B_5	0.077 993 465
A_6	–0.053 323 22	B_6	0.012 475 611
A_7	0.280 213 62	B_7	–0.032 267 127
A_8	0.107 152 24	B_8	–0.075 291 522
A_9	–0.293 028 65	B_9	–0.056 470 670
A_{10}	0.044 598 72	B_{10}	0.076 201 285
A_{11}	0.118 686 32	B_{11}	0.123 893 204
A_{12}	–0.052 481 34	B_{12}	–0.029 201 193
		B_{13}	–0.091 173 542
		B_{14}	0.001 317 696
		B_{15}	0.026 025 526

3.2 ICVGT Definition: 4.2 K to 24.5561 K

The ITS-90 defines temperature over the range 3 K to 24.5561 K via an Interpolating Constant Volume Gas Thermometer (ICVGT). The lower limit of the range can be varied depending on the choice of the lower-most fixed-point temperature in the range from 3.0 K to 5.0 K as derived from ^{4}He vapor pressure measurements.(see section 3.3 below) When the lower temperature limit is in the range 4.2 K to 5.0 K, the ICVGT definition is simplified and temperatures are derived from measurements of the static pressure p of a ^{4}He gas bulb according to the equation,

$$T_{90} \equiv a + bp + cp^2 \tag{3.10}$$

where the coefficients a, b, and c are found by solution of three simultaneous equations using the p,T_{90} data at three ITS-90-defined fixed-point temperatures. The solution is unique to the particular experimental parameters of the gas bulb. In practice the interpolation is predominately linear, with the cp^2 term contributing less than 0.05 % at 24.556 K for a 1 liter bulb of ^{4}He gas. These temperatures are shown in Table 3.4 for the special case where the lower temperature limit of 5.0 K is chosen. This is the version of the ICVGT which is disseminated by NIST (see section 4.1)

Table 3.4 The fixed points of the ITS-90 used for realization of the ICVGT definition at NIST.

Notation	Descriptive Name	T_{90} / K
^{4}He VP	helium-4 vapor pressure at p_{4He}=196 kPa	5.0 K
e-H_2 TP	equilibrium-hydrogen triple point	13.8033
Ne TP	neon triple point	24.5561

3.3 ^{4}He and ^{3}He Vapor Pressure Definitions: 0.65 K to 5 K

The ITS-90 defines temperature over the range 1.25 K to 5 K via the saturated vapor pressure (VP) of ^{4}He and temperature over the range 0.65 K to 3.1 K via the saturated vapor pressure of ^{3}He. The ITS-90 vapor pressure equation is given by,

$$T_{90} = a_0 + \sum_{i=1}^{9} a_i \{[\ln(p) - b]/c\}^i \tag{3.11}$$

where the measurements of the vapor pressures p are expressed in units of Pa and the coefficients are given in table 3.5. The ^{4}He VP range is broken into two ranges with separate coefficient sets, one set for temperatures 1.25 K$\leq T_{90} \leq$2.1768 K below the λ-point, and the other set for temperatures 2.1768 K$\leq T_{90} \leq$ 5.0 K above the λ-point. All three sets of coefficients used for equation 3.11 are given in Table 3.5. The two vapor pressure curves are plotted in Figure 3.4.

.

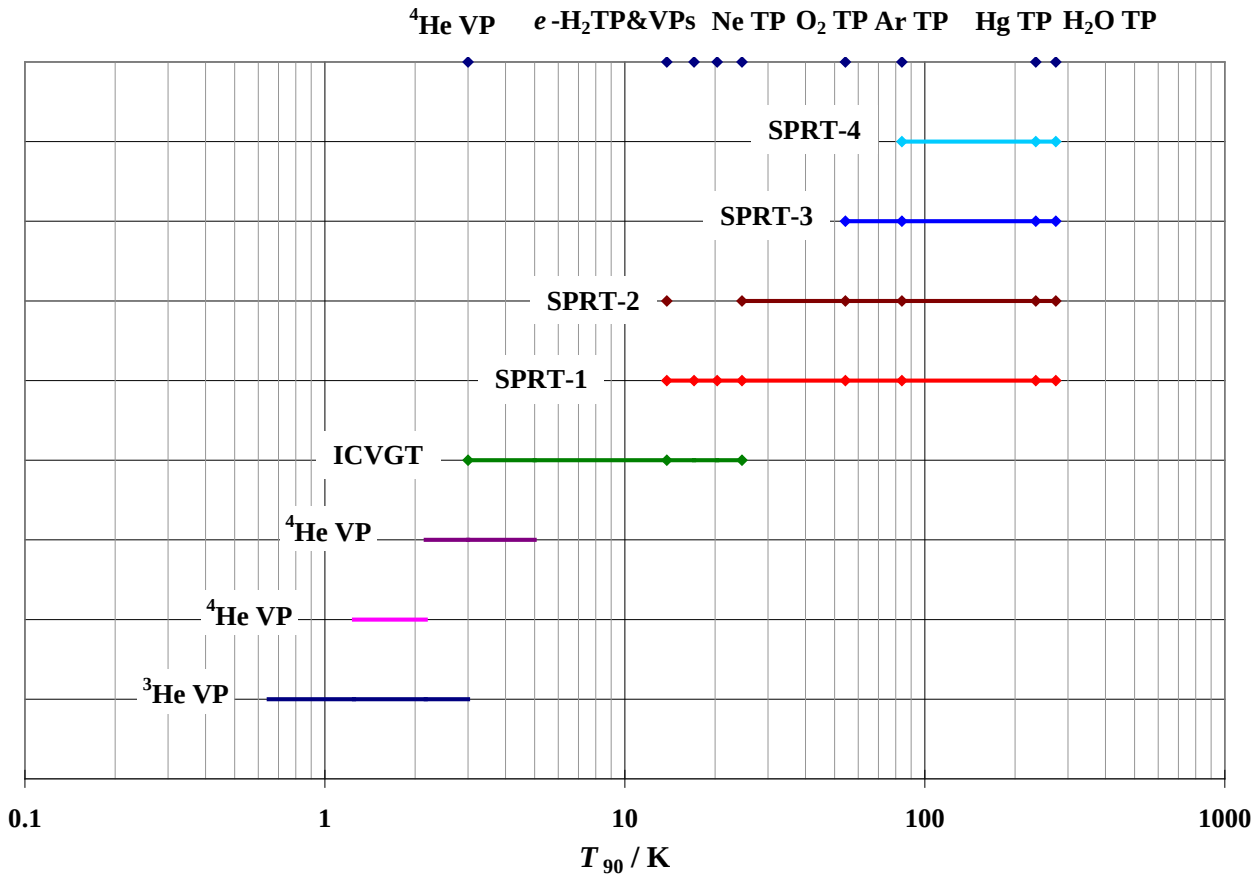

Figure 3.1 The structure of the ITS-90 below 273.16 K showing defining sub-ranges.

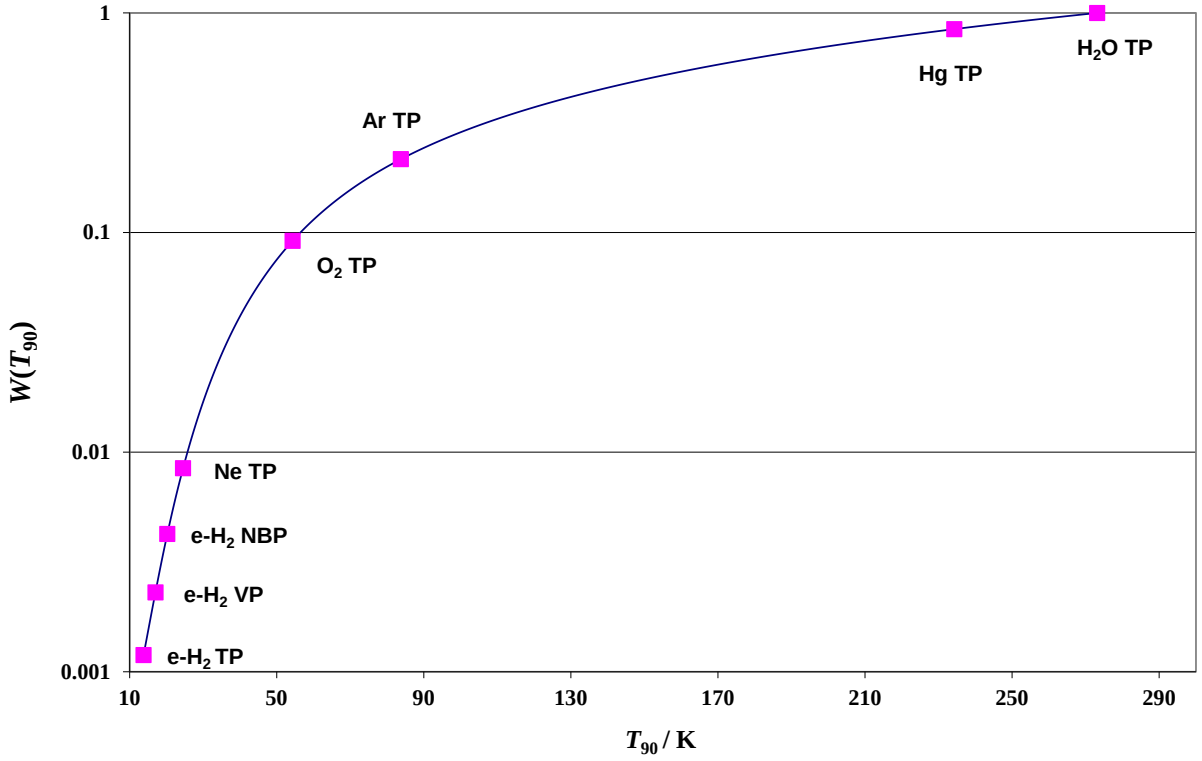

Figure 3.2 The SPRT reference function for T_{90} <5 K. Location of defining fixed points are indicated as square markers on the curve.

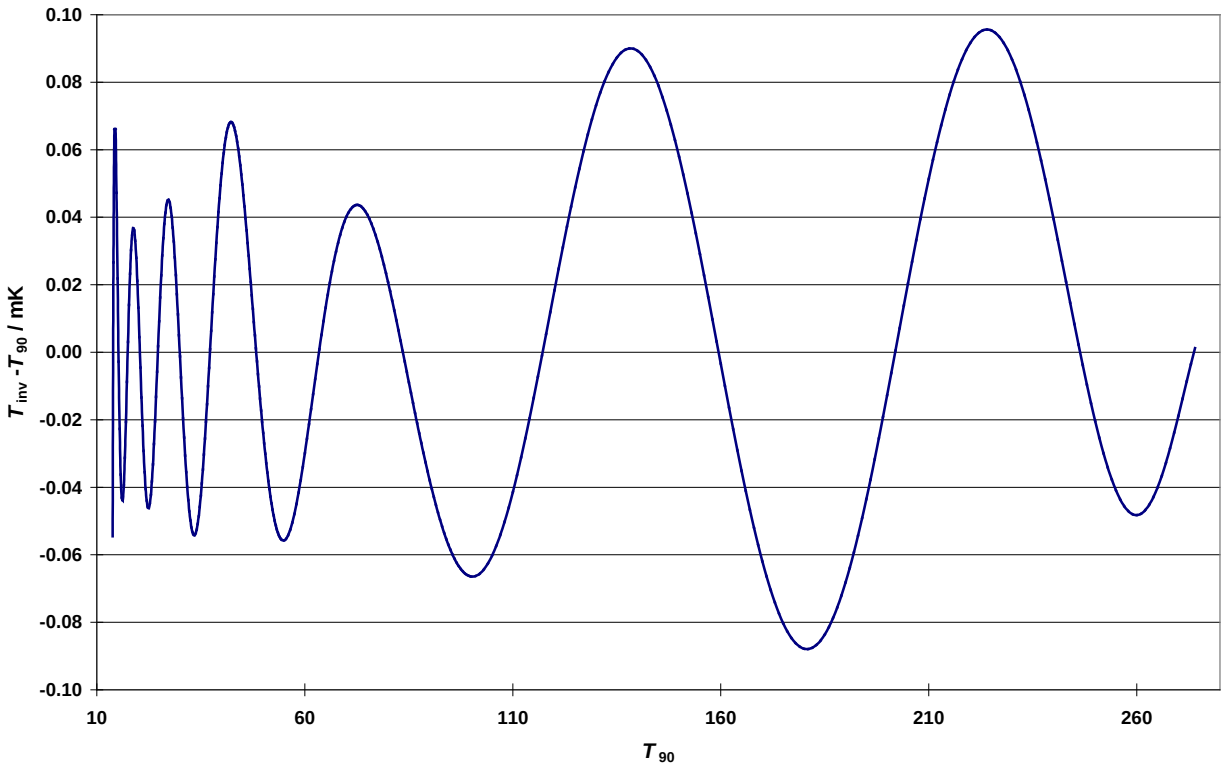

Figure 3.3 The difference in ITS-90 interpolated temperatures for SPRTs as derived from the inverse function T_{inv} and those derived from the reference function T_{90} for T_{90} <273.16 K .

Table 3.5 Coefficients used for the ^{3}He and ^{4}He vapor pressure equations (equation 3.11).

Range	0.65 K to 3.2 K	1.25 K to 2.1768 K	2.1768 K to 5.0 K
Coefficient	^{3}He	^{4}He-II	^{4}He-I
a_0	1.053447	1.392408	3.146631
a_1	0.980106	0.527153	1.357655
a_2	0.676380	0.166756	0.413923
a_3	0.372692	0.050988	0.091159
a_4	0.151656	0.026514	0.016349
a_5	-0.002263	0.001975	0.001826
a_6	0.006596	-0.017976	-0.004325
a_7	0.088966	0.005409	-0.004973
a_8	-0.004770	0.013259	0
a_9	-0.054943	0	0
b	7.3	5.6	10.3
c	4.3	2.9	1.9

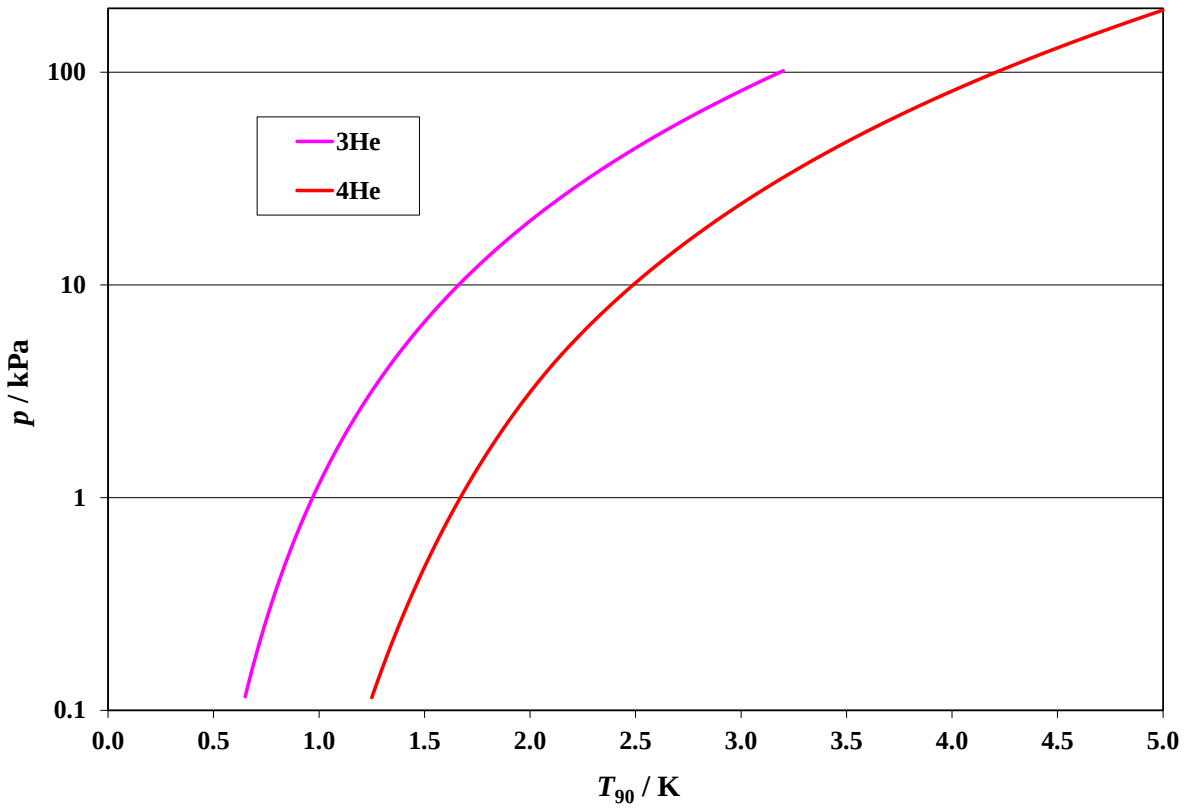

Figure 3.4 The ITS-90 ^{3}He and ^{4}He vapor pressure curves from 0.65 K to 5.0 K.

4 NIST Realizations of the ITS-90: 0.65 K to 273.16 K

NIST maintains three separate facilities which are involved in the realization and dissemination of the ITS-90 over the range 13.8 K to 273.16 K [104]. Two of these three facilities are also involved in the realization and dissemination of the ITS-90 below 83.8 K [117]. In the first facility, the "SPRT Calibration Laboratory", all of the immersion-type fixed-point cells necessary for the ITS-90 realization from the Ar TP to the Ag FP are maintained [100,45]. The second facility, the "Low Temperature Realization Facility" (LTRF), is built around a recirculating ^{3}He cryostat containing a series of six similar fixed-point cells, each dedicated for use with a different gas. These are all machined into one OFHC copper block along with the NIST ICVGT [103]. This system of cells and ICVGT are each connected to one of seven room temperature gas manifolds and described in detail elsewhere [117]. This facility contains all the necessary pressure measurement equipment for the ITS-90 realization in the cryogenic sub-ranges from 0.65 K to 24.5561 K.

A third facility, the "Low Temperature Calibration Facility"(LTCF), houses a similar ^{3}He cryostat dedicated to comparison calibrations of capsule SPRTs, RIRTs, and other cryogenic RTs over the range 0.65 K to approximately 165 K [102]. This cryostat is also used for the realization of triple points with sealed-cells in the range 13.8 K to 161.4 K. A set of NIST check SPRTs and RIRTs are maintained in the LTCF for the purposes of ITS-90 maintenance and dissemination below 83.8 K. The procedures and equipment utilized in the LTCF are the focus of chapter 5.

All three of these laboratory facilities use similar resistance ratio bridges and calibrated resistance standards. The calibrations of the resistance standards are periodically checked against those maintained in the SPRT Calibration Laboratory (CL), or re-calibrated in units of Ω_{90} as maintained via the quantum Hall effect elsewhere at NIST [62].

4.1 Realizations from 0.65 K to 24.556 K

NIST has performed realizations of the ITS-90 from 0.65 K to 273.16 K on in-house SPRTs and RIRTs for the purposes of scale maintenance and dissemination [118]. We refer to these SPRTs and RIRTs as NIST 'check' capsule SPRTs and 'check' RIRTs and their calibrations are all nominally equivalent to within the realization uncertainty. (see section 5.1) This *as-defined* version of the ITS-90 has been disseminated from NIST since 1996 [101]. Prior to 1996, an approximate version of the ITS-90 was disseminated [128].

The ^{3}He and ^{4}He vapor pressure realizations [105] cover the range 0.65 K to 5.0 K and are carried on the NIST check RIRTs described below. The as-disseminated ITS-90 is based on the ^{3}He VP definition for temperatures $T < 2.0$ K and the ^{4}He VP definition for $T \geq 2.0$ K.

NIST has performed a realization of the ICVGT over the range 5.0 K to 24.5561 K [103]. The NIST check RIRTs have been calibrated over this range with temperatures derived from the ICVGT realization. The ICVGT definition is likewise carried on the same set of five RIRTs and covers the range 5.0 K to 24.5561 K. NIST has disseminated the ICVGT definition from 5 K to

13.8 K since 1996, but only since 2004 has the ICVGT definition been disseminated in the range 13.8 K to 24.5561 K.

Above 24.5561 K, NIST disseminates the ITS-90 via the SPRT sub-range 1 definitions when providing comparison calibrations in the LTCF. Other NIST calibration facilities will disseminate comparison temperatures via an SPRT subrange 4 definition for $T \geq 83.8$ K or via direct realization of the fixed points when calibrating SPRTs [45]. The estimation of scale non-uniqueness due to overlapping definitions of the ITS-90 is described in chapter 6.

The region of overlap between the SPRT-1 subrange and the ICVGT range is 13.8 K to 24.5561 K. There is a significant disagreement (i.e. non-uniqueness) in these two original NIST realizations of the ITS-90 in the immediate region of the *e*-H_2 VP_1 (i.e. near 17 K) [119]. The realizations of these two subranges differ by $T_{90\text{-SPRT-1}} - T_{90\text{-IGT}} \cong 0.63 \pm 0.38$ mK. Similar direct comparisons of the SPRT-1 and ICVGT ranges near the *e*-H_2 VP_2 , at 20.27 K, however, show good agreement, or $\left| T_{90\text{-SPRT-1}} - T_{90\text{-IGT}} \right| < 0.1$ mK, well within the combined realization uncertainties. This discrepancy is treated as a source on non-uniqueness in section 6.

Adjustments to the NIST-disseminated ICVGT scale and e-H_2 fixed points became necessary in 2006 and will be fully described elsewhere [132]. These adjustments were a consequence of CCT clarifications [133] on the isotopic specification for realizations of the e-H_2 TP and e-H_2 VP points. For NIST fixed points, the magnitude of the adjustment is 0.33 mK at 13.8 K and smaller over the rest of the ICVGT range. Other related adjustments of slightly smaller magnitude have been applied to the e-H_2 VP points at 17.0 K and 20.27 K for use in the SPRT sub-range 1 definition. This adjustment has the effect of slightly increasing the aforementioned non-uniqueness at 17 K between the SPRT subrange 1 definition and ICVGT definitions to $T_{90\text{-SPRT-1}} - T_{90\text{-IGT}} \cong 0.8 \pm 0.37$ mK. These adjustments are comparable to or less than the NIST-disseminated ITS-90 uncertainties (see chapter 6) for these temperatures, and they are therefore unlikely to be of any significant consequence to the customer.

4.2 Fixed Points

The fixed point cells used at NIST for the calibration of capsule SPRTs are described in a variety of other publications as referenced in Table 4.1. Of these, only the WTP, HgTP, and ArTP are directly involved in the calibration of customer SPRTs. These fixed point cells are either a.) immersion-cell (IC) types, as used for long-stem or as adapted for capsule SPRTs [45], or b.) miniature-calorimetric types which are exclusively used for NIST check capsule SPRTs or RIRTs and not used directly for calibrations of customer SPRTs. The miniature cells are also known as Sealed Triple Point Cells (STPCs) when permanently sealed and Open Triple Point Cells (OTPCs) and Vapor Pressure Point Cells (VPPCs) when connected to an external manifold [111]. A STPC and WTP are shown in Figure 4.1 and 4.2 respectively.

Figure 4.1 A Sealed Triple Point Cell shown suspended in a frame for calorimetric triple point realizations.

Table 4.1 Summary of fixed-point cells currently used at NIST for calibration of as NIST check capsule SPRTs.

Fixed Point	T_{90} / K	types	NIST facilities	References
e-H_2 TP	13.08033	OTPC	LTRF	[114]
		STPC	LTCF	[116], [120]
e-H_2 VP1	17.036	VPPC	LTRF	[119]
e-H_2 VP2	20.2714	VPPC	LTRF	[119]
Ne TP	24.5561	OTPC	LTRF	[114]
		STPC	LTCF	[116]
O_2 TP	54.3584	OTPC	LTRF	[114]
		STPC	LTCF	[115]
Ar TP	83.8058	IC	SPRT CL	[113]
		OTPC	LTRF	[114]
		STPC	LTCF	[110]
Hg TP	234.3156	IC	SPRT CL	[107,108,109]
TPW	273.16	IC	SPRT CL	[130,131]
		IC	LTCF	[130]

4.2.1 Fixed Points 83.8 K to 273.16 K

The use of capsule SPRTs in the immersion-type fixed-point cells at NIST requires an adapter probe for the capsule. For capsule SPRTs, NIST has constructed three varieties of capsule adapter probes. One such probe uses a borosilicate tube of 9 mm inner diameter (ID) and 11 mm outer diameter (OD) as shown in Figure 4.3. Another probe adaptor is made from stainless steel tubing of 11.1 mm OD and 10.6 mm ID [32]. Both of these adapter probe designs require the use of a close-fitting aluminum bushing (see Figure 4.4) to adapt the SPRT sheath diameter to that of the fixed-point cell inner immersion well. A third design uses a borosilicate tube of 5.8 mm inner diameter (ID) and 7.5 mm outer diameter (OD). This third type is only suitable for those capsules with a uniform diameter of 5.7 mm or less [37]. These probes are used to calibrate the SPRTs at the Ar TP, Hg TP, WTP, and GaTP ICs. When in use, the probes are pressurized with He gas to a level slightly above the ambient atmospheric pressure. The immersion characteristics of these capsule probe adaptors have been determined to be adequate when used with NIST immersion-type fixed point cells. When adapted in this way for use in immersion fixed point cells, however, the reproducibility of capsule SPRTs is still inferior to that of most long-stem SPRTs when used in the same way. (see chapter 6)

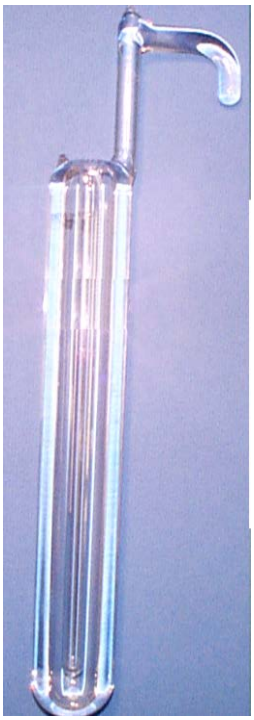

Figure 4.2 A Type B WTP cell.

The standard calibration process control employed within the SPRT CL at NIST for any SPRT calibration using immersion-type fixed-point cells involves the use of NIST long-stem SPRTs (i.e. “check thermometers”) with every fixed point. For the fixed-point cells discussed here, these check

thermometers are long-stem SPRTs, each of which is dedicated for use with a particular fixed point. A complete description is found in reference [45].

Starting in 2006, all customer PTC thermometers which go through the NIST LTCF are checked at the WTP using one of the adaptor probes described above. Some customer NTC thermometers may also be checked using the WTP when appropriate. These WTP cells are maintained in a stirred-water-alcohol bath maintained within the LTCF. The cells are prepared using well established methods [32] which are standard practice at NIST [106]. The NIST check capsule SPRTs and check RIRTs are also checked using LTCF WTP cells on a regular basis. Prior to 2006, the WTP calibrations for capsule check SPRTs were performed in the SPRT CL.[45]

The LTCF WTP cells are commercially manufactured [130] types using distilled water of certified isotopic composition close to the CCT specified VSMOW definition [133]. These cells have been compared with those used in the SPRT CL and are generally equivalent to those to within ± 0.1 mK. A photograph of a glass capsule adapter probe installed in a WTP cell maintenance system is shown in Figure 4.5.

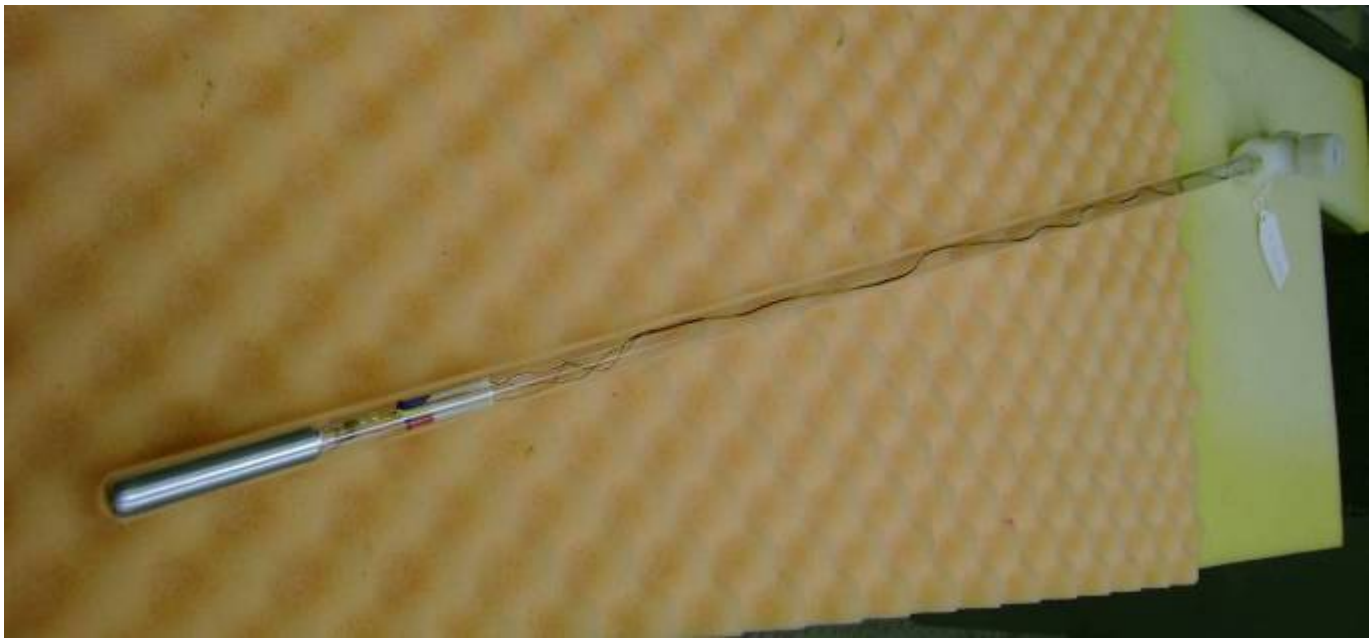

Figure 4.3 A glass adapter probe for use with capsule-type thermometers in immersion-type fixed point cells.

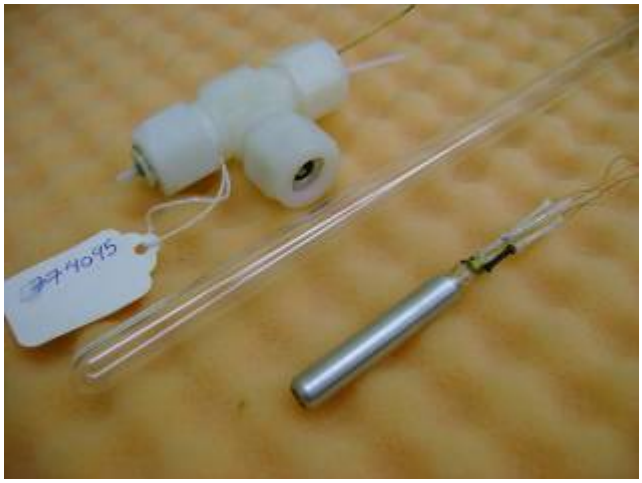

Figure 4.4 The adapter probe assembly showing a capsule SPRT installed in an aluminum bushing.

Figure 4.5. The WTP cell maintenance bath with a glass adapter probe installed in a WTP cell.

4.2.2 Fixed Points 13.8 K to 83.8 K

Prior to 1997, NIST realizations of the ITS-90 cryogenic fixed points (e-H_2 TP, e-H_2 VP1, e-H_2 VP2, Ne TP, O_2 TP, Ar TP) were performed by Meyer and Reilly using the LTRF [114] and NIST check SPRTs and RIRTs. Later realizations were performed using STPCs [116,117,118]. NIST check thermometers were also involved in these later realizations for purposes of maintaining the NIST ITS-90 below 83.8 K. These fixed point cells are not used for customer thermometer calibrations, as all such calibrations are accomplished via comparison methods as described in chapter 5.

STPCs have been maintained in the LTCF since 1996 for purposes of checking the stability of NIST capsule-type check thermometers and providing the basis for adjustments to the as-maintained scales as necessary. These cells are identified in references 22 and 118 and the relative agreement between the realization temperatures of these cells and those used in the LTRF have been summarized [118]. Four of the cells identified in reference 22 have been used in an international comparison of STPCs [136] with 12 other NMIs. All LTRF and LTCF fixed-point realizations have been performed with liquidus-point definitions such that melting plateau temperatures are extrapolated to a melted fraction of F=1.

The most important of the fixed-points available within the LTCF is the e-H_2 TP, T_{H2TP}=13.8033 K, because it is useful for determining the stability of both SPRTs and RIRTs. Three NIST e-H_2 STPCs have been used since 2000 in conjunction with several check RIRTs and SPRTs, with all such realizations using check RIRT B174. The results from some of those realizations are summarized in reference 118 and further details are included in reference 25. The isotopic compositions of the NIST cells are known and, as of 2006, corrections are applied [132] according to a CCT specification [133]. All NIST check RIRTs and check SPRTs have calibrations traceable to e-H_2 TP realizations performed either within the LTRF or LTCF and all such realizations are equivalent to within ±0.02 mK, once the necessary corrections are made.

The Ne TP has been realized using STPCs within the LTCF since 1996 [116]. Results of comparisons of earlier LTRF realizations [19] with those of the LTCF indicate agreement within ±0.25 mK, with observed differences attributable to chemical impurities and/or isotopic variations from different gas sources [22,23]. NIST check SPRT calibrations are traceable to either LTRF or selected STPC NeTP cells and those realization temperatures are equivalent to within 0.15 mK. The ICVGT range carried on the check RIRTs is traceable to the LTRF Ne TP realizations only. Traceability to archival realizations [122] of the NeTP at NIST/NBS is not as well established (e.g. ~1 mK uncertainty).

The O_2 TP has been realized at NIST/NBS since 1986 [115] via STPCs and also in OTPCs within the LTRF in the 1994-1996 time frame [114]. All cells used in those realizations employed the same gas which was synthesized from thermal decomposition of $KMnO_4$. Contemporary realizations of the O_2TP in the LTCF using the same STPCs agree with those performed using OTPCs in the LTRF to within ±0.03 mK which is comparable to the statistical limit of the SPRT resistance measurements. All NIST check SPRT O_2 TP calibrations are traceable to these realizations.

The Ar TP has been realized at NIST since 1978 for capsule SPRTs [110] and since 1971 for long-stem SPRTs [113]. Realizations of the Ar TP were also performed in the LTRF in 1995-1996 [114]. All NIST check capsule SPRTs have calibrations at the ArTP traceable to contemporary realizations [118] in the LTCF using the same STPCs as described in reference [110].

5 Calibration Procedures

Comparison calibrations of customer thermometers at temperatures of 165 K and below are performed in the NIST LTCF. All customer thermometer services for temperatures $T<77.35$ K are handled exclusively in this facility. Other services requiring temperatures 165 K$\geq T\geq$77.35 K may also be handled in this facility or in combination with other NIST calibration facilities, as necessary.

5.1 NIST Check Thermometers

NIST maintains a group of seven check capsule SPRTs, and five check RIRTs for maintenance of the ITS-90 below 83.8 K. The use of check thermometers within the LTCF is different from the practice within the SPRT CL. In the LTCF, the check SPRTs and RIRTs are not dedicated to any particular fixed point, but are all nominally equivalent for a given ITS-90 range definition. Some of these seven check capsule SPRTs have a complete history of all fixed-point realizations at NIST between the e-H_2 TP and the Ga TP, while others have histories with a sub-set of fixed point realizations. However, all of these capsule SPRTs are compared against one another on a regular basis. In addition, three of the seven were part of the original Compton and Ward international comparison [121] and two others were part of the more recent CCT K-2 comparison [134]. The check RIRTs are likewise intercompared with each other and with the check SPRTs on a regular basis. All of these RIRTs were originally calibrated against the NIST ICVGT, ^{4}HeVP realization, and ^{3}HeVP realization during the time period 1994 to 1996. Two of these RIRTs were part of the recent CCT K-1 comparison [135].

For purposes of comparison calibrations, a working reference thermometer is chosen from the group of check SPRTs and RIRTs maintained at NIST (see listing in Table 5.1). From the 1997 through the 2000 comparison runs, SPRT serial no. 1004131 was designated as the working reference for $T\geq$13.8 K because it had been calibrated at NIST according to the ITS-90 in the lowest sub-range using the most recent realizations of all the required fixed points. These fixed-point realizations were performed between December 1994 and May 1996 in the LTRF according to the techniques described by Meyer and Reilly [114,119]. The check thermometers for $T\geq$13.8 K have been taken from different combinations of two or more of the six other capsule SPRTs as shown in Table 5.1. These check thermometers provided some independent fixed-point realization data to gauge the uncertainty of the comparison calibration process. Since 2001, SPRTs 1842385 and 1812284 have served as reference SPRTs and SPRT 1004131 is no longer in use. It's role as a NIST check SPRT has been replaced by SPRT 1842382.

The five NIST check RIRTs have been calibrated at NIST between 0.65 K and 24.5561 K. Three of these, B-168, B-174, and B-211, were compared in the LTRF to SPRTs 1004131 and 1842385 in May of 1996 ("96X" in Table 5.1) to transfer the three e-H_2 fixed point temperatures. In addition, SPRTs 1812282 and 1812284 have similar LTRF comparisons with RIRT B-211 ("96Y" on Table 5.1). For $T\leq$13.8 K, RIRT B-174 has served as the comparison reference thermometer within the LTCF since 1998 and RIRT B-168 has served as the primary check thermometer. Normally, some of these RIRTs are also included to serve as check thermometers during SPRT comparisons at $T\geq$13.8 K in the LTCF. Comparisons between the check SPRTs and

RIRTs B-174 and B-168 have been performed also in the LTCF on a regular (approximately annual) basis since 1998.

The lower section of Figure 5.1 shows the range of use for the NIST check RIRTs and SPRTs, both within the LTCF for $T \leq 165$ K and other NIST facilities for $T \geq 165$ K. The upper section of Figure 5.1 illustrates the regular calibration ranges available for customer RIRTs, GeRTs, PCRTs, and SPRTs. The range for special tests of PTC or NTC cryogenic thermometers within the LTCF is also shown along with the ranges available for calibrations in other NIST facilities.

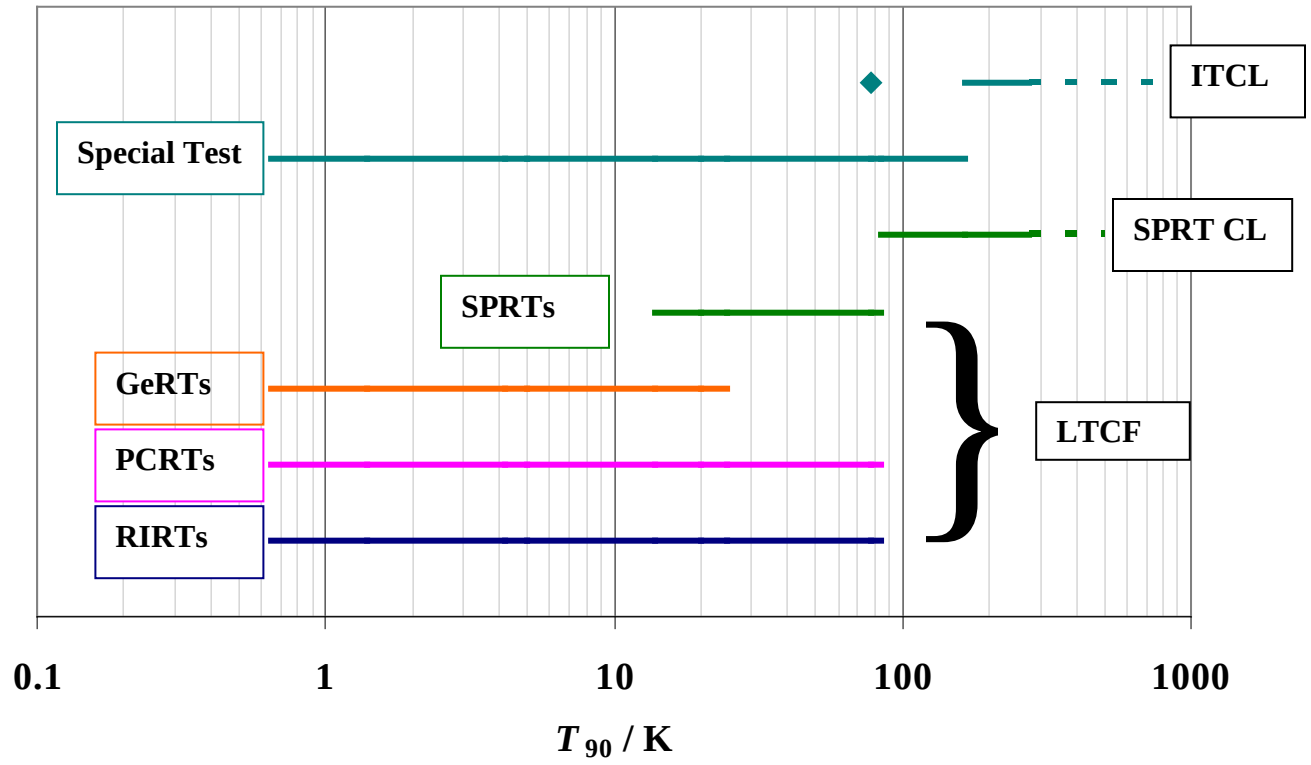

Figure 5.1 Temperature ranges for NIST check thermometers and customer calibrations. Lower plot: Ranges of the NIST check RIRTs and check SPRTs as used in the LTCF, and check SPRTs as used in the Industrial Thermometer Calibration Laboratory (ITCL) . Upper plot: Ranges for calibrations of customer thermometers: RIRTs; PCRTs; GeRTs; capsule SPRTs in the LTCF; capsule SPRTs in the SPRT CL; special tests of cryogenic resistance thermometers in the LTCF; and range for the ITCL.

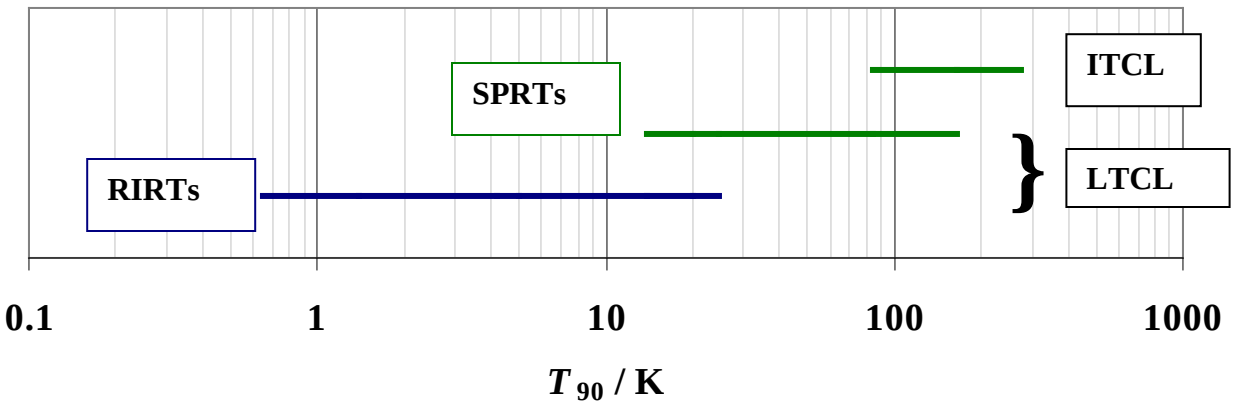

Table 5.1 Summary of calibration history of NIST capsule check thermometers 1996-2007.

Thermometer	Direct Fixed-point Calibrations	NIST Comparisons	Int'l Comparisons
SPRT 1004131†	e-H_2 TP, e-H_2 VP_1, e-H_2 VP_2, Ne TP, O_2 TP, Ar TP, Hg TP, H_2O TP, Ga TP	96X, 97A, 98E, 99A, 00A, 01B, 02A	
SPRT 1842382	O_2 TP, Ar TP, Hg TP, H_2O TP, Ga TP	03A, 05A, 07D	
SPRT 1842385	e-H_2 TP, e-H_2 VP_1, e-H_2 VP_2, Ne TP, O_2 TP, Ar TP, Hg TP, H_2O TP, Ga TP	96X, 97A, 98E, 01B, 02A, 03A, 04B, 05A, 06A, 07D	
SPRT 1812279	O_2 TP, Ar TP, Hg TP, H_2O TP, Ga TP	97A, 98E, 00A, 04B, 05A	Compton & Ward [121]
SPRT 1812282	e-H_2 TP, e-H_2 VP_1, e-H_2 VP_2, Ne TP, O_2 TP, Ar TP, Hg TP, H_2O TP, Ga TP	96Y, 97A, 99A, 00A, 01B, 06A	Compton & Ward [121]
SPRT 1812284	e-H_2 TP, e-H_2 VP_1, e-H_2 VP_2, Ne TP, O_2 TP, Ar TP, Hg TP, H_2O TP, Ga TP	96Y, 97A, 00A, 99A, 01B, 03A, 06A	Compton & Ward [121]
SPRT 1774092	e-H_2 TP, Ne TP, O_2 TP, Ar TP, Hg TP, H_2O TP, Ga TP	97A, 01B, 04B, 05A	CCT K-2 [134]
SPRT 1774095	e-H_2 TP, Ne TP, O_2 TP, Ar TP, Hg TP, H_2O TP, Ga TP	97A, 01B, 03A, 05A, 07D	CCT K-2 [134]
RIRT B174	^{3}He VP, ^{4}He VP, e-H_2 TP, Ne TP	96X, 98E, 99A, 99B, 00A, 01B, 02A, 04B, 05A, 06A, 07D	
RIRT B168	^{3}He VP, ^{4}He VP, e-H_2 TP, Ne TP	96X, 98E, 99A, 00A, 01B, 04B, 05A, 06A, 07D	
RIRT B211	^{3}He VP, ^{4}He VP, e-H_2 TP, Ne TP	96Y, 04B, 05A	
RIRT A128	^{3}He VP, ^{4}He VP, e-H_2 TP, Ne TP	99B, 00A, 01B, 07D	CCT KC-1 [135]
RIRT A129	^{3}He VP, ^{4}He VP, e-H_2 TP, Ne TP	99B, 00A, 04B, 05A, 06A, 07D	CCT KC-1 [135]

† Decommissioned in 2001 and replaced with 1842382.

5.2 Comparison Calibration Process

Comparisons are performed in batches of up to 20 capsule thermometers, including both NIST check SPRTs and check RIRTs. Each batch calibration run is assigned a three character run ID by concatenating the last two digits of the calendar year with a sequential letter (e.g. 99A, 01B, 07D, etc.) Each batch thermometer has a unique installation code, referred to as the "NIST-ID". For calibrations performed in the NIST LTCF, the NIST-ID is generated by combining the run ID with a unique device-under-test (DUT) number, 1 to 24 (e.g. 07D-15, etc.). Each installation code is cross-indexed with a Logical Device number 1 to 40, which corresponds with the 4-wire

address of a scanner switch card for connecting the DUT to the appropriate AC or DC measurement system.

The thermometers of a calibration batch, along with the NIST reference thermometer and various check thermometers, are installed in a series of close-fitting thermowells in a copper comparison block [102]. Several comparison blocks of different sizes are available for use. All of those are machined from OFHC copper in a cylindrical geometry with various-sized vertical thermowells. A cryogenic-grade carbon-based grease [137] or a grease and copper-particle mixture is used to wet the thermometer's sheath surfaces to the interior thermowell surfaces. The comparison block is wired with 24 four-wire harnesses arranged in four sets of six each. Each wiring harness is thermally coupled to a tempering plate above the block via a set of eight copper tempering spools. A large comparison block currently in use is shown in Fig. 5.2.

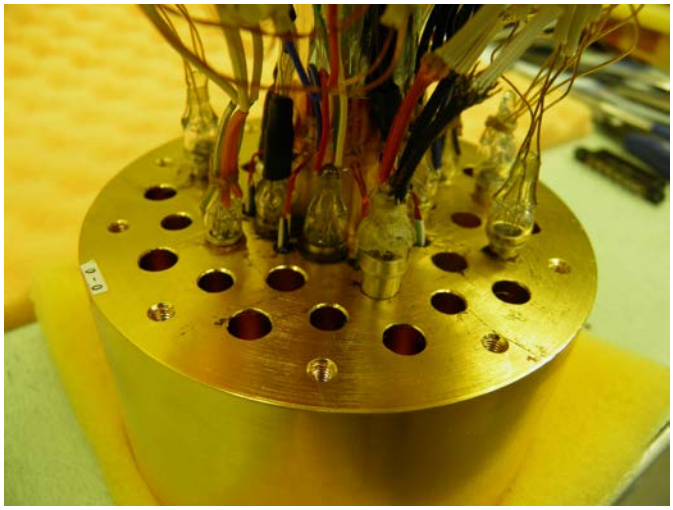

Figure 5.2 A large comparison block with capsule thermometers installed.

Figure 5.3 The ^{3}He cryostat with a large comparison block installed.

Each batch thermometer resistance R_{Bat} is measured at the two excitation currents i_1 and i_2 (see Table 5.3) in a symmetrical sequence, starting and ending with the working reference thermometer resistance R_{Ref}. The sequence is a series of nine measurement records: $R_{Ref}(i_1)$, $R_{Ref}(i_2)$, $R_{Ref}(i_1)$, $R_{Bat}(i_1)$, $R_{Bat}(i_2)$, $R_{Bat}(i_1)$, $R_{Ref}(i_1)$, $R_{Ref}(i_2)$, $R_{Ref}(i_1)$. Each measurement record in the sequence consists of an average of 20 to 36 individual bridge readings (in the case of AC measurements) and the standard deviation of the reading sequence. All reference thermometer measurements are made with two currents and resistance ratios corrected to zero-power dissipation. The average zero-power resistance of the reference thermometer's initial and final records is then used to compute the average block temperature for the particular batch thermometer being measured.

Multiple measurement sequences are incorporated into each comparison run at all calibration point temperatures. The particular set of comparison temperatures which are used in a calibration will depend on the type of thermometer being calibrated. Table 5.3 lists a typical set of calibration temperatures and currents appropriate for SPRTs, RIRTs, and GeRTs over the range

0.65 K to 83.8 K. For SPRTs, there are always one to three additional comparison points taken which are intermediate to the fixed-point temperatures. Even though these temperatures are not required for the calibration, the data are useful for the purpose of evaluating the interpolation uncertainties. Measurement currents vary from one thermometer type to another and change with temperature as is shown in Table 5.3. The values shown for GeRTs are approximate only, and in practice these would be chosen such that the excitation voltage remains in the range of 2 mV to 4 mV.

5.3 Cryostat refrigeration modes and control

The cryostat used at NIST for the comparison calibrations is a re-circulating ^{3}He refrigerator (see Figure 5.3) as described previously. [102] The ^{3}He is circulated through the cryostat for cooling to temperatures $\lesssim$ 4 K. The system can also be used at higher temperatures without circulating ^{3}He, by employing refrigeration via either simple pool boiling of liquid ^{4}He and N_2 or solid-N_2 sublimation. The system permits operation via the following five basic refrigeration modes as shown in Table 5.2

Table 5.2 Cryostat Refrigeration Modes as used in the NIST LTCF.

Mode #	Range	Cooling Method	Active Control Zones
1	0.5 K to 4 K	re-circulating ^{3}He, pumped ^{4}He, pool boiling ^{4}He	1
2	≈3 K to 12.0 K	pumped ^{4}He, pool boiling ^{4}He	1
3	10.0 K to 50 K	liquid ^{4}He pool boiling at ~100 kPa	2
4	50 K to 75 K	solid/slush N_2 sublimation	2
5	78 K to 165 K	liquid N_2 pool boiling	2

The comparison block is installed in the vacuum space below the lowest control stage of the cryostat as shown in Figure 5.4a. The block is controlled at an appropriate constant temperature under high vacuum conditions and surrounded by a series of isothermal shields. Heating power is applied to the two inner-most shields, which entirely surround the comparison block, but not directly to the block itself. Two-zone active heating control is utilized at $T \geq 13.8$ K (refrigeration modes 3, 4, and 5 above), with single zone heating control below that point. The benefits of control zones, however, are not just limited to heated zones. In practice, refrigeration mode 2 utilizes two effective control zones since the ^{4}He pot is pumped to an approximately constant pressure, which serves to stabilize the temperatures of that additional zone. Similar considerations apply in mode 1, where both the ^{3}He still and the ^{4}He pot serve as additional stabilized zones. Heating power varies from a minimum of about 0.25 mW at 0.65 K, 5.0 mW at 13.8 K, to as high as 200 mW at 54 K under liquid ^{4}He pool boiling conditions. The power applied at 54.358 K under solid N_2 sublimation conditions is less than 9 mW, and 80 mW or less at 83.8 K under liquid N_2 boiling conditions.

The primary control zone heater is located above the comparison block in order to minimize any inducted thermal gradients in the block. The degree of isothermal conditions in the comparison block has been verified by tests using various check SPRT comparisons at 54.358 K, under both mode 3 and mode 4 operation which differ by a factor of 20 in the applied power. The results of

such comparisons have not been significantly dependent on which of the two refrigeration modes are used, despite the large difference in heating power levels.

The control integration time constants are generally set as low as possible while still avoiding oscillation behavior. The time constant for the comparison block is determined by the thermal diffusivity $\alpha_{\text{d-Cu}}$ of the copper which is assumed to be in a work-hardened state such that X_{RR}~50.

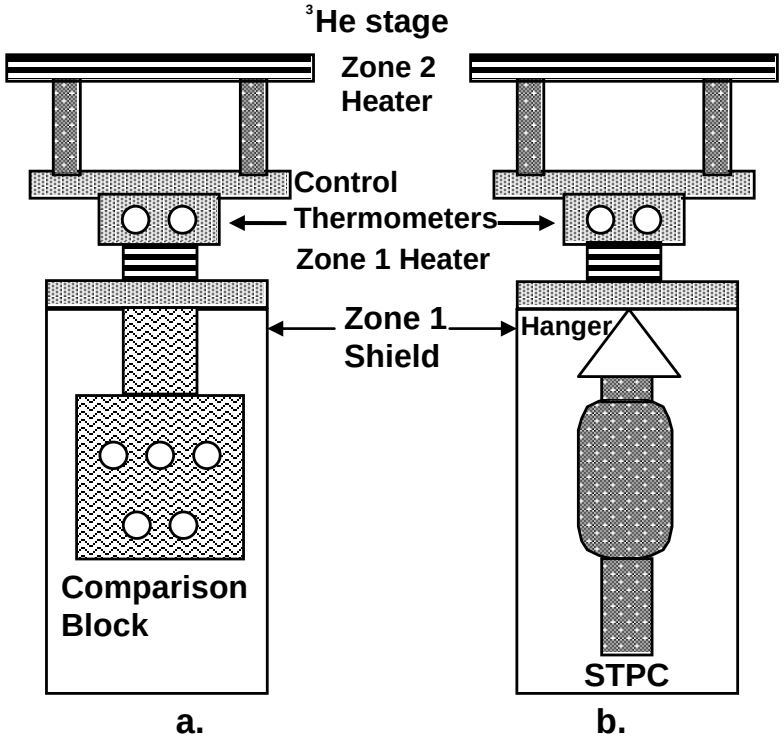

Figure 5.4. Control zones for ^{3}He cryostat shown in both operating modes: a.) with comparison block installed for comparison calibrations and. b.) with and STPC installed for adiabatic triple-point realizations.

The thermal diffusion time constant of the block is $\tau_{\text{blk}} \sim D^2/\alpha_{\text{d-Cu}}$ which is the dominant factor governing transient response for temperatures $\gtrsim$60 K. For temperatures $\lesssim$50 K, the thermal response times of the check thermometers themselves can exceed τ_{blk}. Figure 5.5 shows estimated values for τ_{blk} together with estimates for τ_{int} and τ_{ext} for a typical NIST check thermometer (see section 1.4.1).

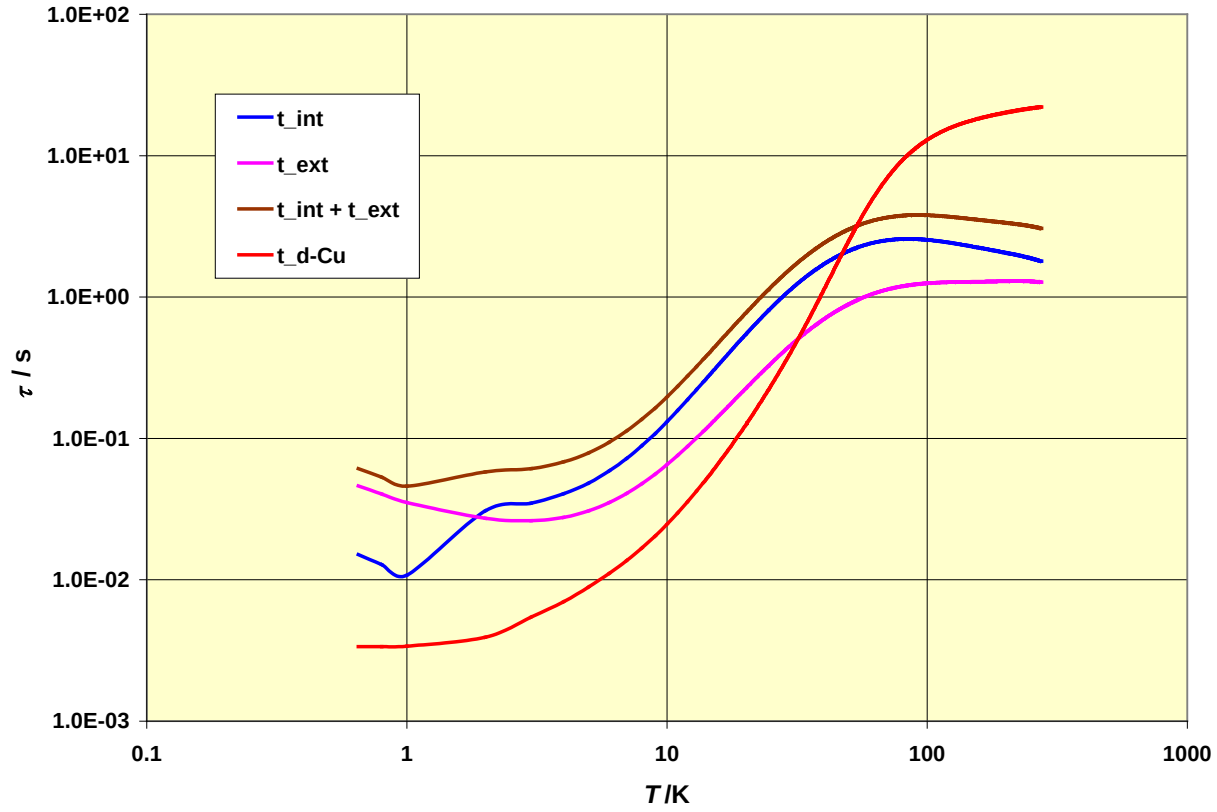

Figure 5.5 Estimated time constants for the LTCF comparison block, and estimated thermal response times associated with a typical NIST check thermometer (i.e. capsule RIRT or SPRT) from 0.65 K to 273 K. (Legend: t_int= τ_{int} ; t_ext= τ_{ext} ; t_d-Cu= $\tau_{blk,}$ or the thermal diffusion time constant for a copper block with $X_{RR} \approx 100$).

Table 5.3 The typical set of comparison temperatures, definitions, and measurement currents used for calibrations of cryogenic RTs. Empty cells indicate no data are necessary for that temperature.

			Currents I_1 and I_2 (in mA or otherwise as shown)			
T(K)	Definition	Reference Thermometer	25.5 Ω SPRTs	100 Ω MPRTs	RIRTs & PCRTs	250 Ω GeRTs (μA)
0.650	^{3}He VP	RIRT			0.141, 0.2	0.1 to 0.2
0.746						0.1 to 0.2
0.851					0.141, 0.2	0.285
1.000						0.4
1.180					0.141, 0.2	0.705
1.400						0.8
1.650					0.141, 0.2	1.414
1.900						2
2.200	^{4}He VP				0.141, 0.2	3
2.500						5
2.800					0.141, 0.2	10
3.100						10
3.414					0.141, 0.2	10
3.800						10
4.221					0.141, 0.2	14
4.600						14
5.100	ICVGT or SPRT-1				0.2, 0.282	20
6.100					0.2, 0.282	20
7.200					0.2, 0.282	30
8.300					0.2, 0.282	30
9.400					0.2, 0.282	50
10.600					0.2, 0.282	50
11.800					0.2, 0.282	70
12.800					0.2, 0.282	100
13.803		RIRT or SPRT	5.0, 7.07	2.83, 5.0	0.282, 0.5	100
15.400			5.0, 7.07	2.83, 5.0	0.282, 0.5	141
17.035			5.0, 7.07	2.83, 5.0	0.282, 0.5	141
18.650			5.0, 7.07	2.83, 5.0	0.282, 0.5	200
20.271			5.0, 7.07	2.83, 5.0	0.282, 0.5	283
21.500					0.282, 0.5	283
22.600			5.0, 7.07	2.83, 5.0	0.282, 0.5	283
23.600					0.282, 0.5	500
24.556			2.823, 5.0	2.0, 2.83	0.282, 0.5	500
26.00	SPRT-1	SPRT			0.282, 0.5	
27.10					0.282, 0.5	
30.0			2.823, 5.0	2.0, 2.83	0.282, 0.5	
35.0					0.282, 0.5	
40.0			2.823, 5.0	2.0, 2.83	0.282, 0.5	
50.0					0.282, 0.5	
54.358			2.0, 2.83	1.0, 1.414	0.282, 0.5	
60.0			2.0, 2.83	1.0, 1.414	0.282, 0.5	
65.0					0.282, 0.5	
71.0			2.0, 2.83	1.0, 1.414	0.282, 0.5	
78.0			2.0, 2.83	1.0, 1.414	0.282, 0.5	
83.806			1.0, 2.0	0.5,0.707	0.282, 0.5	

5.4 Instrumentation

The LTCF normally employs two resistance measurement systems. One is an AC resistance ratio bridge based on a decade-type IVD with 9 ½ digits resolution which covers a ratio range from 0 to 1.29 [138]. The other system is a precision DC voltage divider based on a bi-polar current source and precision ADC. The measurement of PTC device resistances are performed on the AC system for all resistances $R(T)<250\ \Omega$ and $I>0.1$ mA. Otherwise the DC system is used. In the case of NTC devices, the DC system is normally used unless some special requirement exists and the above criteria for AC measurements are met.

The AC system uses a set of stable reference resistors (1 Ω, 10 Ω, 100 Ω, and 200 Ω) with AC/DC difference specifications of $<10^{-7}$ [139]. The reference resistors are maintained in an oil bath controlled at 25 °C. These resistors are periodically calibrated at NIST and their calibration history is sufficient to establish bounds on their drift rates, to the extent that any such drifts are in fact measurable. This type of resistance bridge has a linearity specification of 1×10^{-7} of the measured ratio, but measurement statistics and or parasitic loading effects may sometimes exceed this level (see chapter 6). Bridge linearity is verified via resistance network ratio calibrators using combinatoric techniques [140,141]. The resistance bridge sources alternating currents of frequency f=30 Hz in the range 0.1 mA to 10 mA rms through both the reference resistor R_S and the DUT (thermometer) resistance R_x and balances the two via the IVD to the nearest integral transformer ratio n (see Fig. 5.6). The residual detector voltage is then integrated over a 0.1 Hz bandwidth and digitized to provide an additional 2.5 digits of interpolation to derive the resistance ratio reading X. Data are acquired as X values which are averaged and the DUT resistance is then calculated via $R_x=XR_S$.

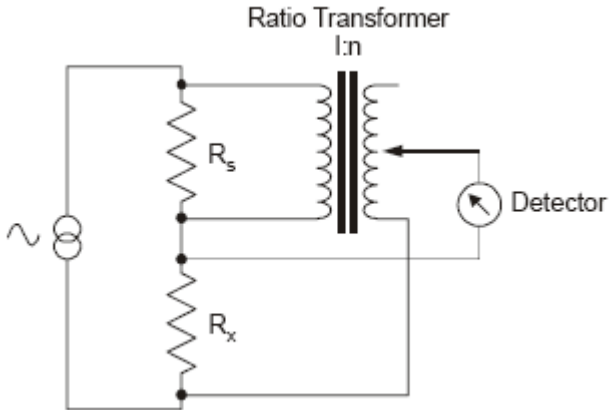

Figure 5.6 The basic principle of the AC resistance ratio bridge based on an IVD.

Measurements of SPRTs and MPRTs from 13.8 K to 165 K require that three AC reference resistors are used (1 Ω, 10 Ω, 100 Ω), depending on the temperature range. Table 5.4 shows the normal temperature ranges of use for each standard resistance. RIRTs and PCRTs are measured using the 100 Ω reference only. A 200 Ω reference resistor is available for special test purposes for RTs having $130\ \Omega<R<250\ \Omega$.

Table 5.4 Temperature ranges and reference resistor values for AC resistance measurements of MPRTs and SPRTs.

Range	100 Ω MPRT	25.5 Ω SPRT
13.8 K – 24.56 K	1 Ω	1 Ω
24.56 K – 54.35 K	10 Ω	10 Ω
54.35 K – 125 K	100 Ω	10 Ω
125 K – 165 K	100 Ω	100 Ω

The DC system uses one of several stable reference resistors R_s (normally1 kΩ, 10 kΩ, and 100 kΩ) in series with the DUT and a bipolar DC current source. The potential leads are switched between the reference and DUT to the input of a 22-bit ADC. The ADC is part of an auto-calibrating 8.5 digit DMM [142] which is used in the DC voltage mode. These DMMs are known to exhibit non-linearity in voltage of $<1\times10^{-7}$ [143]. Referring to figure 5.7, the excitation current is sourced directly through the reference resistor R_S and the DUT (thermometer) resistance R_x and two voltages are measured on the DMM, V_{R+} and V_{S+}, which are the potential differences across the unknown and the reference, respectively. Then the current is reversed and the reverse voltages V_{R-} and V_{S-} are acquired and the unknown resistance R_x is computed via

$$R_x = \frac{V_{R+} - V_{R-}}{V_{S+} - V_{S-}} R_S \,. \qquad 5.1$$

In this case the resistance ratio is a ratio of potential differences and most systematic measurement errors will be canceled. The system can achieve linearity for a fixed range which is limited only by that of the ADC. In practice the resistance measurement uncertainty can be limited by a combination of type A statistics, common mode errors, range (i.e. gain) errors, and the reference resistor calibration uncertainty (see chapter 6).

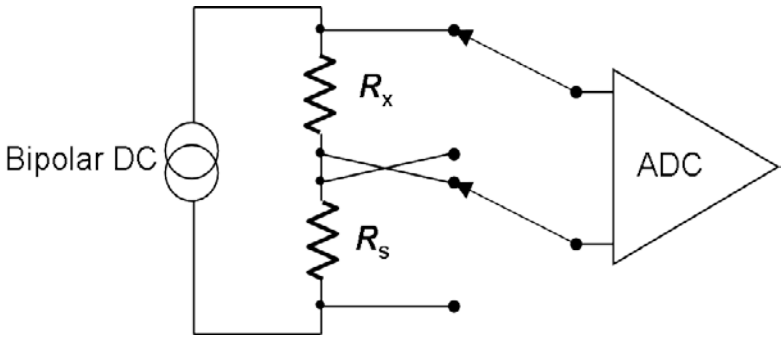

Figure 5.7 Simplified diagram for the DC resistance measurement system.

The selection of the DC reference resistors depends on the type of NTC thermometer under test and the temperature, which in turn determine the appropriate excitation current. The reference resistor is chosen such that the reference voltages $V_S = iR_s$ are comparable to or somewhat larger than V_R, while ideally remaining less than 200 mV. The DC reference resistors have calibrations which are traceable to the NIST as-maintained Ohm [62]. Stable 100 Ω AC-DC resistors are used to verify the accuracy of the DC measurement system by comparison to the AC system and 10 kΩ transfer standards allow verification and traceability to the NIST Quantum-Hall-Resistance standard.

5.5 Interpolation

The interpolation of capsule SPRTs is defined by the ITS-90 over all subranges. As described in chapter 3, these are unique solutions to the deviation equations for each sub-range according to the fixed-point calibration values for the resistance ratios $W(T)$. The full cryogenic range from 13.8 K to 273.16 K (i.e. SPRT subrange 1) requires eight calibrations points as given in table 3.1. The uncertainties associated with these interpolations are covered in chapter 6.

All other cryogenic RTs may be used to interpolate temperature according to whatever equation is found to be both convenient and sufficiently accurate. The interpolation equation is normally expressed as resistance as a function of temperature, $R=f(T)$, with typically seven to twelve parameters. The parameters or coefficients are determined via a standard Least-squares (LS) statistical minimization process. Ideally, such LS-fits possess ~10 or more degrees of freedom. For GeRTs and most other NTC devices, log(R) and log(T) are the preferred variables for curve fitting.

Simple N^{th}-order polynomial functions such as,

$$f(T) = \sum_{j=0}^{N} a_j T^j \qquad 5.2a$$

are suitable for most interpolation purposes when both the temperature range and resistance range are limited to approximately one decade. A common approach for treating larger range calibrations is to break the calibration range into two or more sub-ranges, each sub-range having a separate solution to Eqn. 5.2 with different coefficients. The break points may be chosen with some degree of overlap between the sub-ranges or by including spline-type fitting constraints for continuity in df/dT. Once the thermometer is calibrated and in use by the customer, temperatures are normally derived from resistance data by numerical iteration of the temperature via the fitting functions. Analogous considerations apply equally well to the approximately exponential characteristics found in the NTC thermometers, in which case,

$$\log(R) = f(T) = \sum_{j=0}^{N} a_j \log^j(T) \qquad 5.2b$$

Alternatively, an inverse function $g(R)=T$ may be used to express temperature directly as a function of resistance. In the case of special tests, customers may ask for the calibration data to be fitted to a specific functional form. In the case of inverse functions, a Cragoe parameter [144] $Z(T)=\{R(T)-R(T_1)\}/\{R(T_2)-R(T_1)\}$ where $T_1 \leq T \leq T_2$, is sometimes useful to serve as the independent variable. In this case the values of $R(T_2)$ and $R(T_1)$ are treated as two normalization parameters and $Z(T)$ is treated as an independent variable for interpolation of temperature via a function $h(Z)=T$.

The goal of the LS fitting process is to achieve fitting residuals which are comparable to the calibration uncertainties for each temperature. There is no realistic purpose to adding any more coefficients or other enhancements to the functional form once this limit has been achieved. The report of calibration will normally list the residuals of the LS-fitting function and give the interpolation coefficients in a separate table (see appendices).

5.5.1 Tables

Historically, calibration reports have included tables of calculated R and T values in regular intervals of 1 K or even 0.1 K when necessary. The original use of such tables was to allow simple numerical interpolation of temperature. Since the advent of desktop computing where double precision arithmetic is no longer at a premium, however, such uses have become rare. NIST still provides tables on all reports where there is sufficient data to support a fitting function. For cryogenic resistance thermometers, these tables will usually be in 1 K intervals, but

may not be suitable for numerical interpolation at the same level as the calibration uncertainties. The table's primary purpose is for the user to check his calculations using the specified fitting function.

5.6 Reporting Calibration Results

Examples of calibration reports are found in Appendix A1-A3. The first of these shows a Report of Calibration for an SPRT calibrated from the e-H_2 TP to the Sn FP. This report contains ITS-90 deviation function coefficients for 2 mA, 1 mA and 0 mA excitation currents, calibration uncertainties, the last measured R(WTP) values for 1 mA and 0 mA, and the stability of the SPRT during calibration.

The second example shows a Report of Calibration for an RIRT calibrated from 0.65 K to 83.8 K. The calibration is data are adjusted to an extrapolated zero-power resistance.

The third example shows a Report of Calibration for a GeRT calibrated from 0.65 K to 24.5 K. In this example, the calibration data are derived from piecewise constant current excitations and then adjusted for a constant excitation voltage of 2 mV for the entire calibration range.

Upon return of the thermometer to the customer, the first measurement should be either the R(WTP) for PTC thermometers or R(4.222 K) for most NTC thermometers. To compare a R(WTP) value with that given on the Report of Calibration, several factors should be kept in mind: a.) there may be differences between the NIST ohm and customer's in-house realization of the ohm; b.) mechanical strain can sometimes cause resistance shifts in the sensor due to mechanical shocks experienced during shipping; and c.) differences in the self-heating coefficient may exist between the customer's WTP installation and that used by NIST. Small differences in the WTP may also be possible from one cell to another, but these are normally less than 0.1 mK. NIST technical staff should be contacted for consultation if the difference between R(WTP) values exceed the equivalent of 10 mK (e.g. 0.001 Ω for a 25.5 Ω SPRT) when shipped, or 1 mK when hand carried.

Similarly, several factors can influence comparisons of an NTC thermometer's resistance as calibrated at 4.2 K with that as measured in a liquid helium bath: a.) small differences in the helium normal boiling point (NBP) temperatures due to atmospheric pressure variations from weather and altitude; b.) typical variations in resistance due to the thermometer's thermal cycling stability; and c.) differences in the self-heating coefficient $\eta(T)$ from a vacuum installation and that found in liquid helium. NIST normally calibrates thermometers at a comparison temperature of 4.222 K ± 0.001 K which corresponds to 101.3 kPa for the ^{4}He saturated vapor pressure. For NTC thermometers, any differences between the NIST ohm and customer's in-house ohm are usually of negligible influence on comparisons of R(4.2 K) when expressed in mK. For GeRTs which are known to be stable, the pressure-corrected R(4.222 K) value, as measured by the customer, should be within ± 2 mK of that given in the report of calibration. NIST technical staff should be contacted for consultation if this is not the case.

5.7 Recalibration Intervals and re-normalization

NIST has no recommended re-calibration intervals for resistance thermometers. The calibration status of any resistance thermometer depends on its design, construction, and the amount of thermal and mechanical stress that it incurs over time. Customers who wish to evaluate the calibration status of a resistance thermometer should maintain records of the calibration history and track the thermometer's reproducibility for at least one fixed-point resistance value.

In the case of capsule SPRTs, mechanical shocks can change the R(WTP) value and somewhat proportionally change all other $R(T)$ values. Therefore, it is important that the R(WTP) be determined at an interval that is appropriate for the SPRT's service. The most recent R(WTP) values should then be used to renormalize the $W(T)$ value when calculating temperature.

In the case of other types of cryogenic RTs, single point renormalization methods are usually not as successful and are not generally recommended. In some cases, however, a two-point renormalization process, as could be applied to calibrations in terms of a Cragoe parameter $Z(T)$ (e.g. T_1= 4.222 K and T_2=273.16 K), may be partially successful. The efficacy of these methods can only be accessed by the use of a third and intermediate reference point $T_1 \leq T_3 \leq T_2$ which is used to compare the interpolated T_3 with that supplied by an independent reference thermometer or fixed point.

5.8 Quality System Checks

NIST maintains a quality system based on the ISO/IEC 17025 [145] specifications. The documentation consists of quality manuals (QMs) and technical appendices arranged according to the administrative level: QM-I for all of NIST; QM-II for each organizational division and; QM-III for each calibration service. An outline of the NIST Quality System program is available at: http://nist.gov/qualitysystem/index.cfm. The NIST quality manual is available at: http://nist.gov/qualitysystem/upload/NIST-QM-I-V8-Controlled.pdf .

The QM-III for the LTCF documents general aspects of the calibration quality control process and lists locations for specific information and data maintained in a series of loose-bound paper-copy appendices and corresponding electronic files. The LTCF quality system is assessed on a 3-year schedule through internal quality audits conducted by the NIST Sensor Science Division. The overall management of the NIST Quality System programs is administered internally by the NIST Associate Director for Laboratory Programs.

The principal metric for the LTCF QM-III is the check thermometers' control charts. These are plots of the differences between the interpolated temperatures derived from the various NIST check thermometers in use during a comparison calibration run and those of the designated reference thermometer. An example of a control chart for SPRT comparisons is shown in Figure 5.8 and a chart for RIRT comparisons in Figure 5.9.

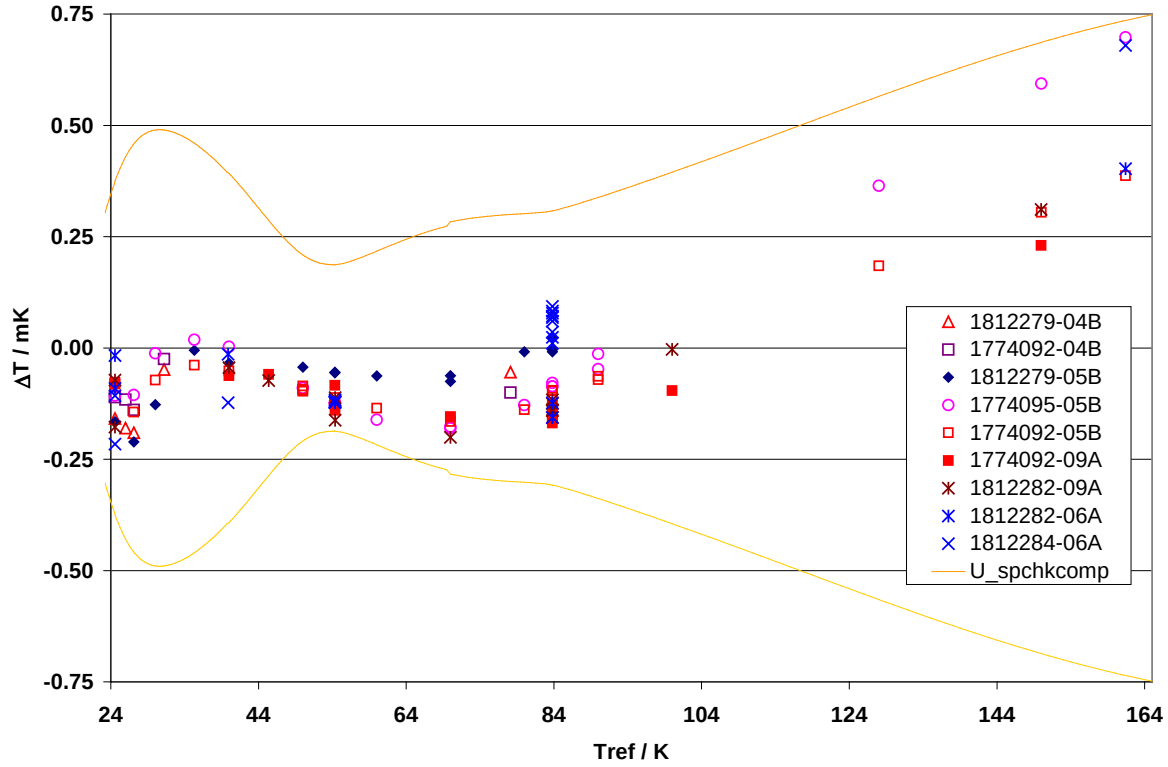

Figure 5.8. Comparison calibration control chart for NIST check SPRTs, 24.556 K to 165 K.

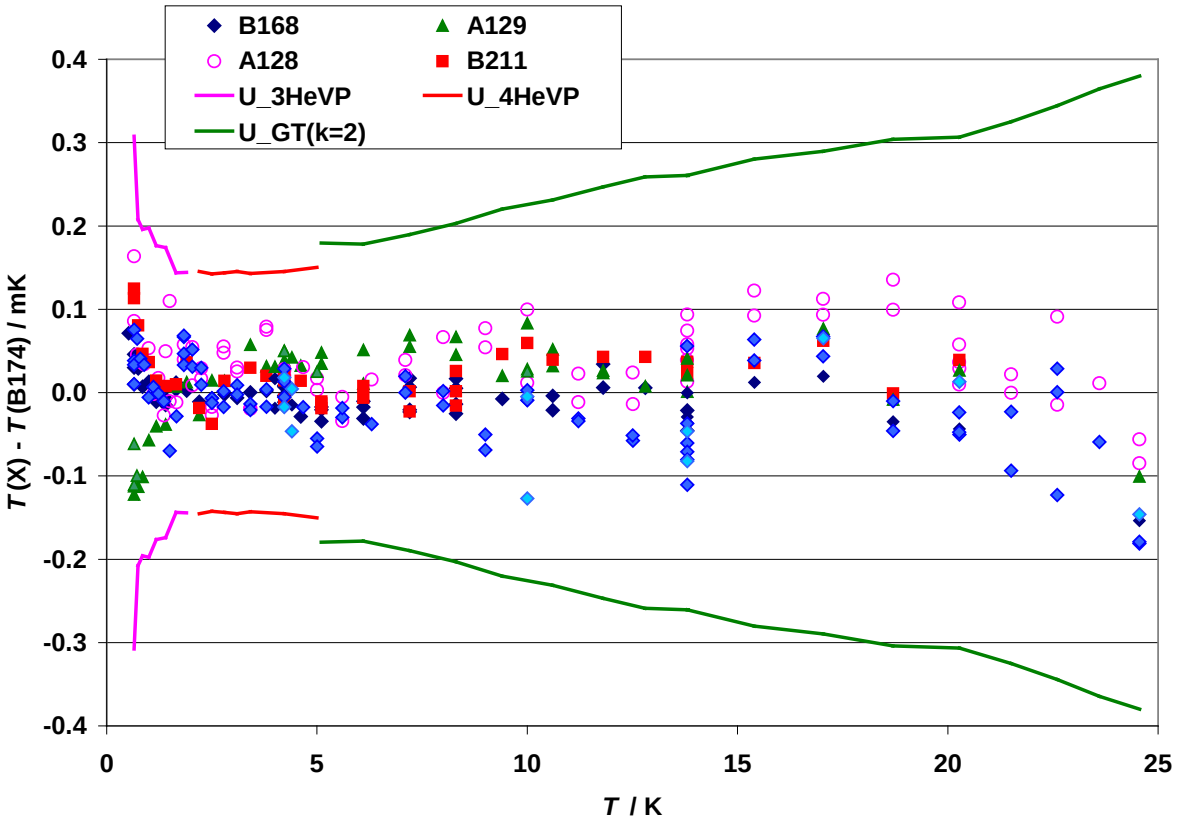

Figure 5.9. Comparison calibration control chart for NIST check RIRTs, 0.65 K to 24.56 K.

6 Calibration Uncertainties

This chapter concerns the ITS-90 calibration uncertainties of capsule SPRTs, RIRTs, and GeRTs at NIST. The specific examples treated here are for: 1.) capsule SPRTs calibrated on the ITS-90 over sub-range 1, 13.8033 K to 273.16 K; 2.) RIRTs calibrated on the ITS-90 over the range 0.65 K to 24.5561 K; and GeRTs calibrated on the ITS-90 over the range 0.65 K to 24.5561 K. The uncertainties are organized in three basic categories: 1.) Resistance Measurement; 2.) Temperature Scale Realization; and 3.) Comparison Process.

6.1 Capsule SPRTs: 13.8 K to 273.16 K.

This calibration involves data derived from the NIST realization of eight different fixed points. Three of these fixed points (H_2O TP, Hg TP, Ar TP) are realized directly with immersion-type fixed-point cells using the customer SPRT [100]. The other five fixed points (e-H_2 TP, e-H_2 VP_1, e-H_2 VP_2, Ne TP, and O_2 TP) were realized at an earlier time using fixed point cells with various other NIST check capsule SPRTs [101]. The lower four fixed-point temperatures are then transferred to the customer SPRT via comparison to the check SPRTs [102].

The example here is for a 25.5 Ω capsule SPRT as the customer ('batch') thermometer and NIST 25.5 Ω capsule check SPRT as the reference thermometer. Measurements of each SPRT's resistance at the respective fixed-point temperatures are made via an IVD-based AC resistance-ratio bridge. The ratio measurements are performed at a carrier frequency of 30 Hz, using either a 1 Ω, 10 Ω, or 100 Ω resistance standard, R_s, and the various excitation currents, i_1, i_2, as shown in Table 6.1. Other parameters shown in Table 6.1 are the values of the SPRT reference function $W_r(T_{90})$, and the approximate measured resistance ratio $X \equiv R(T_{90})/R_s$.

Table 6.1. Measurement parameters for the eight fixed-point temperatures used for calibration of a customer capsule SPRT over the range 13.8033 K to 273.16 K.

Fixed Point	T_{90} / K	$W_r(T_{90})$	X	R_s / Ω	i_1, i_2 / mA
WTP	273.16	1.00000000	0.255	100	1.0, 2.0
Hg TP	234.3156	0.84414211	0.218	100	1.0, 2.0
Ar TP	83.8058	0.21585975	0.55, 0.055	10, 100	1.0, 2.0
O_2 TP	54.3584	0.09171804	0.234	10	2.0, 2.83
Ne TP	24.5561	0.008449736	0.215, 0.0215	1, 10	2.83, 5.0
e-H_2 VP_2	20.2714	0.004235356	0.108	1	5.0, 7.07
e-H_2 VP_1	17.036	0.002296459	0.058	1	5.0, 7.07
e-H_2 TP	13.8033	0.001190068	0.030	1	5.0, 7.07

6.1.1 SPRT Resistance Measurement Uncertainties

The SPRT resistance measurement uncertainty components actually refer to the uncertainty in the determination of ratio $W(T)$ at each of the required calibration points. This causes some correlations of uncertainty components in $R(T)$ with those of $R(T_{WTP})$ and the net uncertainty in $W(T)$ becomes lower than what might otherwise be calculated [146]. The treatment presented here generally ignores such correlations for the assignment of uncertainties for most of fixed point $W(T)$ values used in the calibrations of the NIST check SPRTs. This choice reflects the historical pattern of ITS-90 realizations at NIST which have taken place within multiple laboratory facilities, utilizing multiple measurement systems over extended periods of time. In the case of the contemporary utilization of these check SPRTs as reference thermometers during comparison calibrations, however, some obvious correlations in the determination of $W(T)$ are taken into account. Likewise, correlations that pertain to determination of the $W(T)$ for the batch SPRTs (e.g. customer) comparison calibration are also taken into account.

The following treatment follows that given by the CCT Working Group 3 for SPRT uncertainties.[147] Starting from the basic AC bridge measurement of the SPRT resistance ratio X, where $R_x = XR_s$, the uncertainty in R_x is given by,

$$u^2(R_x) = u^2(X) + u^2(R_s)\,. \tag{6.1}$$

The uncertainty in the resistance standard $u(R_s)$ is primarily due to an uncertainty $u(T_{RS})$ in its maintenance bath temperature T_{RS} (nominally 25°C) and uncertainty in its calibration $u(R_{s,cal})$. During both fixed-point and comparison calibrations above 84 K, the same 100 Ω standard resistor is used to determine both $R(T)$ and $R(T_{WTP})$ for SPRTs. Hence, in those cases $u(R_{s,cal})$ is omitted from the uncertainty in $W(T)$, but it does contribute for T<70 K where other resistance standards must be utilized (see Tables 6.1 and 5.4).

The uncertainty in the bridge ratio $u(X)$ involves two forms of bridge non-linearity, integral (INL) and differential (DNL) and associated uncertainties $u(X_{INL})$ and $u(X_{DNL})$. In addition, when values for R (or X) are extrapolated to zero-current values, there is an uncertainty component $u(X_{sh})$ in the self-heating correction due to uncertainties $u(I)$ in the currents I. A further complication exists from parasitic reactance in cables and cryostat wiring which loads the bridge input creating errors in the measured ratio. A parasitic loading uncertainty $u(X_{PL})$ accounts for these effects. Finally, the bridge noise creates a type A uncertainty component $u(X_n)$.

The total uncertainty in the measured resistance R_x is then estimated via the expression,

$$\begin{aligned} u^2(R_x) = X^2\left\{u^2(R_{s,cal}) + A(I_1,I_2)R_s^2\beta_s^2u^2\left(T_{RS}\right)\right\} + R_s^2u^2\left(X_{PL}\right) + \\ R_s^2\left\{u^2\left(X_{INL}\right) + A(I_1,I_2)\left[u^2\left(X_{DNL}\right) + u^2\left(X_n\right)\right] + 8\Delta X_{sh}^2B(I_1,I_2)\frac{u^2(I)}{I^2}\right\}, \end{aligned} \tag{6.2}$$

where $A(I_1,I_2)=(I_2^4+I_1^4)/(I_2^2-I_1^2)^2$, $B(I_1,I_2)=I_2^4/(I_2^2-I_1^2)^2$, ΔX_{sh} is the self-heating correction in X for $I=I_1$, and β_s is the TCR of the resistance standard. It is assumed that both $u(I)$ and $u(X_n)$ are independent of current, which is approximately true for small increments between the currents I_1 and I_2.

The general expression for the SPRT resistance ratio is $W(T)= R_T/R_{WTP}= (X_T/X_{WTP})(R_{sT}/R_{sWTP})$ where R_{sT} and R_{sWTP} are the standard resistors and X_T and X_{WTP} are the measured resistance ratios at the temperature T and at the water triple point, respectively. The total measurement uncertainty in $W(T)$ is then derived from the uncorrelated approximation,

$$u^2(W) = W^2 \left\{ \frac{u^2(X_T)}{X_T^2} + \frac{u^2(R_{sT})}{R_{sT}^2} + \frac{u^2(X_{WTP})}{X_{WTP}^2} + \frac{u^2(R_{sWTP})}{R_{sWTP}^2} \right\} \quad . \tag{6.3}$$

By combining Eqn. 6.3 and Eqn. 6.2, it is then straightforward to show that,

$$u^2(W) = \frac{1}{R_{WTP}^2} \left\{ \begin{array}{l} X_T^2 u^2(R_{sT,cal}) + W^2 X_{WTP}^2 u^2(R_{sWTP,cal}) + A_{12} u^2(T_{RS}) \left[R_{sT}^2 \beta_{sT}^2 + W^2 R_{sWTP}^2 \beta_{sWTP}^2 \right] \\ + R_{sT}^2 \left[u^2(X_{PL\text{-}T}) + u^2(X_{INL}) \right] + W^2 R_{sWTP}^2 \left[u^2(X_{PL\text{-}WPT}) + u^2(X_{INL}) \right] \\ + A_{12} \left[\left(R_{sT}^2 + W^2 R_{sWTP}^2 \right) u^2(X_{DNL}) + R_{sT}^2 u^2(X_{n\text{-}T}) + W^2 R_{sWTP}^2 u^2(X_{n\text{-}WTP}) \right] \\ + 8 B_{12} \left[R_{sT}^2 \Delta X_{sh\text{-}T}^2 + W^2 R_{sWTP}^2 \Delta X_{sh\text{-}WTP}^2 \right] \dfrac{u^2(I)}{I^2} \end{array} \right\} \tag{6.4}$$

Subscripts which contain '*T*' refer to the measurement of the SPRT at an arbitrary temperature *T* and subscripts which contain 'WTP' refer specifically to the measurement of the WTP resistance. In the special case where $R_{sT} = R_{sWTP} \equiv R_s = 100\ \Omega$ for $T>\sim 84$ K, the first two terms in Eqn. 6.4 are omitted and the remaining terms simplify to

$$u^2(W) = \frac{1}{X_{WTP}^2} \left\{ \begin{array}{l} \left(1+W^2\right) A_{12} u^2(T_{RS}) \left[\beta_s^2 \right] \\ + \left[u^2(X_{PL\text{-}T}) + u^2(X_{INL}) \right] + W^2 \left[u^2(X_{PL\text{-}WPT}) + u^2(X_{INL}) \right] \\ + A_{12} \left[\left(1+W^2\right) u^2(X_{DNL}) + u^2(X_{n\text{-}T}) + W^2 u^2(X_{n\text{-}WTP}) \right] \\ + 8 B_{12} \left[\Delta X_{sh\text{-}T}^2 + W^2 \Delta X_{sh\text{-}WTP}^2 \right] \dfrac{u^2(I)}{I^2} \end{array} \right\} . \tag{6.5}$$

The RSS of the individual uncertainty components may be expressed as a dimensionless value $u(W)$ or in units of mK via $u(T)=1000\ u(W)/(\mathrm{d}W_r/\mathrm{d}T)$.

6.1.1.1 Resistance Standards Uncertainties

The resistance standards used in the LTCF have differing but known values for β_s and $u(T_{RS})=0.025$ K is assigned to represent the resistor maintenance oil bath control stability. The uncertainty parameters for a set of 4 LTCF standard resistors are listed in Table 6.2. The first two

terms in Eqn. 6.4 are the uncertainties $u_{Rs}(W)$ associated with the calibration uncertainties $u(R_s)$. The next two terms are the uncertainties $u_{TRs}(W)$ associated the thermal stability of the resistance standards.

Table 6.2 Uncertainty parameters for 4 LTCF standard Resistors used in batch calibrations.

Serial Number	Nominal Value	$u(R_s)$ [μΩ/Ω]	β_s μΩ/Ω-K	Drift μΩ/Ω-Yr
268950	1	0.5	±1.0	–
16954/12	10	0.25	–0.5	–
268185	100	0.25	–0.4	–
270985	200	0.5	1.6	–

6.1.1.2 Parasitic Loading Uncertainties.

The parasitic loading uncertainty $u(X_{PL})$ is negligible for the WTP measurement, but is dominant at low temperatures due to the large and variable (i.e. channel dependent) reactance and series resistance of the cryostat wiring. The net effect is modeled as a simple offset term R_{offset} =0.5 μΩ in the bridge readings which represents the average errors present due to series resistance and lossy shunt capacitance of the wiring.

6.1.1.3 Bridge Non-linearity.

The bridge INL uncertainty $u(X_{INL})$ can in principle be corrected by using $\Delta X_{INL}(X)$ data derived from ratio calibration networks [140]. While such data are periodically used for resistance bridge verification at NIST [141], it is not customary to apply bridge corrections for routine calibrations. Rather, the bridge verification data are used to estimate $u(X_{INL})$. In the special cases of the HgTP calibration and other measurements near X=0.255 (i.e.W~1), $u(X_{INL})$ is simply omitted due to the obvious correlations that will exist when using the same resistance bridge as is used to determine R(WTP). In contrast, the DNL uncertainty $u(X_{DNL})$ has a pseudo-random characteristic and a single uncorrelated term of 3×10^{-8} is sufficient to characterize this component.

6.1.1.4 Bridge Noise.

The bridge noise contribution $u(X_n)$ is obviously random, but temperature dependent due to variable signal voltages and sensitivity. This component is modeled as two voltage noise terms, $v_{n\text{-}ip}$ and $v_{n\text{-}qs}$, the in-phase and quadrature-servo bridge noise voltages. The quadrature-servo noise is produced by a fraction of the phase-shifted reference voltage being fed back into the IVD and its effect is most noticeable when IR_s is small.

6.1.1.5 Self-Heating Correction.

The self-heating correction uncertainties are treated as uncorrelated in Eqns. 6.4 and 6.5, as would be expected for random variations in the resistors used to set the excitation currents assuming 0.5% tolerances. However, there are correlations in the uncertainty terms for T and

WTP readings when the same currents are used on the same bridge for both measurements. In this case the self-heating correction uncertainty $u_{sh}(W)$ (the term in the bottom row) in equation 6.5 is modified to account for this correlation by

$$u_{sh}^2(W) = 8B_{12}\left[\Delta X_{sh-T} - W\Delta X_{sh-WTP}\right]^2 \frac{u^2(I)}{I^2}, \qquad 6.6$$

which is slightly smaller than the uncorrelated form in Eqn. 6.5. This modification is included for T>84 K.

6.1.1.6 Combined SPRT Measurement Uncertainties

When the SPRT measurement uncertainties are combined according to Eqn. 6.4 and Eqn. 6.5, the result exhibits discontinuities due to the changes in excitation currents and resistors as indicated in Tables 5.3 and 5.4. The combined measurement uncertainty $u_{cm}(T)$ is shown in Figure 6.1 for the range 13.8 K to 165 K. This represents the uncertainties in the measurement of a 25.5 Ω batch SPRT resistance ratio within the NIST LTCF only.

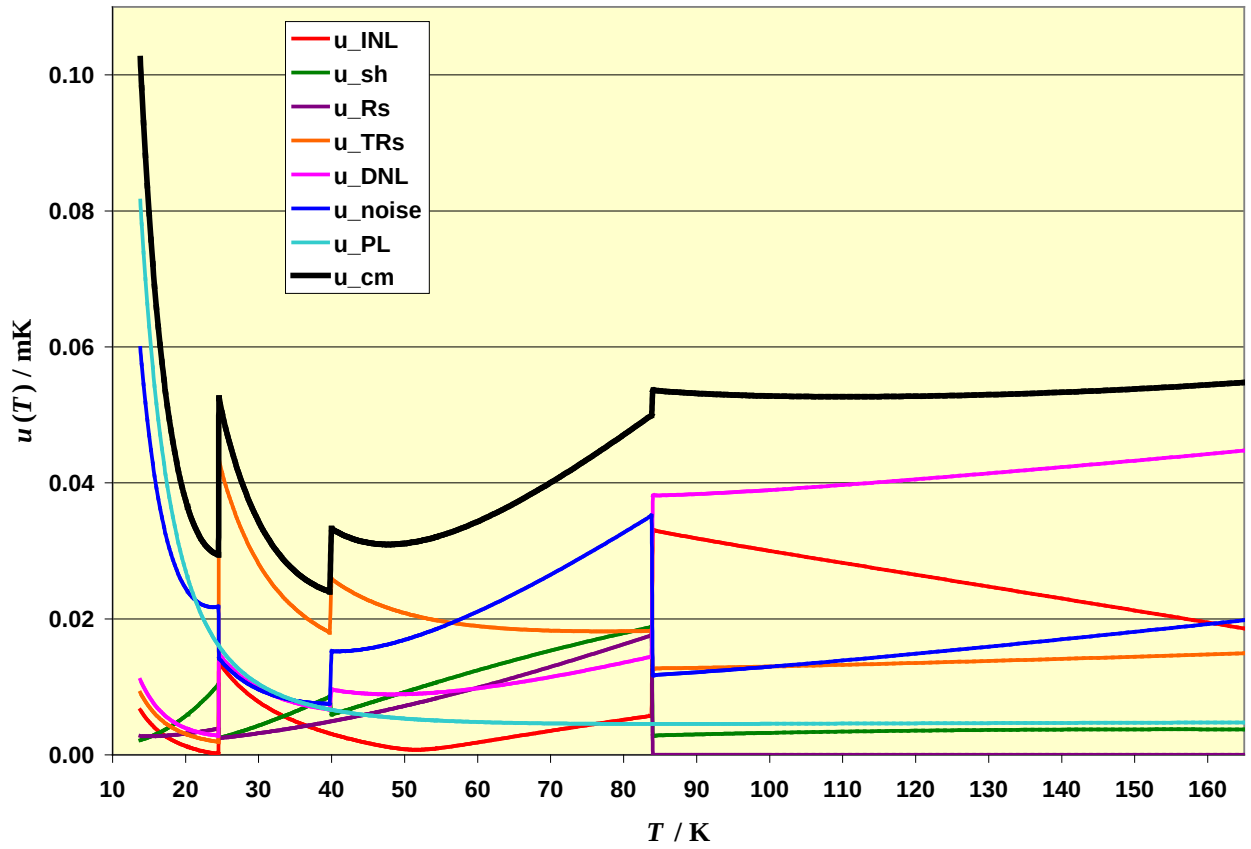

Figure 6.1 The combined measurement uncertainty for a batch SPRT.

6.1.2 SPRT Realization Uncertainties

These are mostly type B uncertainty components [125, 126] associated with NIST fixed-point realizations and the resulting ITS-90 interpolation uncertainty over the SPRT subrange 1 from 13.8 K to 273.16 K. These realizations are the basis for the NIST check SPRT calibrations. The uncertainties are quoted as symmetric distributions and any asymmetric residual parts are ignored. In many cases, the probability distributions are unknown, but modeled as rectangular with half-widths b such that the standard uncertainty is $u=b/(3)^{1/2}$. The distribution widths are estimated, based on upper bounds for the size of the effects, as derived from reasonable assumptions about the relevant physical and chemical processes. The individual uncertainty components are assumed uncorrelated so that the total realization uncertainty is calculated as the RSS.

6.1.2.1 Fixed Point Repeatability

This is a type A uncertainty which is estimated from variations in repeated FP realizations.

6.1.2.2 Chemical Impurities

These are type B uncertainty estimates based on the observed melting curves as used in the FP realizations together with either information from specific gas lot assays or some reasonable assumptions about the possible impurities present. Impurity concentrations on a volume basis are commonly expressed as μL/L, meaning 10^{-6} liters impurity in a standard liter of gas.

For the e-H_2 fixed points, the only chemical impurity of any consequence is Ne. However, commercial research grade H_2 gas is generally dominated by impurities of H_2O, CH_4, CO, CO_2, and N_2. The observed melting range of 0.03 mK, observed in the LTRF, between 50% and 100% melted fractions could be almost entirely accounted for by the HD content alone (see next section below). The assigned uncertainty component of u=0.02 mK is a conservative estimate, but impurity contributions at that level cannot be ruled out.

For the Ne TP, approximately 1/3 or more of the observed melting range (≈0.15 mK from F= 50% to 100%) can be accounted for by the effects of isotopic segregation between the liquid and solid phases. A possible impurity concentration of 10 μmol H_2/mol Ne cannot be ruled out, corresponding to a ≈0.05 mK depression in the liquidus point. A lot analysis from Matheson of Ne gas of origin similar to the bottle used in the LTRF gives an upper limit of 1 μL N_2/L impurity by volume, but concentrations of ≈5 μL/L are probably more realistic for cells filled via typical gas manifolds, corresponding to ≈0.04 mK depression in the liquidus point. We assume a rectangular distribution of width 2b=0.150 mK so that u=0.04 mK.

For the O_2 TP, there is no observable indication of impurities from the melting curves of the NIST O_2 cells, leaving only Ar as a potential undiscoverable problem. This is unlikely for these

samples which are not derived from the atmosphere, but impurity concentrations ≈1 μL/L cannot be ruled out, corresponding to plateau elevations of ≈0.012 mK. We assign an uncertainty component u=0.012 mK to reflect an effect of this magnitude.

The NIST Ar TP cells, both the capsule type (sealed-cells and the LTRF cell) as well as the immersion-type cells, have melting curves which suggest the presence of impurities at approximately 1 μL/L to 2 μL/L. These are assumed to be a mixture of N_2, O_2, CO, and light hydrocarbons which would normally produce depressions in the liquidus point of 20 μK/ μL/L to 30 μK/ μL/L each. We assume u=0.050 mK to account for probable effects of this magnitude.

The chemical uncertainty components for NIST Hg TP and WTP ICs are discussed in the NIST SP-250-81 document for long-stem SPRTs [45].

6.1.2.3 Isotopic corrections/variations:

The CCT has issued a "Mise-en-practique" for the ITS-90 [133] which defines the isotopic composition for e-H_2 fixed point realizations to be equivalent to Standard Light Antarctic Precipitation (SLAP) or $x_{SLAP}(D)$=89 μmol/mol. NIST has used a lighter composition for all such realizations of $x_{NIST}(D)$=29 μmol/mol [117]. This necessitates applying corrections of +0.33 mK for the *e*-H_2 TP, +0.15 mK for the *e*-H_2 VP point at 33 kPa, and +0.174 mK for the VP point at 101 kPa. The uncertainties associated with these corrections plus those arising from the composition measurement are estimated to be 0.019 mK, 0.038 mK, and 0.044 mK at those three fixed point temperatures respectively [132].

In the case of the Ne TP, recent evidence [148] has indicated that commercial Ne gas may exhibit a range of fractionation as large as 320×10^{-6} in the relative atomic weight. The extent of fractionation appears to be much larger than previously estimated, corresponding to extreme variations of ~0.48 mK in the TP realization temperature. NIST is in the process of determining the isotopic composition of Ne used for TP realization but at present these factors remain unknown. The ITS-90 currently specifies "natural isotopic composition" for all such fixed points. This is, however, somewhat ambiguous in the case of Ne in light of the large fractionation associated with distillation processes. We assign a standard uncertainty of 0.14 mK=0.48 mK/$(12)^{½}$ for this effect based on reasonable estimates for the probable range of variation and knowledge of the mass sensitivity coefficient [149].

In the case of the WTP, the CCT "Mise-en-practique" [133] defines the isotopic composition for the water triple point to be equivalent to that of Vienna Standard Mean Ocean Water (VSMOW) or $x_{VSMOW}(D)$=156 μmol/mol. NIST WTP cells are either made with water of the VSMOW composition or otherwise corrected when the actual composition is known. An uncertainty of 0.006 mK is assigned to account for variations from the defined VSMOW composition.

6.1.2.4 Static Head Corrections

This uncertainty applies to those fixed-point realizations in immersion type cells for which a static pressure head correction is applied, i.e., the H_2O TP, the Hg TP, and the immersion type Ar TP. The dominant uncertainty is the location of the effective center of the Pt element, for which

we assign a standard uncertainty of 0.5 cm. The other factors such as material density, column height, and $\partial T/\partial P$ are assigned relative standard uncertainties of 2% or less.

6.1.2.5 Immersion/ Heat Leaks

Immersion Cells: The degree to which adequate immersion is maintained depends on the flux of heat through the probe adaptor into the re-entrant well. Estimates of the immersion uncertainty associated with the NIST capsule SPRT adapter probes are based primarily on the measured immersion profiles. Rectangular distributions are assumed based on estimates of the upper limits on the possible size of immersion errors

LTRF: In this case there exist steady–state gradients from heat leaks into and out of the FP cells. The values assumed are estimates based on experience, primarily from the size of the effects observed near the final portion of the melts.

Sealed-Cells: In this case the heat leaks from lead wires are the primary source of error. Again, the values assumed are estimates based on experience, primarily from the size of the effects observed near the final portion of the melts.

6.1.2.6 Thermal Equilibrium

This component is an estimate of the degree to which a fixed point cell is in true thermal equilibrium during the realization measurements. The values are based on observations of the variability of fixed point realizations when variable equilibration times are used. No specific model is assumed.

6.1.2.7 Spin Equilibrium / Phase Equilibrium

The uncertainties due to incomplete spin conversion in the e-H_2 points are, in principle, asymmetric. For the sake of calculation, however, a symmetric rectangular distribution is assumed with u= 0.012 mK.

6.1.2.8 Pressure Calibrations

These uncertainties apply to the e-H_2 VP points only. They are based on a 12 ppm standard calibration uncertainty for the piston gauge used to generate the reference pressures in the LTRF. A zero offset uncertainty of 0.1 Pa has also been included.

6.1.2.9 Liquid-Vapor Volume Dependence

These uncertainties apply to the e-H_2 VP points only. They are based on the theoretical range of VP equilibrium between the condensation and evaporation isobars [150]. For the particular

isotopic composition used for NIST realizations of the e-H_2 VP points, these ranges are 67 μK and 81 μK for the 101 kPa and 33 kPa VP points, respectively. The standard uncertainties are derived by assuming a rectangular distribution for these ranges and dividing by $(12)^{1/2}$.

6.1.3 Uncertainties in the Comparison Process.

The comparison process involves measurements of a check SPRT (i.e. designated reference SPRT) and a batch SPRT (e.g customer SPRT being calibrated), but some of the measurement uncertainties discussed in section 6.1.1 are correlated and do not contribute to the comparison uncertainty. Those measurement uncertainties which remain uncorrelated between the two measurements are included. In addition, thermal uncertainties are included which account for limitations in the equilibrium and uniformity that can be established during the comparison process. The RSS of all comparison-specific uncertainty components is designated as $u_{comp}(T)$ and it represents the extent to which the resistance ratios of two similar SPRTs can be compared at the same temperature without regard for the actual indicated temperatures of either one. The individual components are summarized in Table 6.3 for the SPRT calibration temperatures.

6.1.3.1 Thermal Uniformity

This uncertainty component accounts for the thermal non-uniformity within the comparison block. The comparison block heater is located above the zone where the thermometers are installed. This spatial separation serves to minimize induced thermal gradients from the main controller power. The comparison block is subject to local heating, however, from the combined thermometer-element, lead-wire and wiring-harness resistances under normal measurement excitations. The OFHC copper is assumed to have $X_{RR} \approx 50$ which corresponds to reductions in the thermal conductivity from the highly annealed state by factors of ≈7 at 13.8 K, but only by a factor of ≈1.1 at 83.8 K. Even with this derating of the copper, however, the uncertainty estimate does not exceed 0.014 mK in the range 13.8 K to 165 K.

6.1.3.2 Temperature Control

The effects of variations in the comparison block temperature over time due to imperfect temperature control mostly cancel over the averaging intervals employed in the LTCF comparison process. The control fluctuations, however, have Fourier components which span over time scales comparable to the basic comparison measurement cycle of ~35 minutes for AC resistance measurements of SPRTs. Therefore, the Fourier components of the control fluctuations which match this measurement cycle time are the only ones that really matter in producing comparison errors. The uncertainty component $u_{TC}(W)$ accounts for this effect and is estimated by 0.03 mK +1 μK/K of the temperature.

6.1.3.3 Thermal Equilibrium

This component accounts for imperfect equilibrium of the comparison system under changing conditions such as switching between thermometers and switching currents. The data acquisition system pauses for a fixed wait time τ_{wait} after each such change before resuming data acquisition. The relative effect of these thermal perturbations is estimated by summing all major system time

constants and dividing by the wait time of 60 s for 13.8 K<T<54.56 K and 120 s for T≥54.56 K. The major system time constants are those associated with: 1.) total self-heating resistance and the internal heat capacitance, $\tau_{int}=(\eta_{int}+\eta_{ext})C_{int}$; 2.) external self-heating resistance and heat capacitance, $\tau_{ext}=\eta_{ext}C_{ext}$ and ; 3.) the thermal diffusivity time constant of the comparison block $\tau_d=l^2/\alpha_d$, for l=5 cm. The uncertainty estimate is calculated from the time constant ratio multiplied by the magnitude of the self-heating perturbations or $u_{TE}(W)=\Delta T_{sh}\Sigma\,\tau_i/\tau_{wait}$.

6.1.3.4 Reference Thermometer Measurement

This component accounts for the measurement uncertainty associated with the determination of the temperature during comparisons with a check SPRT. It includes all of the uncorrelated terms described in section 6.1.1 but excludes terms corresponding to common systematic errors for all SPRTs and channels in the comparison process. Specifically, the uncertainty is estimated as the RSS of $u_{TRs}(W)$, $u_{DNL}(W)$, $u_{noise}(W)$, and $u_{PL}(W)$.

6.1.3.5 Reference Thermometer Stability

This component is an estimate of uncertainty associated with instability of an SPRT reference thermometer's residual resistance. The standard uncertainty estimate is 0.3 μΩ.

6.1.3.6 Batch Thermometer Measurement.

This component accounts for the measurement uncertainty associated with the determination of the W value for the batch SPRT under calibration. The terms are identical to those for the reference thermometer measurement described above in section 6.1.3.4. Since they are either random in nature or otherwise uncorrelated with those associated with the reference thermometer, both sets of measurement uncertainties contribute to the total comparison uncertainty.

Table 6.3 Comparison uncertainties in mK for NIST comparison calibrations of SPRTs from 13.8 K to 83.8 K.

Comparison Temperatures	**13.8**	**17.03**	**20.27**	**24.56**	**54.36**	**83.8**
Description						
Thermal Uniformity	0.013	0.012	0.011	0.005	0.005	0.012
Temperature Control	0.033	0.034	0.036	0.039	0.062	0.089
Thermal Equilibrium	0.000	0.001	0.002	0.002	0.020	0.070
Check Thermometer Meas.	0.102	0.055	0.036	0.050	0.029	0.042
Check Thermometer Stability	0.059	0.036	0.026	0.020	0.013	0.013
Batch Thermometer Meas.	0.102	0.055	0.036	0.050	0.029	0.042
RSS Combined Comparison Uncertainty. $u_{comp}(k=1)$	**0.160**	**0.093**	**0.068**	**0.084**	**0.079**	**0.130**

6.1.4 Check SPRT Calibration Uncertainty

The check SPRTs as previously calibrated on the ITS-90 at NIST have calibration uncertainties which are a combination of previous ITS-90 realization uncertainties and SPRT measurement uncertainties. The individual uncertainty components have already been discussed in sections 6.1.1 and 6.1.2 above. Table 6.4 is a summary of the relevant components for the NIST check SPRTs for the 8 fixed points in the range 13.8 K to 273.16 K. The RSS of individual components is referred to as $u_{\text{chkcal-}j}$ for j=1 to 8 representing the 8 fixed points in this subrange.

When using the check SPRT as a reference thermometer to determine temperatures between the ITS-90 fixed-point temperatures, the calibration uncertainty propagates from each of the individual fixed-point calibration temperatures. The net uncertainty at any intermediate temperature T is a complicated function formed by the combination of each uncertainty propagation function $u_{\text{chkcal-}j}(T)$ of the individual fixed-point uncertainties for each specific subrange definition.[146,147]. The existence of correlations in some of the individual uncertainty components between two or more fixed-point temperatures complicates matters further. The case of the WTP is the most obvious and possibly the most complicated because the exact correlation depends on a variety of factors pertaining to how the WTP resistance value is obtained. For the purposes of calibrations within the LTCF these correlations are generally small contributions in the overall uncertainty and are ignored. Therefore, the propagated uncertainty for the entire subrange is approximated as a simple RSS of the individual propagated uncertainty terms $u_{\text{chkcal-}j}(T)$, or

$$u^2_{\text{chkcal}} = \sum_{j=1}^{8} u^2_{\text{chkcal-}j}(T)\,. \qquad 6.7$$

Figure 6.2 shows the individual contributions $u_{\text{chkcal-}j}(T)$ to u_{chkcal} over the 13.8 K to 273.16 K range of temperatures. The individual uncertainty components, $u_{\text{chkcal-}j}(T)$, are derived from numeric solutions[146] to the ITS-90 subrange 1 deviation equation under defined perturbations to the fixed-point W values.

Table 6.4 Calibration uncertainties for NIST Check SPRTs as used in the LTCF.

Description	*e*-H_2 TP†	*e*-H_2 VP_1†	e-H_2 VP_2†	Ne TP†	O_2 TP†	Ar TP†	Ar TP‡	Hg TP‡	WTP ‡
Realizations									
Melting plateau reproducibility	0.064	0.050	0.050	0.091	0.020	0.050	0.030	0.200	0.040
Chemical Impurities	0.020	0.020	0.020	0.040	0.012	0.050	0.050	0.010	0.010
Isotopic Variations/corrections	0.019	0.037	0.043	0.139	0.010				0.006
static-head correction		0.005	0.005				0.008	0.036	0.005
Heat Leaks/Immersion	0.020	0.020	0.020	0.020	0.020	0.020	0.030	0.080	0.050
Thermal Equilibrium	0.020	0.010	0.010	0.020	0.020	0.020			0.020
Spin/Phase Equilibrium	0.020	0.020	0.020						
Pressure Gauge Cal.		0.042	0.032						
liq./vapor Vol. dependence		0.023	0.019						
SPRT Measurement									
SPRT repeatability	0.060	0.033	0.024	0.014	0.018	0.035	0.002	0.005	0.033
INL	0.016	0.009	0.006	0.032	0.014	0.021	0.018	0.019	0.000
DNL	0.011	0.006	0.004	0.015	0.009	0.014			0.057
Parasitic Loading	0.081	0.043	0.026	0.016	0.005	0.005	0.005	0.006	0.005
bath stability	0.009	0.005	0.003	0.043	0.020	0.018	0.005	0.006	0.019
resistance standards	0.003	0.003	0.003	0.002	0.008	0.018	0.005		
SPRT self-heating	0.002	0.004	0.006	0.002	0.011	0.016	0.010	0.012	0.000
RSS Check cal. unc. $u_{chkcal}(k=1)$	**0.129**	**0.103**	**0.092**	**0.183**	**0.052**	**0.093**	**0.070**	**0.220**	**0.097**

† Cryogenic fixed point , either sealed cell or open cell.
‡ Immersion-type fixed point cell.

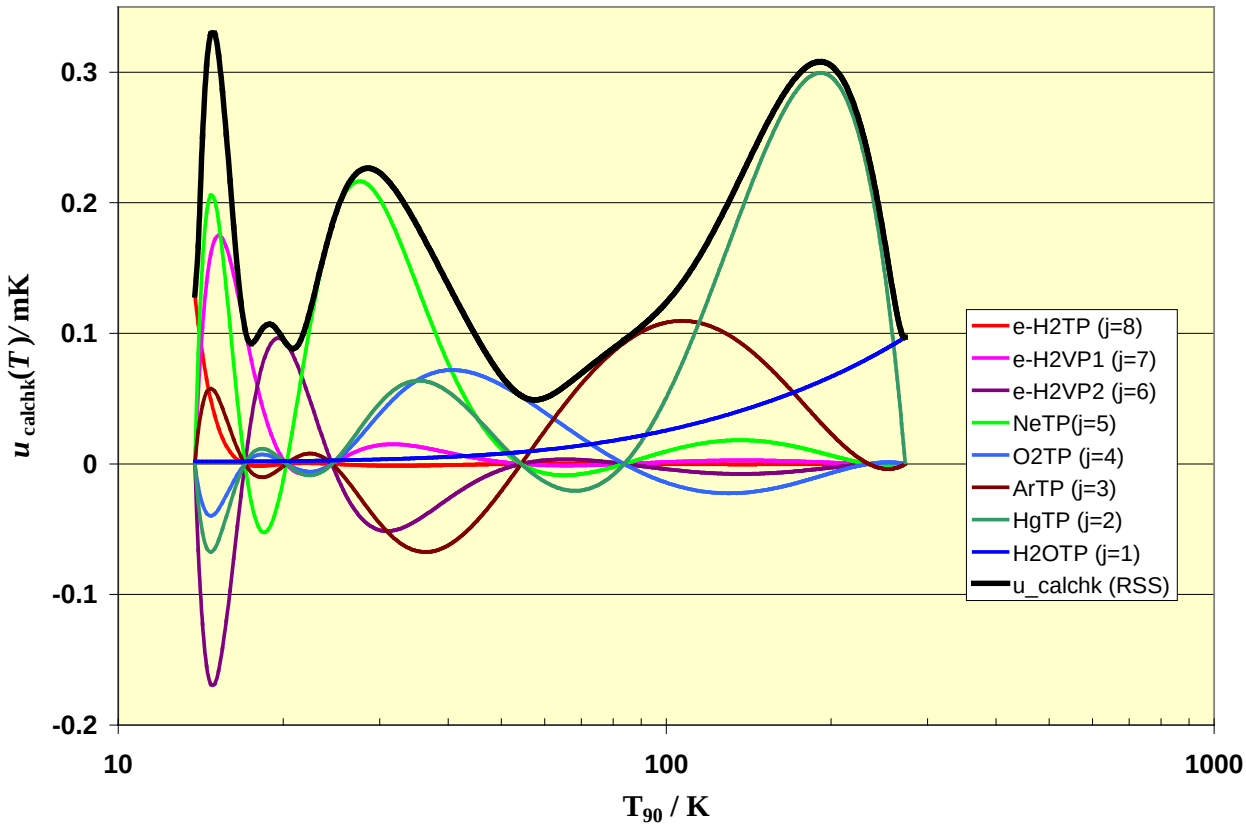

Figure 6.2 The individual contributions to a check SPRT propagated calibration uncertainty from 13.8 K to 273.16 K and the RSS value $u_{\text{calchk}}(T)$. All values are k=1 standard uncertainties.

6.1.5 Non-Uniqueness

The ITS-90 has multiple overlapping definitions for the SPRT Subranges. All NIST check SPRTs in the LTCF are utilized according to the SPRT subrange-1 definition. However, other alternative definitions exist in higher but overlapping temperature subranges (see section 3.1) which can yield slightly different interpolated temperatures between the defined fixed points. This results in an inherent ambiguity in the ITS-90 in these overlapping subranges, even for a single SPRT. This ambiguity is referred to as 'subrange inconsistency' or simply 'Type-1 Non-uniqueness [151]. The type-1 non-uniqueness has been estimated for the SPRT subrange overlap temperature range 24.556 K to 273.16.[152] The CCT-recommended non-uniqueness uncertainty for the subrange 1 has the form

$$u_{\text{NU1},i} = \sum_{j=1}^{5} A_{\text{NU1},ij}\,(T_{90} - T_{0i})\,, \qquad 6.8$$

where the coefficients $A_{\text{NU1},ij}$ and T_{0i} are given in reference [152].

There are two overlapping definitions for the ITS-90 in the interval 13.8 K to 24.556 K which involve two completely different interpolating instruments, the SPRT and the ICVGT. This introduces a second type of non-uniqueness, the so-called type-2 [151]. Meyer, *et. al*.[119] have evaluated this specific case of type-2 non-uniqueness for the NIST ICVGT realization and e-H_2 fixed-point realizations in conjunction with NIST check SPRTs. That evaluation from 1999 was based on H_2 gas [117] with an isotopic composition lighter than what was later defined for the ITS-90 by the CCT [133]. The subsequent adjustment [132] in the NIST ICVGT and SPRT subrange-1 disseminated scales resulted in an increase in the observed type-2 non-uniqueness over most of the 13.8 K to 24.556 K temperature interval. The adjusted difference $T_{SP1} - T_{ICVGT}$ is calculated to increase to ~0.8 mK at 17.036 K. More recent direct comparisons of SPRT subrange 1 and ICVGT temperatures at NIST suggest slightly smaller differences, but even these are larger than data from international key comparisons [134,135] would otherwise suggest. An empirical function for estimating the type-2 non-uniqueness standard uncertainty is

$$u_{NU2} = A_{NU2}\left(T - 13.8033\right)^{0.5}\left(20.2714 - T\right)^{1.5} \quad , \tag{6.9}$$

where the coefficient A_{NU2} =0.07/(3)$^{1/2}$ mK·K^{-2}, treating the observed non-uniqueness as essentially an upper bound value. The u_{NU2} uncertainty estimate applies to the interval 13.8 K<T<20.2714 K only, and is assumed to be zero above 20.2714 K.

A third type of non-uniqueness exists over all SPRT subranges due to differences in interpolation characteristics from one SPRT to another (i.e. sample-dependence). The type-3 non-uniqueness for capsule SPRTs over the range 13.8 K to 273.16 K has been evaluated by Hill and Steele.[153] The CCT Working Group 3 has recommended a functional form for this uncertainty component,

$$u_{NU3} = A_{NU3-i}\left(T - T_{1i}\right)^{m}\left(T_{2i} - T\right)^{n}, \tag{6.10}$$

for the i=1 to 4 intervals bounded by the 5 fixed points at 24.5561 K, 54.3584 K, 83.8058 K, 234.3156 K, and 273.16 K [147]. The coefficients are given in reference 147.

In general, since 1996, NIST has disseminated both the SP-1 definition and the ICVGT definition in the overlap range of 13.8 K to 24.556 K. The choice being primarily based on what type of customer thermometer is being calibrated. In previous ITS-90 uncertainty assessments [123], NIST had not included uncertainty allowances for non-uniqueness. This omission was due to the fact that, until relatively recently, not enough data were available to make reliable assessments of these scale defects. As of 2009, the certain non-uniqueness uncertainties will be included in NIST ITS-90 uncertainty statements for cryogenic thermometer calibrations. In the case of SPRTs, all three types described here are relevant and will be included in the uncertainty statement. Figure 6.3 is a plot over the SPRT subrange 1 of all three non-uniqueness uncertainty components for SPRTs as given by Equations 6.8, 6.9 and 6.10.

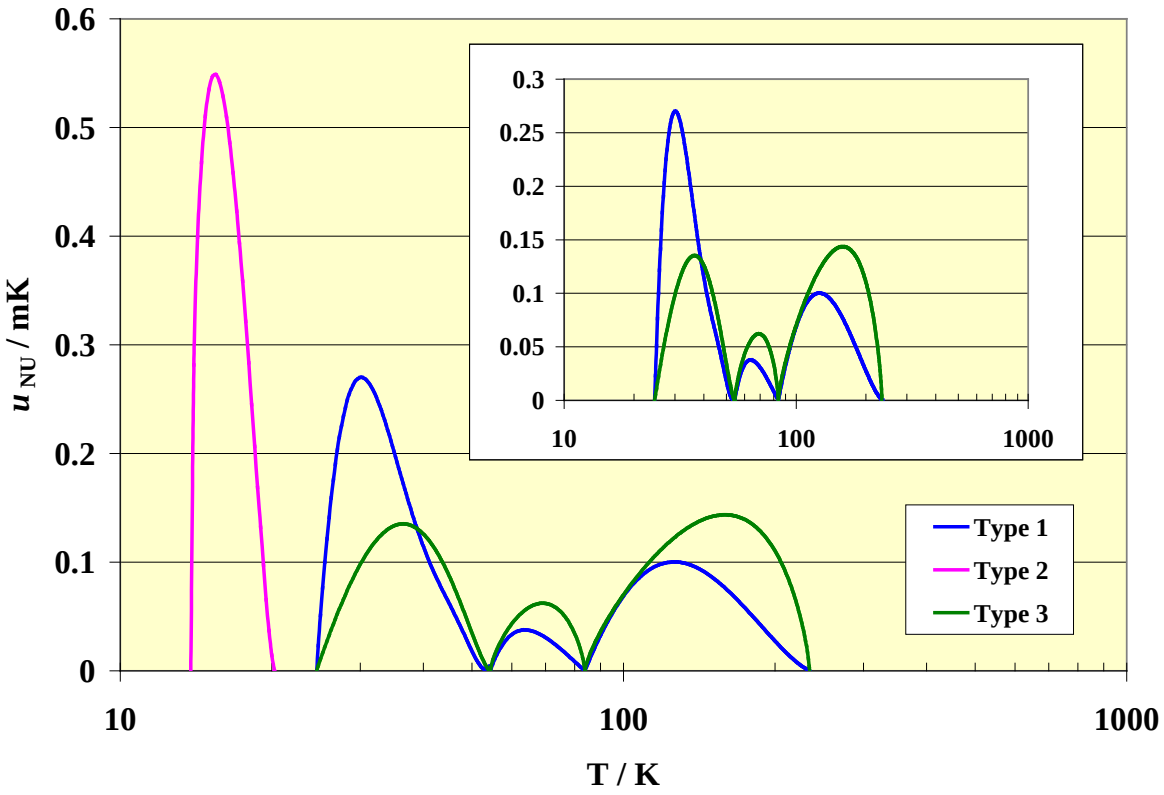

Figure 6.3 The non-uniqueness uncertainties for SPRTs from 13.8 K to 273.16 K.

6.1.6 Total Comparison Calibration Uncertainty

The batch SPRT calibration uncertainty $u_{\text{batcal-i}}$ for each calibration point i is calculated as the RSS of the comparison uncertainty u_{comp}, the check calibration uncertainty u_{chkcal}, and the batch SPRT measurement uncertainty u_{batm},

$$u^2_{\text{batcal-}i} = u^2_{\text{comp}}(T_i) + u^2_{\text{chkcal}}(T_i) + u^2_{\text{batm}}(T_i). \qquad 6.11$$

for i=4 to 8, corresponding to the lowest five calibration temperatures which are performed by comparison. The other three calibration temperatures, i=1 to 3 (Ar TP, Hg TP, and WTP), are performed by direct realization in immersion cells within the NIST SPRT calibration laboratory (see section 5 and reference [45]) so that u_{comp} and u_{batm} are zero and $u_{\text{batcal-i}} = u_{\text{chkcal-i}}$.

The batch SPRT measurement uncertainty u_{batm} is a partial RSS of the components of the combined measurement uncertainty u_{cm} (see section 6.1.1) excluding those components already included in u_{comp} (see section 6.1.3). Specifically,

$$u^2_{\text{batm}} = u^2_{\text{Rs}} + u^2_{\text{INL}} + u^2_{\text{sh}}\ , \qquad 6.12$$

which includes only those uncertainty components that are of a purely systematic nature. These components are separated from u_{comp} because they occur for both the check SPRT and the batch SPRT so that any associated errors cancel in the comparison of like SPRTs. They should be counted once in the total calibration uncertainty for the comparison, but not twice. Similar terms do contribute to the check calibration uncertainty u_{chkcal} , but in that case they usually occur in other measurement systems as utilized at some earlier time and are therefore assumed to be uncorrelated with those occurring during the comparison process.

The total calibration uncertainty $u_{batcal\text{-}Total}(T)$ for the batch SPRT is the propagated RSS uncertainty from all $u_{batcal\text{-}i}$ values and the various appropriate non-uniqueness uncertainty components u_{NU1}, u_{NU2}, u_{NU3}. Specifically,

$$u^2_{batcal\text{-}Total}(T) = \left[\sum_{i=1}^{8} u^2_{batcal\text{-}i}(T)\right] + u^2_{NU1}(T) + u^2_{NU2}(T) + u^2_{NU3}(T) \qquad 6.13$$

The propagated uncertainty functions $u_{batcal\text{-}i}(T)$ are essentially the same as those used for the propagation of the check SPRT calibration uncertainties in Eqn. 6.7 except that they are now scaled by $u_{batcal\text{-}i} > u_{chkcal\text{-}i}$ for i=4 to 8.

In the special case of the WTP (i=1), however, the exact form of the propagation uncertainty function $u_{batcal\text{-}1}(T)$ depends on how the end user obtains a WTP value in use of the SPRT.[146] In the example treated here, the end user obtains $R(T_{WTP})$ with an uncertainty $u_{user}(T_{WTP})$ through a direct realization using the same measurement system for all subsequent measurements of the SPRT for the purposes of determining temperatures. In this way the user does not incur uncertainties from resistance calibrations as long as the same standard resistor is used for determination of $R(T_{WTP})$. Figure 6.4 is a summary plot of the principle components for the total calibration uncertainty.

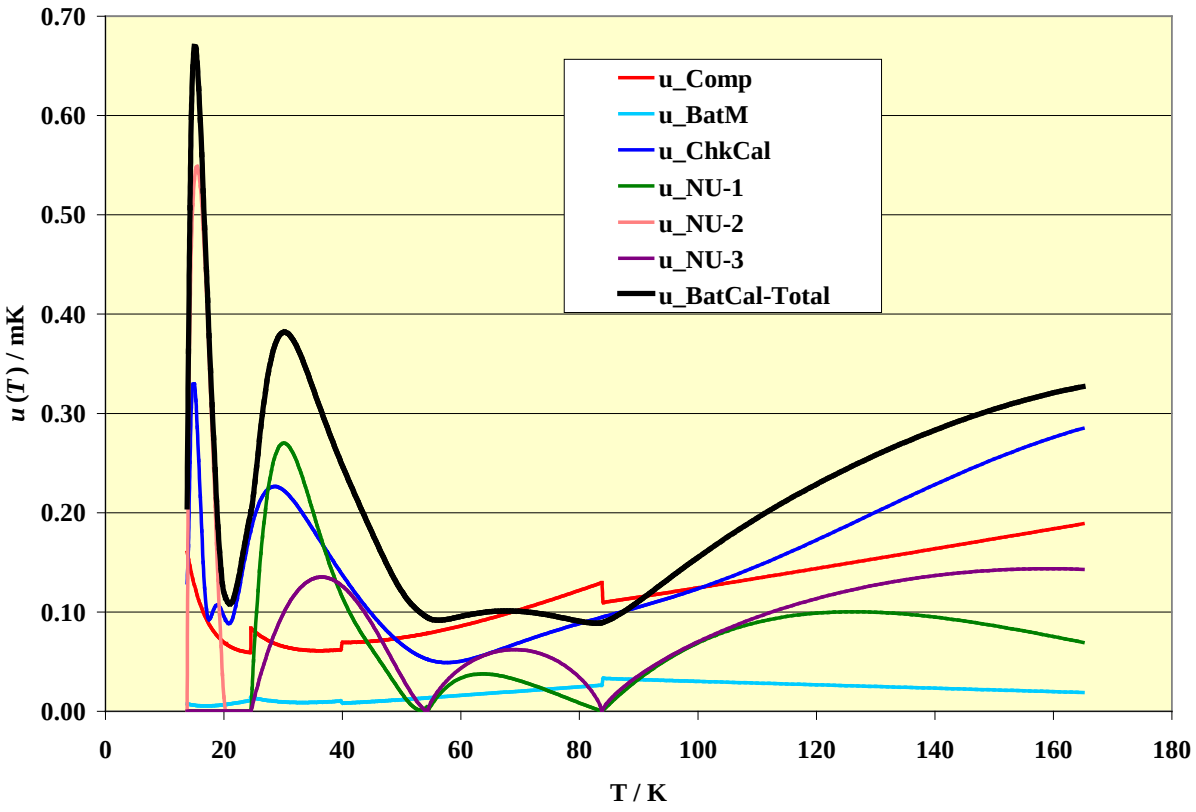

Figure 6.4 The total calibration standard uncertainty for a batch SPRT from 13.8 K to 165 K. Also shown are the comparison uncertainty, the batch measurement uncertainty, the check SPRT calibration uncertainty and the three types of non-uniqueness uncertainties.

6.2 RIRTs 0.65 K to 83.8 K

RIRTs are calibrated on the ITS-90 at temperatures as low as 0.65 K. The upper limit is somewhat flexible but NIST offers two standard services with upper limits at 24.556 K and 83.8 K. The batch RIRT is calibrated by comparison to similar NIST check RIRTs at temperatures below 24.556 K. Above this point, the check thermometer will be an SPRT as calibrated on the SPRT subrange 1. Table 6.5 shows the relevant scale definitions (see section 3) and measurement parameters (see sections 5.3 and 5.4) used for calibrations up to 83.8 K.

Table 6.5. ITS-90 Calibration parameters for a batch (customer) RIRT (R(273.15 K)≈100 Ω, typical).

Definition	T_{90} / K	$R_{\mathrm{RIRT}}(T_{90})$ / Ω	X	R_{std} / Ω	i_1, i_2 / mA
^{3}He VP	0.65 to 2.0	5.1 to 6.0	0.051 to 0.06	100	0.14, 0.2
^{4}He VP	2.0 to 5.0	6.0 to 7.4	0.06 to 0.074	100	0.2, 0.283
ICVGT	5.0 to 24.5561	7.4 to 12.4	0.074 to 0.124	100	0.283, 0.5
SPRT	24.5561 to 83.8	12.4 to 28	0.124 to 0.28	100	0.5, 0.707

6.2.1 RIRT Resistance Measurement Uncertainty

The example here is for a 100 Ω capsule RIRT. Measurements of each RIRT's resistance at the respective calibration-point temperatures are made via an automatically balancing AC resistance-ratio bridge. The resistance ratio measurements are performed at a carrier frequency of 30 Hz, using only a single calibrated 100 Ω resistance standard, R_s, and the various excitation currents, i_1, i_2 , as shown in Table 6.5. The measured resistance ratio is $X \equiv R(T_{90})/R_s$.

Calibration data for RIRTs consist of resistance values, $R(T_{90})$, taken at about 25 points distributed over the range 0.65 K to 24.556 K and another 12 points for extended range calibrations covering 26 K to 83.8 K in order to construct an accurate interpolation function for that range. Since the RIRT is not a defining instrument of the ITS-90, there is no officially adopted reference function for interpolation. A combination of two simple polynomial expansions in T_{90} is generally sufficient to represent the resistance in the range 0.65 K to 24.6651 K. A third polynomial is adequate to complete the interpolation for calibrations up to 83.8 K (see Table 5.4 for specific temperatures).

Starting from Equation 6.2 (see section 6.1.1) for the total uncertainty $u(R_x)$ in the measured resistance R_x, the terms specific to an RIRT measurement are evaluated as follows. Each uncertainty component is plotted as a function of temperature in Figure 6.5 over the range 0.65 K to 83.8 K.

6.2.1.1 Resistance Standards' Uncertainties

The 100 Ω resistance standard listed in Table 6.2 is used for the entire range. The first term in Eqn. 6.2 is the uncertainty $u_{Rs}(R)$ associated with the calibration uncertainties $u(R_{s\text{-}Cal})$. The next

term is the uncertainty $u_{TRs}(R) \equiv u(T_{RS})$ associated the thermal stability of the resistance standards. The contributions u_{Rs} do not exceed ≈0.022 mK for a 100 Ω RIRT.

6.2.1.2 Parasitic Loading Uncertainties.

The parasitic loading uncertainty $u(X_{PL})$ is negligible (i.e., <0.01 mK) for the entire range of RIRT calibrations.

6.2.1.3 Bridge Non-linearity.

The bridge INL uncertainty $u(X_{INL})$ is treated similarly to that for SPRTs in section 6.1.1. The bridge verification ΔX_{INL} data are used to estimate $u(X_{INL})$ and no corrections are applied. The DNL uncertainty $u(X_{DNL})$ is treated as a pseudo-random uncertainty and a single uncorrelated term of 3×10^{-8} is again used to characterize this component.

6.2.1.4 Bridge Noise.

The random bridge noise contribution $u(X_n)$ is again temperature dependent due to variable signal voltages and sensitivity. As in the SPRT case, this component is modeled as two voltage noise terms, $v_{n\text{-}ip}$ and $v_{n\text{-}qs}$, the in-phase and quadrature-servo bridge noise voltages.

6.2.1.5 Self-Heating Correction.

The self-heating correction uncertainties are treated as uncorrelated (from the resistance bridge standpoint) as the correction originates from random variations in the internal resistors used to set the excitation currents assuming 0.5 % tolerances. The effect is correlated, however, from the standpoint of thermometers using the same current settings. The uncertainty is estimated according to the last term in equation 6.2.

6.2.1.6 Combined RIRT Measurement Uncertainty

Equation 6.2 as written is the combined form for all RIRT measurement uncertainties. The solid black line in Figure 6.5 represents the RSS standard combined uncertainty u_{cm} for the resistance measurement of the batch RIRT.

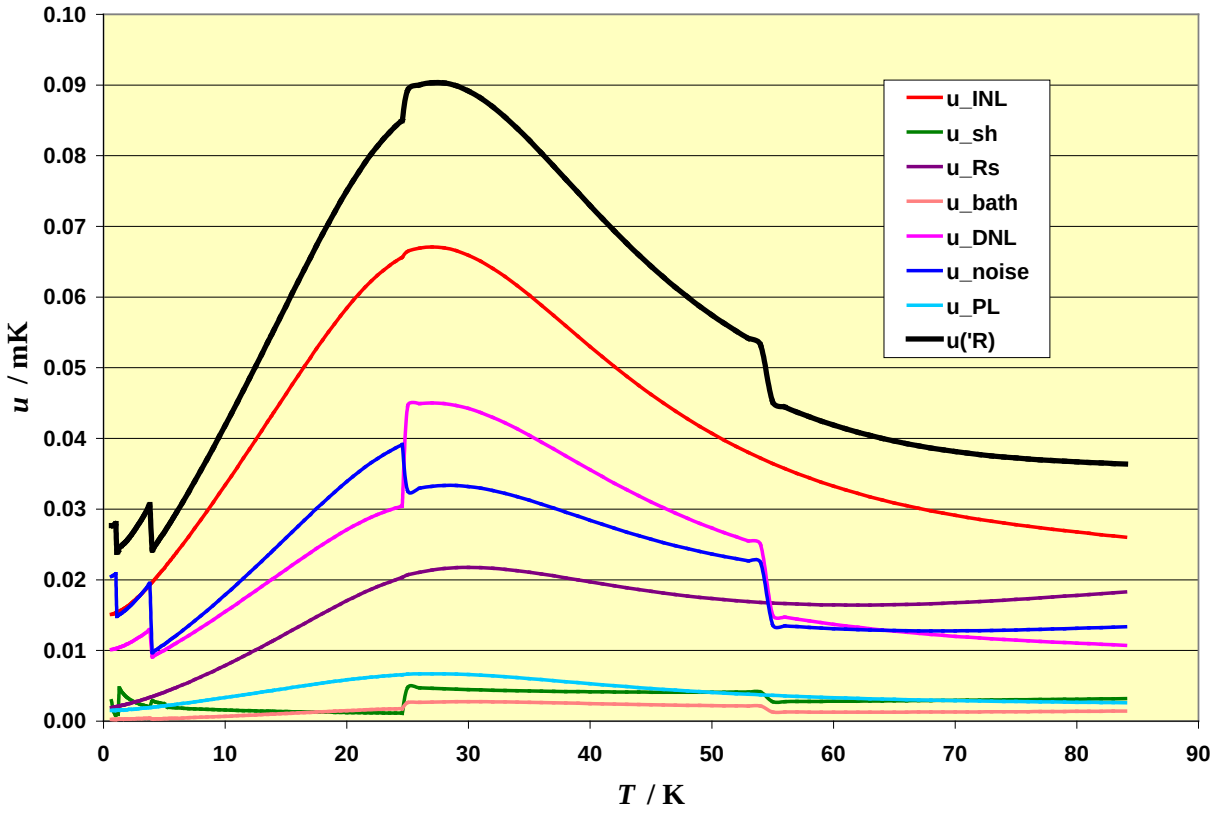

Figure 6.5 Batch RIRT measurement uncertainty components as a function of temperature over the range 0.65 K to 83.8 K.

6.2.2 ITS-90 Realization Uncertainties 0.65 K to 83.8058 K

These uncertainty components pertain to the thermo-physical aspects of the ITS-90 realizations as performed at NIST in the range 0.65 K to 84.8058 K. In the range $T \leq 24.5561$ K, these are essentially the same as those prepared for the CCT K1 comparison [135]. The combined realization uncertainty u_{cr} is the RSS of the individual uncertainty components.

6.2.2.1 ^{3}He and ^{4}He VP, 0.65 K to 5.0 K

These uncertainties have been previously discussed by Meyer and Reilly [105]. In this assessment we have made the following modification to that original treatment. The uncertainty of the piston gauge calibration has been augmented to include an offset or "zero" uncertainty of 0.1 Pa, [120] in addition to the common 12 μPa/Pa proportional term. The ^{3}He VP definition is used below 2.0 K, and the ^{4}He VP definition is used above 2.0 K.

6.2.2.2 ICVGT definition, 5.0 K to 24.556 K

These uncertainties have been previously discussed by Meyer and Reilly [103]. In this assessment we have simply allowed for an error propagation between the ICVGT calibration points.

6.2.2.3 SPRT definition, 24.556 K to 83.806 K

These uncertainties are derived from the propagation of fixed-point calibration uncertainties already treated in section 6.1 for SPRTs.

6.2.3 Comparison Process

6.2.3.1 Thermal Uniformity

As in the case of SPRT comparison uncertainties described in section 6.1.3.1, the comparison block is subject to local heating from the combined thermometer-element, lead-wire and wiring-harness resistances under normal RIRT measurement excitations. These local heating effects are generally negligible for RIRT comparisons since excitation currents are generally lower than those used during SPRT comparisons.

6.2.3.2 Temperature Control

As in the case of SPRTs discussed in section 6.1.3.2, there are Fourier components to the control fluctuations which span time scales comparable to the basic comparison measurement cycle of ≈35 minutes for AC RIRT measurements. Therefore, these Fourier components of the control fluctuations produce comparison errors. The uncertainty component $u_{TC}(W)$ accounts for this effect and is estimated by 0.03 mK + 1 μK/K of the temperature.

6.2.3.3 Thermal Equilibrium

This component accounts for imperfect equilibrium of the comparison system under changing conditions such as switching between thermometers and switching currents. For comparisons between 0.65 K and ~ 10 K, the data acquisition system pauses for a 30 second wait time τ_{wait} after each such change before resuming data acquisition. The relative effect of these thermal perturbations is estimated by summing all major system time constants and dividing by the wait time. The major system time constants are those associated with: 1. total self-heating resistance and the internal heat capacitance, $\tau_{int}=(\eta_{int}+\eta_{ext})C_{int}$; 2. external self-heating resistance and thermometer package heat capacitance, $\tau_{ext}=\eta_{ext}C_{ext}$ (see section 1.4.1 and Figure 5.5); and 3. the

thermal diffusivity time constant of the comparison block $\tau_d = l^2/\alpha_d$, for l=5 cm. The uncertainty estimate is calculated from the time constant ratio multiplied by the magnitude of the self-heating perturbations or $u_{TE}(W) = \Delta T_{sh} \Sigma \tau_i / \tau_{wait}$. For RIRTs at temperature $\lesssim$10 K, the longest time constant is that for equilibration, or $\tau_{ext} \lesssim 0.1$ s, which is sufficiently short to make this uncertainty component negligible in this range.

6.2.3.4 Reference Thermometer Measurement

This component accounts for the measurement uncertainty associated with the determination of the temperature during comparisons with the reference RIRT. It includes all of the uncorrelated terms described in section 6.2.1 but excludes terms corresponding to common systematic errors for all RIRTs and channels in the comparison process. Specifically, the uncertainty is estimated as the RSS of $u_{TRs}(R)$, $u_{DNL}(R)$, $u_{noise}(R)$, and $u_{PL}(R)$.

6.2.3.5 Reference Thermometer Stability

This component is an estimate of uncertainty associated with instability of an RIRT reference thermometer's calibration. The standard uncertainty is estimated as 10 μK + 10 μΩ/(dR/dT).

6.2.3.6 Batch Thermometer Measurement

This component accounts for the measurement uncertainty associated with the determination of the resistance of the batch RIRT under calibration. The terms are identical to those for the RIRT reference thermometer measurement described above in section 6.2.3.4. Since they are either random in nature or otherwise uncorrelated with those associated with the reference thermometer, both sets of measurement uncertainties contribute to the total comparison uncertainty.

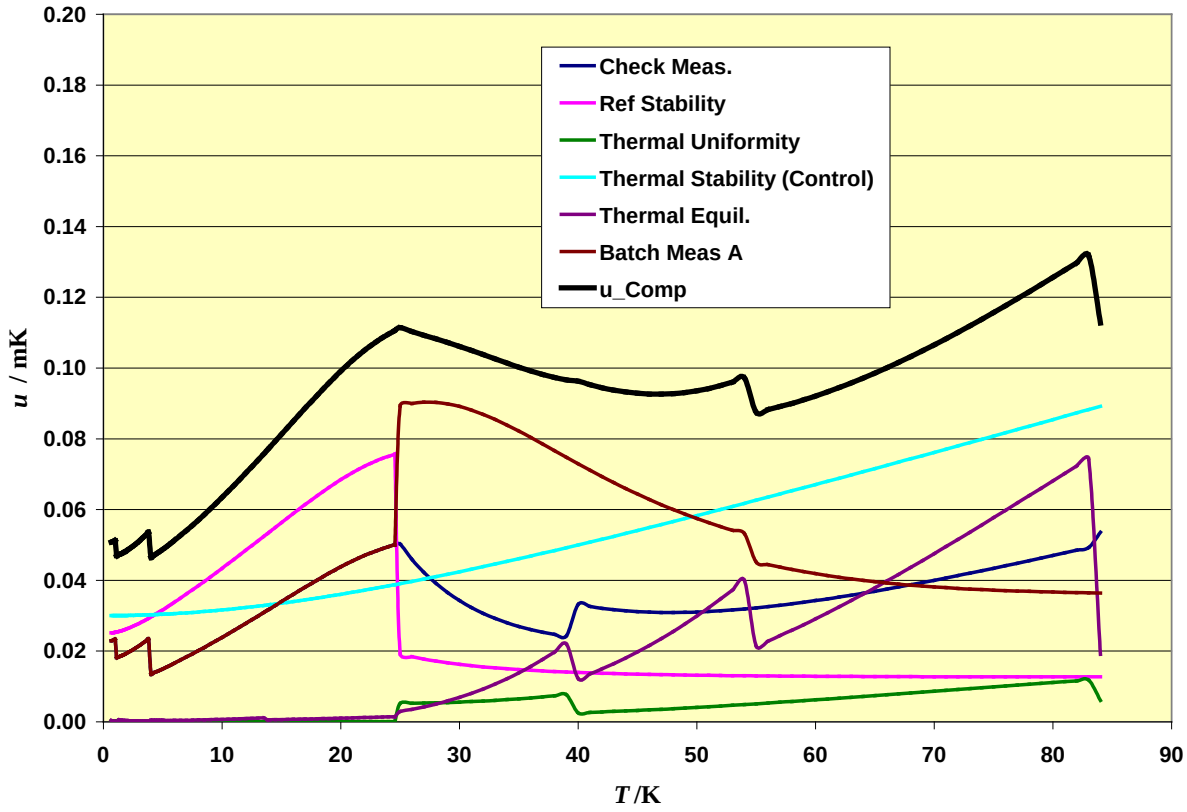

Figure 6.6 Comparison uncertainties for extended range RIRT calibrations.

6.2.4 Check RIRT or SPRT Calibration Uncertainties

In the range 0.65 K to 24.556 K where an RIRT reference is employed, this component accounts for the check RIRT calibration uncertainty. This uncertainty component $u_{\text{chkcal}}(T)$ includes the combined realization uncertainty u_{cr} described in section 6.2.2 as appropriate to the various ITS-90 scale definitions used over this range. In addition, $u_{\text{chkcal}}(T)$ includes the RIRT measurement uncertainties u_{cm} for this range of temperatures according to

$$u^2_{\text{chkcal}} = u^2_{\text{cr}} + u^2_{\text{cm}} . \qquad 6.14$$

The measurement systems associated with the original NIST check RIRT calibrations are different from those employed in the LTCF. Therefore, all measurement uncertainty components described in section 6.2.1 are included in calculating u_{cm} .

For extended range calibrations of RIRTs above 24.556 K, an SPRT reference is used whose interpolation calibration uncertainty $u_{\text{chkcal}}(T)$, is governed by Eqn. 6.7 for the fixed-point uncertainty and the normal error propagation as described above in section 6.1.4.

6.2.5 Non-Uniqueness

For the range 0.65 K to 24.556 K, calibrations are accomplished with respect to a NIST check RIRT which has been calibrated at NIST as described in section 5.1. The calibration data are used to produce a statistical fit to various polynomial $R(T)$ functional forms as described in section 5.5. The statistical fit is imperfect and introduces some degree of non-uniqueness to the check thermometer calibration process. This is a type of interpolation non-uniqueness and for the purposes of this discussion we refer to this uncertainty component as "type 0" non-uniqueness. This uncertainty is accounted for by a simple linear uncertainty component u_{NU0}=0.03 mK + 0.000003×T applied over this range.

A type 2 non-uniqueness exists in the ITS-90 for the range 1.25 K to 3.2 K where the ^{3}He and ^{4}He vapor pressure definitions overlap. The magnitudes are typically $u_{\mathrm{NU2}} \lesssim 0.1$ mK. For the interval 13.8 K<T<20.2714 K, the type 2 non-uniqueness uncertainty u_{NU2} is the same as that described above in section 6.1.5. This applies even though the ICVGT definition is being disseminated for RIRT calibrations over this range.

For the extended range RIRT calibrations above 24.556 K, the same two non-uniqueness uncertainty components u_{NU1} and u_{NU3} (type 1 and type 3), as described under section 6.1.5, also apply since a check SPRT serves as the reference thermometer in this range. Hence, from 13.8 K to 273.16 K, the non-uniqueness uncertainties applicable to RIRT calibrations are identical to those shown in Figure 6.3.

6.2.6 Total RIRT Comparison Calibration Uncertainty

The procedure used here is analogous to that described in section 6.1.6 above for SPRTs, except that the complications of the fixed-point versus comparison calibration methods are no longer relevant. The batch RIRT calibration uncertainty u_{batcal} is calculated as the RSS of the comparison uncertainty u_{comp}, the check calibration uncertainty u_{chkcal}, the correlated batch RIRT measurement uncertainty $u_{\mathrm{batm\text{-}c}}$, and the correlated check thermometer measurement uncertainty $u_{\mathrm{chkm\text{-}c}}$, or

$$u_{\mathrm{batcal}}^2 = u_{\mathrm{comp}}^2(T) + u_{\mathrm{chkcal}}^2(T) + u_{\mathrm{batm\text{-}c}}^2(T) + u_{\mathrm{chkm\text{-}c}}^2(T), \qquad 6.15$$

for a given temperature in the calibration range.

The correlated batch and check RIRT measurement uncertainties $u_{\mathrm{batm\text{-}c}}$ and $u_{\mathrm{chkm\text{-}c}}$ are assumed to be zero when like RIRTs are being compared. These components are separated from u_{comp} because they occur for both the check RIRT and the batch RIRT so that any associated errors cancel in the comparison of like RIRTs. For the range 0.65 K to 24.556 K this is normally the case.

For the extended range calibrations from 24.556 K to 83.8 K, the reference (SPRT) and batch (RIRT) thermometers are different in this range. In this case both $u_{\mathrm{batm\text{-}c}}$ and $u_{\mathrm{chkm\text{-}c}}$ must be accounted for since the systematic measurement uncertainties are different. Each of these

uncertainties are a partial RSS of the purely systematic components of the combined measurement uncertainty u_{cm} (see section 6.1.1 and 6.2.1) excluding those quasi-random components already included in u_{comp} (see section 6.2.3). Specifically,

$$u_{batm\text{-}c}^2 = u_{Rs}^2 + u_{INL}^2 + u_{sh}^2, \qquad 6.16$$

and similarly for $u_{chkm\text{-}c}$.

In the range 0.65 K to 24.556 K, the total calibration uncertainty $u_{batcal\text{-}Total}(T)$ for the batch RIRT is the RSS uncertainty from the RIRT check calibration uncertainty and the various appropriate non-uniqueness uncertainty components u_{NU0},u_{NU1}, u_{NU2}, u_{NU3}. Specifically,

$$u_{batcal\text{-}Total}^2(T) = u_{batcal}^2(T) + u_{NU0}^2(T) + u_{NU1}^2(T) + u_{NU2}^2(T) + u_{NU3}^2(T) \qquad 6.17$$

For the extended range calibrations from 24.556 K to 83.8 K equation 6.13 is used.

Figure 6.7 is a summary plot of the principle components for the RIRT total calibration uncertainty.

The NIST total calibration uncertainty in temperature as given in Eqn. 6.17 includes the NIST resistance measurement uncertainty. Since the calibration is expressed in Ohms, however, the user's resistance measurement uncertainty must also be considered. When a calibrated RIRT is used by the customer to calculate temperature, the customer must add his or her own resistance measurement uncertainty as well as other system-related temperature uncertainties to Eqn. 6.17 in order to calculate the total user uncertainty in the temperature as determined by the RIRT.

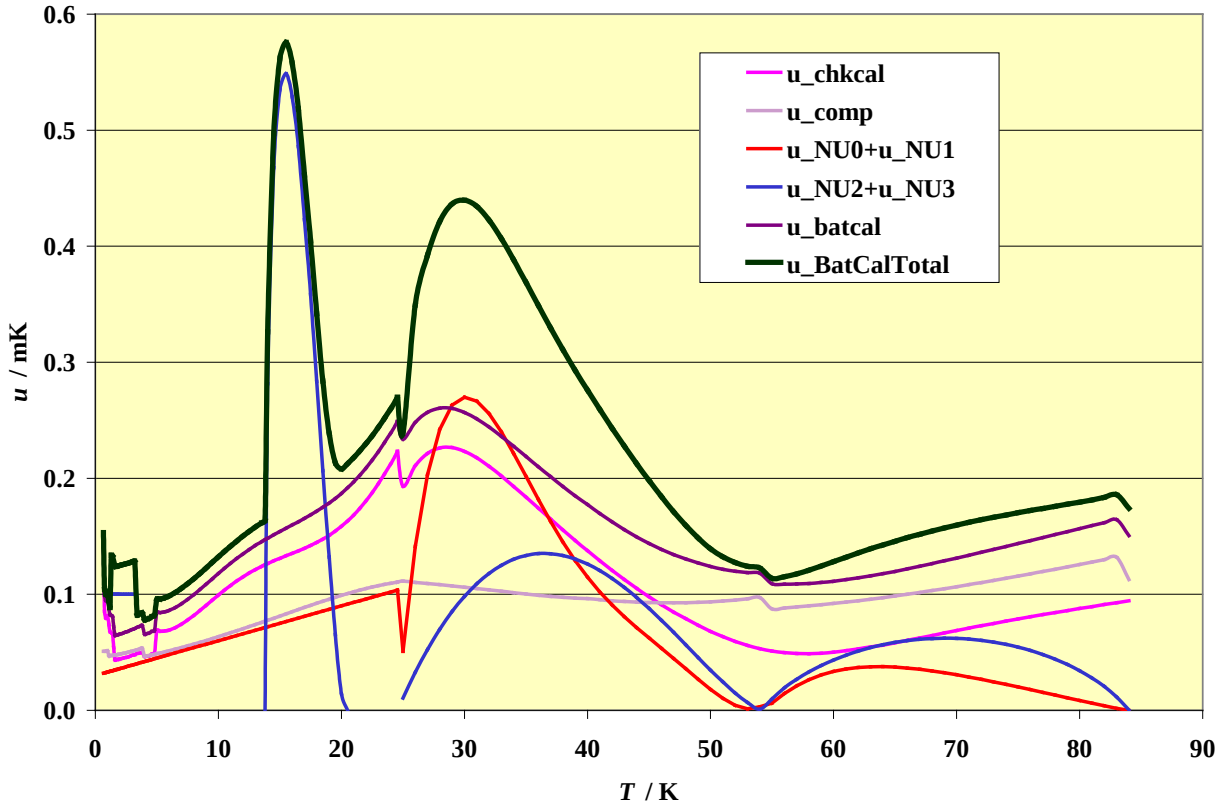

Figure 6.7 Principal uncertainty components and total batch RIRT calibration uncertainty for an extended range calibration from 0.65 K to 83.8 K.

6.3 GeRT Uncertainties 0.65 K to 24.556 K

In this case we are treating the calibration of a device which is in many ways different from the RIRT check thermometers used as references in the comparison process. The comparison of dissimilar thermometers precludes the possibilities of correlated measurement and comparison uncertainties so that all systematic uncertainty components must be explicitly included in the uncertainty budget.

6.3.1 GeRT Resistance Measurement Uncertainty

A typical GeRT will be calibrated using DC excitation over nearly 4 decades in resistance and excitation current. In some cases, AC excitation is also used for $T \gtrsim 13.8$ K and $I \geq 100$ μA. The currents are adjusted down as temperature is lowered to keep the excitation voltage approximately constant or within the range of 2 to 6 mV. This in turn causes the dissipation power to also drop with temperature over almost 4 decades. Table 6.6 shows the approximate calibration parameters appropriate for a typical GeRT with $R_{GeRT}(4.2\ K) \approx 250\ \Omega$.

Table 6.6. ITS-90 Calibration parameters for a batch (customer) GeRT ($R(4.2\ K) \approx 250\ \Omega$, typical).

Definition	T_{90} / K	$R_{GeRT}(T_{90})$ / Ω	X	R_s / Ω	I/ μA
^{3}He VP	0.65 to 2.0	50 k to 1.0 k	5 to 0.1	10 k	0.1 to 5†
^{4}He VP	2.0 to 5.0	1.0 k to 200	1.0 to 0.2	1 k	5 to 25†
ICVGT	5.0 to 24.5561	200 to 6	2.0 to 0.06	100	25 to 1000†
ICVGT	13.8 to 24.5561	18 to 6	0.09 to 0.03	200	100 to 1000‡

†DC; ‡AC

In this example the resistance ratio measurements are performed with bi-polar DC excitation, using a set of three resistance standards, $R_{s,}$ and various excitation currents, I_1, I_2, as shown in Table 5.3 and $V_{cal}=I_{cal}R_{GeRT}=2$ mV. The measured resistance ratio is $X \equiv R_{GeRT}(T_{90})/R_s$ as constructed from DC voltage data via equation 5.1.

Calibration data for GeRTs consist of resistance values, $R(T_{90})$, in ohms taken at about 25 points distributed over the range 0.65 K to 24.556 K which allows the construction of an accurate interpolation function for the calibration range. A lower-range polynomial expansion in $\log(T_{90})$ in the form shown in equation 5.2b is generally sufficient to represent $\log(R_{GeRT})$ with approximately 12 coefficients in the range 0.65 K to 13 K. A second similar but lower-order polynomial starting at ~ 13 K is adequate to complete the interpolation for calibrations up to 24.6 K or slightly higher (see Table 5.4 for specific temperatures).

The individual uncertainty components in the resistance measurement uncertainty are similar to those already discussed for SPRT and RIRT measurements with a few notable differences as explained below. Equation 6.18 (a modified form of equation 6.2) may be used to calculate the combined form for all GeRT measurement uncertainties.

$$u_{\mathrm{cm}}^2(R_{\mathrm{GeRT}}) = X^2\left\{u^2(R_{\mathrm{s,cal}}) + A(I_1,I_2)R_{\mathrm{s}}^2\beta_{\mathrm{s}}^2u^2\left(T_{\mathrm{RS}}\right)\right\} + u_{\mathrm{sh}}^2\left(R_{\mathrm{GeRT}}\right) \\ +R_{\mathrm{s}}^2\left\{u^2\left(X_{\mathrm{INL}}\right) + A(I_1,I_2)\left[u^2\left(X_{\mathrm{DNL}}\right) + u^2\left(X_{\mathrm{n}}\right)\right]\right\} \tag{6.18}$$

It should be noted that in the case of finite current calibrations where $I_{\mathrm{cal}} \cong I_1$, the parameter $A(I_1,I_2) \cong 1$ because there is no significant extrapolation in current or power being made.

6.3.1.1 Resistance Standards Uncertainties

The three resistance standards listed in Table 6.6 are sufficient for the entire calibration range. The first term in Eqn. 6.17 is the uncertainty $u_{R\mathrm{s}}(R)$ associated with the calibration uncertainties $u(R_{\mathrm{s\text{-}Cal}})$. The next term is the uncertainty $u_{TR\mathrm{s}}(R) \equiv u(T_{\mathrm{RS}})$ associated the thermal stability of the resistance standards (≈0.05 K) and is generally negligible. The contributions u_{Rs} do not exceed 0.5 μΩ/Ω or ≈0.008 mK at 24.56 K for a 250 Ω GeRT.

6.3.1.2 Non-linearity.

The DC measurement INL uncertainty $u(X_{\mathrm{INL}})$ is treated similarly to that for AC bridge measurements in section 6.1.1. The physical origin is different, however, being a combination of ADC non-linearity, range-dependent offsets, and range-dependent gain errors. A conservative estimate of $u(X_{\mathrm{INL}})$=1 μV/V is used for the entire calibration range. The DNL uncertainty $u(X_{\mathrm{DNL}})$ is treated as a pseudo-random uncertainty due to quantization noise and is negligible (≈ 1 nV/2 mV=0.5 μV/V) in this case.

6.3.1.3 Measurement Noise.

The random noise contribution $u_{\mathrm{n}}(X)$ from the DC measurement system is temperature dependent due to the variable resistance and sensitivity. This component is modeled as two noise terms, a voltage noise v_{n} and a current noise i_{n}, such that the observed rms measurement noise is $v_{\mathrm{n\text{-}obs}} = (v_{\mathrm{n}}^2 + i_{\mathrm{n}}^2 R_{\mathrm{GeRT}}^2)^{½}$ for the GeRT voltage measurement at signal amplitude V_{cal} and similarly for the standard resistor voltage measurement at signal amplitude V_{cal}/X. It is then straightforward to show that

$$u_n^2\left(X\right) = X^2\left[\frac{v_n^2}{V_{\mathrm{cal}}^2}\left(1+X^2\right) + 2\frac{i_n^2R_{\mathrm{GeRT}}^2}{V_{\mathrm{cal}}^2}\right]. \tag{6.18}$$

The DC instrumentation presently being used in the NIST LTCF has characteristic noise components of v_{n}=20 nV and i_{n}=30 pA, or $R_{\mathrm{n}} \equiv v_{\mathrm{n}}/i_{\mathrm{n}}$=667 Ω. The current noise will always dominate at high resistance (i.e. $R_{\mathrm{GeRT}} >> R_{\mathrm{n}}$) and the voltage noise will dominate at low resistance (i.e. $R_{\mathrm{GeRT}} << R_{\mathrm{n}}$).

6.3.1.4 Self-Heating.

GeRT calibrations are usually provided at a constant excitation voltage $V_{\mathrm{cal}} \approx I_1R_{\mathrm{GeRT}}$ and not corrected for self-heating. This means that a finite self-heating is effectively “built-in” to the

calibration. This is a practical compromise which introduces an uncertainty originating from the imperfect reproducibility of the self-heating coefficient η from one installation to another. This is due to the variable nature of the external self heating contribution, η_{ext} (see discussion in section 1.3). The finite-self-heating uncertainty in the resistance measurement is estimated as 50% of the observed self-heating at the calibration voltage or $u_{sh}(R_{GeRT})=0.5(dR/dT)\eta V_{cal}^2/R_{GeRT}$. This uncertainty is larger than the normal self-heating correction uncertainty for zero-power calibrations as given by the last term in equation 6.2.

6.3.1.5 Combined GeRT Measurement Uncertainty

The individual contributions to the GeRT resistance measurement uncertainty are shown in figures 6.8a in μΩ/Ω and 6.8b in mK. The combined GeRT resistance measurement uncertainty $u_{cm}(R_{GeRT})$ is calculated using equation 6.17 and plotted as the solid black line in Figure 6.8. The resistance measurement uncertainty is dominated by self-heating uncertainty and measurement noise, with current noise always dominating at the lowest temperatures (i.e. highest resistances). Unlike the case of capsule-type SPRT or RIRT calibrations, the resistance measurement in GeRT calibrations represents a significant contribution to the overall calibration uncertainty, particularly at the upper end of the calibration range. Given this fact, NIST will normally tabulate $u_{cm}(R_{GeRT})$ separately from the temperature related uncertainties (i.e. $u(R_{GeRT})$ is not combined with $u(T)$) for GeRT calibration reports.

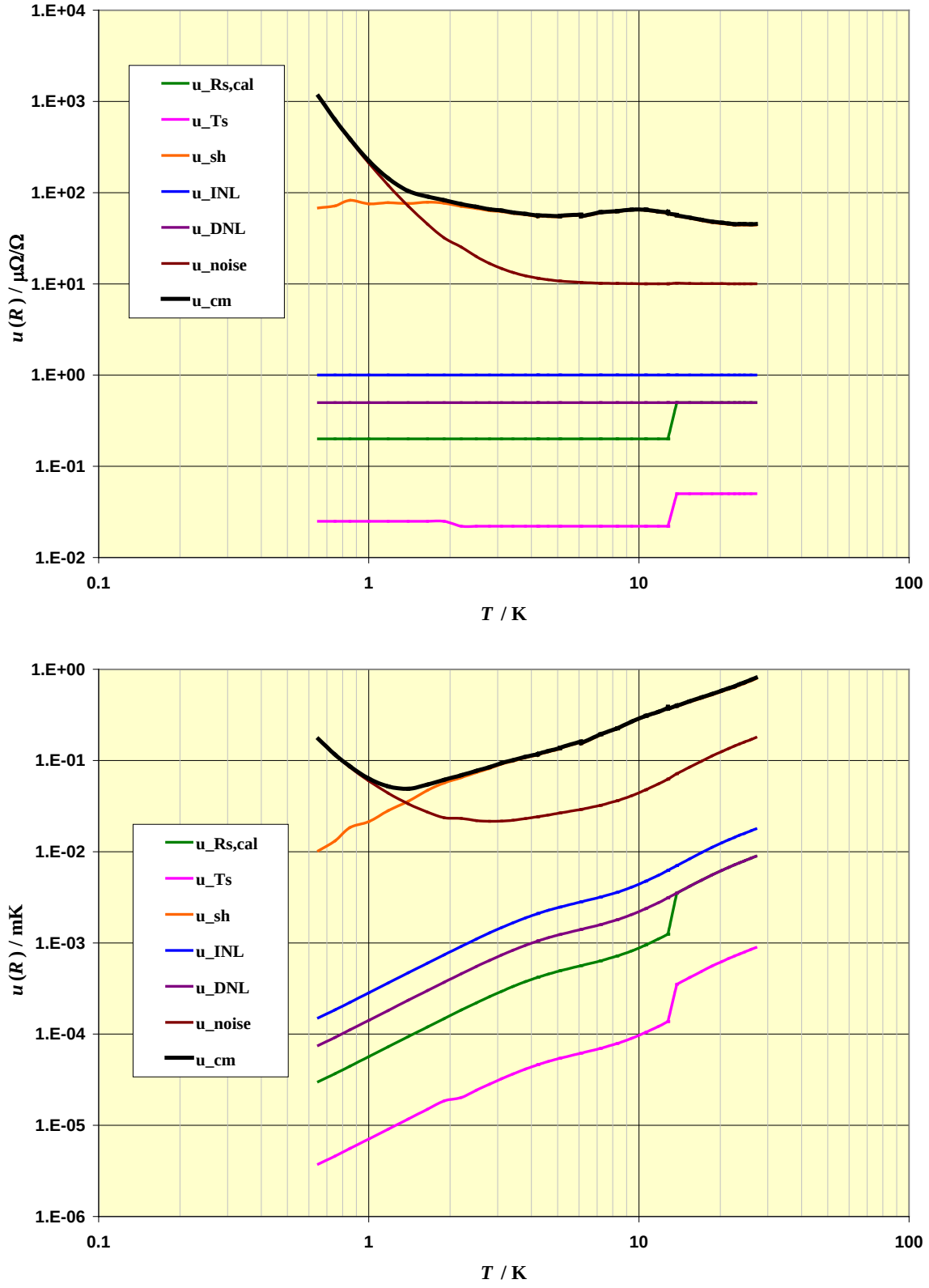

Figure 6.8 The resistance measurement uncertainties for a 250 Ω GeRT calibration at 2 mV, **a**. expressed as relative uncertainties in μΩ/Ω, **b**. expressed as thermometric uncertainties in mK.

6.3.2 ITS-90 Scale-Related Uncertainties

The ITS-90-related uncertainties for a GeRT calibration are those which arise in the calibration of the NIST check RIRT and in the various ITS-90 non-uniqueness terms already described. As treated in section 6.2.4, the uncertainty component $u_{\mathrm{chkcal}}(T)$ includes the combined realization uncertainty u_{cr} described in section 6.2.2 for the various ITS-90 scale definitions and the RIRT combined measurement uncertainties u_{cm} described in section 6.2.1 for the range of temperatures 0.65 K≤T≤24.5561 K. The non-uniqueness uncertainties are limited to the same type 0 and type 2 terms already described in section 6.2.5. The u_{NU0} term exists over the entire calibration range from the RIRT fit statistics. The u_{NU2} term exists in the He vapor pressure overlap interval from 1.25 K to 3.2 K and also in the ICVGT/*e*-H_2 VP overlap interval 13.8 K<T<20.2714 K.

6.3.3 GeRT versus RIRT Comparison Process Uncertainties

The comparison calibration of a batch GeRT against a check RIRT is in many ways analogous to the calibration of a batch RIRT and the comparison uncertainties will be essentially the same in most cases. Referring to the descriptions in section 6.2.3, there are several terms which would be expected to differ from the RIRT vs. RIRT case given there. The combined comparison uncertainty $u_{\mathrm{comp}}(T)$ is given by the RSS of all the terms discussed here except for the batch GeRT resistance measurement uncertainty, which is handled separately.

6.3.3.1 Thermal Uniformity

As is the case for batch RIRT calibrations, the local heating effects are generally negligible for GeRT calibrations since the power levels are even smaller than the 1 μW level for RIRTs.

6.3.3.2 Temperature Control

This uncertainty component $u_{\mathrm{TC}}(W)$ is the same as given in section 6.2.3.2 and is estimated by 0.03 mK + 1 μK/K of the temperature.

6.3.3.3 Thermal Equilibrium

As discussed in section 6.2.3.3 for RIRTs, the thermal response time of the thermometers under comparison determines the net system response for T≲50 K. The τ_{tr} for GeRTs would be expected to differ from that of RIRTs due to the fact that the observed self-heating coefficients η are factors of 40 to 400 times greater than that of typical capsule RIRTs over the range 0.65 K to 24.56 K. However, the mass of 3 mm diameter GeRT capsules are typically a factor of 10 to 20 times smaller than that of capsule RIRTs. The net result is that the predicted effect would be perhaps a factor 2 to 20 times longer response times in GeRTs over this temperature range. The relatively high thermal diffusivity of the single crystal Ge, the base heat sink, and the copper sheath materials tend to mitigate the relative time constants further still, such that at 4.2 K the thermal time constant of a 3 mm GeRT is only ≈200 ms compared to ≈100 ms for a capsule RIRT. Given the 30 s to 60 s wait times employed in the NIST LTCF calibration software, the resulting thermal equilibration uncertainties are again negligible.

6.3.3.4 RIRT Check Thermometer Measurement

In this case, the reference RIRT resistance measurement uncertainty must include all of the individual terms described in section 6.2.1 for the comparison process. Specifically, the uncertainty is estimated as the RSS of $u_{\mathrm{Rs}}(R)$, $u_{\mathrm{INL}}(R)$, $u_{\mathrm{sh}}(R)$, $u_{\mathrm{TRs}}(R)$, $u_{\mathrm{DNL}}(R)$, $u_{\mathrm{noise}}(R)$, and $u_{\mathrm{PL}}(R)$.

6.3.3.5 Reference Thermometer Stability

This uncertainty component is the same as previously described in section 6.2.3.5.

6.3.3.6 Batch Thermometer Measurement

As previously discussed, the batch GeRT resistance measurement uncertainty, as described in section 6.3.1, is not combined with the other temperature-specific uncertainties. Rather, these uncertainties $u(R_{\mathrm{GeRT}})$ are tabulated as a separate category in GeRT calibration reports.

6.3.4 Total Comparison Calibration Uncertainty for GeRTs

The batch GeRT calibration uncertainty u_{batcal} is calculated as the RSS of the comparison uncertainty u_{comp}, and the check calibration uncertainty u_{chkcal}, as described above, or

$$u^2_{\mathrm{batcal}} = u^2_{\mathrm{comp}}(T) + u^2_{\mathrm{chkcal}}(T), \tag{6.19}$$

for the calibration temperature range 0.65 K to 24.556 K.

In the range 0.65 K to 24.556 K, the total calibration uncertainty $u_{\mathrm{batcal\text{-}Total}}(T)$ for the batch GeRT is the RSS uncertainty from the batch calibration uncertainty and the two appropriate non-uniqueness uncertainty components u_{NU0} and u_{NU2}. Specifically,

$$u^2_{\mathrm{batcal\text{-}Total}}(T) = u^2_{\mathrm{batcal}}(T) + u^2_{\mathrm{NU0}}(T) + u^2_{\mathrm{NU2}}(T) \tag{6.20}$$

These principal uncertainty components are shown in Figure 6.9 for the calibration range 0.65 K to 24.556 K. By comparing the GeRT resistance measurement uncertainty, shown in Figure 6.8b, with the batch calibration temperature uncertainty $u_{\mathrm{batcal\text{-}Total}}(T)$, one can see that the GeRT resistance measurement uncertainty is dominant over the entire range with the exception of two small intervals between ≈1 K to ≈3 K and between ≈14 K to ≈17 K. This is the primary reason why the two uncertainty components are not combined for GeRT calibration reports.

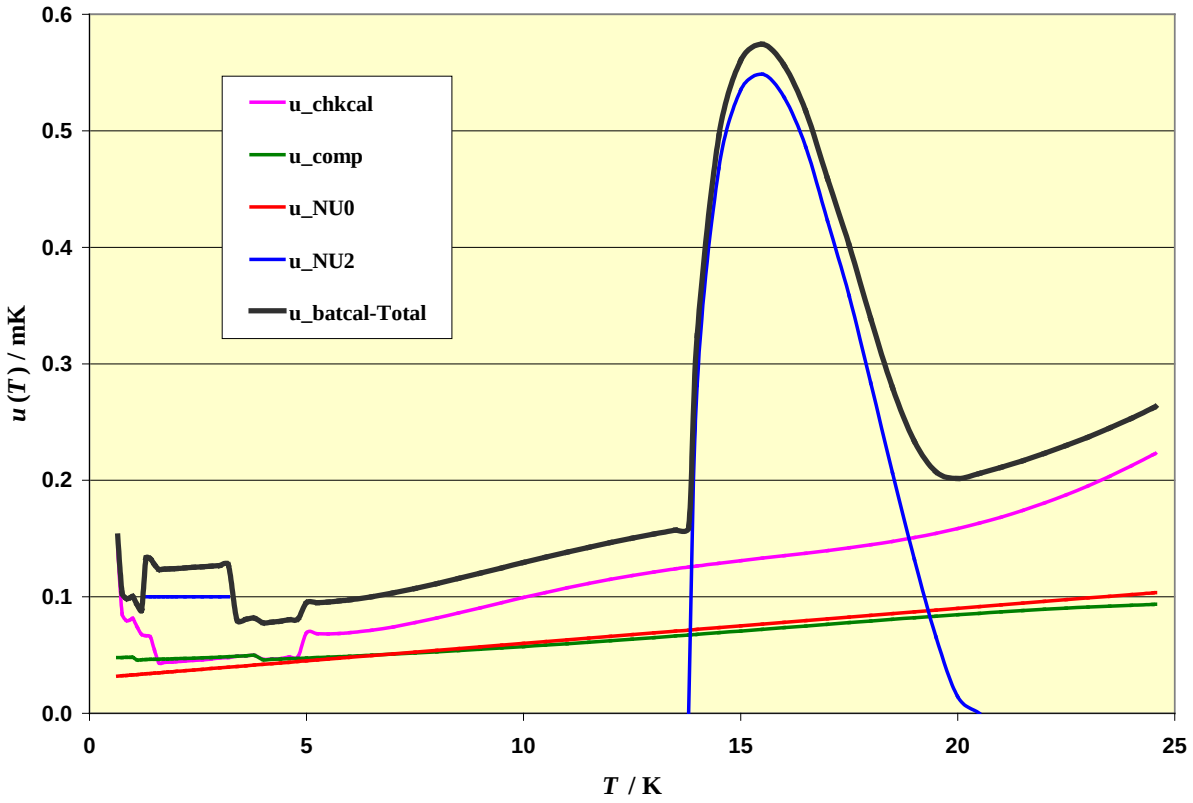

Figure 6.9 The principal uncertainty components for the total batch calibration uncertainty in temperature for a GeRT comparison calibration from 0.65 K to 24.556 K.

The end user should add the resistance measurement uncertainty appropriate to his or her own measurement system to equation 6.20 in order to determine the uncertainty when the GeRT is used as a reference to determine temperature on the ITS-90.

6.4 Other Thermometer Types

Other cryogenic resistance thermometers not explicitly treated here will yield calibration uncertainties which are comparable to those already described, providing that they are sufficiently stable and exhibit moderate to low self heating.

6.4.1 PTC

Other PTC devices such as PCRTs will achieve calibration uncertainties comparable to those given here for RIRTs. The main difference will be that the PCRT resistance measurement uncertainty will exhibit a maximum close to 12 K rather than ≈26 K as in the case of RIRTs (see figure 6.5. This is a consequence of the Pt-Co sensitivity exhibiting a relative minimum near 12 K.

6.4.2 NTC

Other NTC resistance thermometers such as ZNRTs and RORTs will exhibit calibration uncertainties in temperature similar to those given here for GeRTs. Differences will exist in the resistance measurement uncertainty depending on the self heating and sensitivity of the device.

7 References

1. H. Preston-Thomas, "The International Temperature Scale of 1990 (ITS-90)", *Metrologia* 27, 3 (1990); *ibid*, 107 (1990).
2. L. G. Rubin, *Cryogenics* , 37 (7), 341-356 (1997).
3. R. J. Corruccini, "Temperature Measurements in Cryogenic Engineering", in: *Advances in Cryogenic Engineering*, Vol. 8, 315-333, Timmerhaus, Ed., (Plenum Press, New York, 1962).
4. L. G. Rubin, *Cryogenics*, 10 (1), 14-22 (1970).
5. L. G. Rubin, B. L. Brandt, and H. H. Sample, *Cryogenics*, 22, 491-503, (1982).
6. L. L. Sparks, "Temperature, Strain, and Magnetic Field Measurements", Chapter 14, in: Materials at Low Temperatures, R. P. Reed and A. F. Clark, Eds., American Society for Metals, Metals Park Ohio, (1983) pp. 515-571.
7. S. S. Courts, D. S. Holmes, P. R. Swinehart, and B. C. Dodrill, "Cryogenic Thermometry, An Overview", in: *Applications of Cryogenic Technology*, Vol. 10, J. P. Kelly, Ed., 55-69 (Plenum Press, New York, 1991).
8. C. J. Yeager and S. S. Courts, *IEEE Sensors Journal*, 1, 352-60 (2001).
9. J. W. Ekin, "Experimental Techniques for Cryostat Design, Material Properties and Superconductor Critical-Current Testing", Chapter 5, Oxford University Press, (2006) pp. 185-225.
10. D. S. Holmes and S. S. Courts, "Resolution and Accuracy of Cryogenic Temperature Measurements", in: *Temperature: Its Measurement and Control in Science and Industry*, Vol. 6, 1225-1230, J.F. Schooley, ed., American Institute of Physics, New York (1992).
11. E. R. Pfeiffer, NIST Unpublished data, (1992).
12. G. K. White and S. B. Woods, *Phil. Trans. Royal Soc. Lond. Ser. A*, 251, 273-302 (1959).
13. Lake Shore Cryotronics Inc, Temperature Measurement and Control Catalog, Appendix G "Temperature Sensor Response Data Tables", pp. 200-206 (2004).
14. P. C. F. Wolfendale, J. D. Yewen, and C. I. Daykin, "A New Range of High Precision Resistance Bridges for Resistance Thermometry", *in*: "Temperature: Its Measurement and Control in Science and Industry", Vol. 5, 729-737, J. F. Schooley, ed., American Institute of Physics, New York (1982).
15. X. G. Feng, S. Zelakiewicz, and T. J. Gramila, *Rev. Sci. Instrum.*, 70, 2365-2371 (1999).
16. P. Bramley and J. R. Pickering, Cal Lab, Oct.-Dec., 21-26 (2006).
17. Automatic Systems Laboratories, Models F700, F18, and F900 AC Resistance Ratio Bridges.
18. Lakeshore Cryotronics, Inc, Model 370 AC Resistance Bridge.
19. Isotech North America, Inc., Model MicroK-400.
20. W. J. M. Moore and P. M. Miljanic, Current Comparator, 120 pp., (Peter Peregrinus, London, 1988).
21. Measurements International, Inc., Model 6015T.
22. Hart Scientific, Inc., Models 1575A and 1590.
23. P. Ptak, A. Kolek, Z. Zawislak, A. W. Stadler, and K. Mleczko., *Rev. Sci. Instrum.*, 76, 014901 (2005).
24. J. V. Nicholas and D. R. White, "Traceable Temperatures",2nd. Ed., 450 pp. (Wiley, 2001).
25. D. S. Holmes and S. S. Courts, in: *Advances in Cryogenic Engineering*, Vol.41, P. Kittel, Ed., 1699-1706, (Plenum Press, New York, 1996).

26. G. X. Mack, A. C. Anderson, and P. R. Swinehart, *Rev. Sci. Instrum*, 54, 949-951 (1983).
27. L. M. Besley and L. Hai, *Rev. Sci. Instrum*., 64 (3) 748-755 (1993).
28. S. S. Courts, W. E. Davenport, and D. S. Holmes, in: *Advances in Cryogenic Engineering*, Vol. 45B, Quan-Sheng Shu, Ed., pp. 1849-1856, (Plenum Press, New York, 2000).
29. Thermometrics, Inc., Edison N.J. "NTC Thermistors" (1981). Available at: http://www.thermometrics.com/assets/images/ntcnotes.pdf
30. C. J. Yeager, S. S. Courts, and W. E. Davenport, in: *Advances in Cryogenic Engineering*," Vol. 49A, J. Waynert, Ed., pp. 412-419 (American Institute of Physics, NY, 2004).
31. R. Rusby, "Rhodium-Iron, Ten Years On", in: *Temperature, Its Measurement and Control in Science and Industry*, Vol. 5, J. Schooley, Ed., AIP, New York, (1982).
32. J. L. Riddle, G. T. Furukawa, and H. H. Plumb, "Platinum Resistance Thermometry", NBS Monograph 126, US Dept. of Commerce, April 1973, 126 pp.
33. D. J. Curtis, "Thermal Hysteresis and Stress Effects in Platinum Resistance Thermometers" *in*: "Temperature: Its Measurement and Control in Science and Industry", Vol. 5, 803-812, J. F. Schooley, ed., American Institute of Physics, New York (1982).
34. H. M. Edlow and H. H. Plumb, in: *Advances in Cryogenic Engineering*, Vol. 6, 542, Timmerhaus, Ed., (Plenum Press, New York, 1961).
35. Lakeshore Cryotronics, Inc., Temperature Measurement and Control Catalog, Appendix C "Sensor Packaging and Installation", pp. 166-178 (2004).
36. American Society for Testing and Materials, Standard Test Method for Testing Industrial Resistance Thermometers, E 644-06, Section 9, 2006, ASTM International, West Conshohocken, PA, USA.
37. W. L. Tew and G. F. Strouse, "Standard Reference Material 1750: Standard Platinum Resistance Thermometers 13.8033 K to 429.7484 K", NIST Special Publication 260-139, Dec, 2001.
38. C. H. Meyers, "Coiled Filament Resistance Thermometers", *Bur. Stand. J. Res*., 9, 807-813 (1932).
39. D. J. Curtis, "Platinum Resistance Interpolation Standards", in: "*Temperature: Its Measurement and Control in Science and Industry*", Vol. 4, 951-961, H. H. Plumb, ed., Instrument Society of America, Pittsburgh (1972).
40. L. Crovini, H. J. Jung, R. C. Kemp, S. K. Ling, B. W. Mangum, and H. Sakurai., *Metrologia*, 28, 317-325 (1991).
41. R. Rusby, NPL, Private communication, 2001.
42. R. L. Powell, L.L. Sparks, and J. G. Hust, "Standard Thermocouple Material Pt-67: SRM 1967", NBS Special Publication 250-56, 40 pp., U.S. Government Printing Office (1978).
43. R. W. Phillips, in: *Advances in Cryogenic Engineering*, Vol. 45, 1809-1815, Q-S Shu, Ed., (Kluwer Academic, New York, 2000).
44. L. Hai and L. M. Besley, *Rev. Sci. Instrum*., 64 (3) 741-747 (1993).
45. G. F. Strouse, "Standard Platinum Resistance Thermometer Calibrations from the Ar TP to the Ag FP", NIST Special Publication 250-81, 79 pp. (2008).
46. Minco, Inc., Model S1059, (Manufactured from ~1965 to 2010). Starting in 2013, a replacement model has been commercially available from Temflex Controls, Inc., Quebec.
47. D. A. Lucas, "Miniature Precision Platinum Resistance Thermometers", in: "*Temperature: Its Measurement and Control in Science and Industry*", Vol. 4, 963-969, H. H.. Plumb, ed., Instrument Society of America, Pittsburgh (1972).

48. International Electrotechnical Commission, “Platinum Resistance Thermometers and Platinum Sensors” IEC 60751-2008.
49. American Society for Testing and Materials, “Standard specification for Industrial Platinum Resistance Thermometers”, ASTM E1137-2003.
50. C. D. Vaughn and G. F. Strouse, in: *Proceedings of the 8th International Symposium on Temperature and Thermal Measurements in Industry and Science, TEMPMEKO 2001,* B. Fellmuth, Ed., 629-634 (VDE Verlag, Berlin 2002).
51. Hereaus Sensor Technology GmbH, Models C220 and C420 PRTD (2007).
52. O. Tamura, H. Sakurai, and T. Nakajima, “Low-Temperature Characteristics of some Industrial Grade Platinum Resistance Thermometers”, in: *Temperature: Its Measurement and Control in Science and Industry,* Vol. 6, 443-448, J.F. Schooley, ed., American Institute of Physics, New York (1992).
53. Goodrich Sensor Systems, Model 162D.
54. Chino Works of America, Model R800-0.
55. Leeds and Northrup, Inc., Model 8164 (no longer in production, but widely used).
56. Hart Scientific Division, Fluke, Inc., Model 5686.
57. R. L. Rusby, in: "*Temperature: Its Measurement and Control in Science and Industry*", Vol. 4, 865-869, H. H.. Plumb, ed., Instrument Society of America, Pittsburgh (1972).
58. B. R. Coles, *Phys. Lett*. 8, 243-244 (1964).
59. R. L. Rusby, “Resistance Thermometry using Rhodium-iron, 0.1 K to 273 K”, in: *Temperature Measurement*, Conference Series No. 26 (Institute of Physics, London) 125-130 (1975).
60. Englehard, Ltd., UK, Alloy 1200, (discontinued as of 2000).
61. Consultative Committee on Thermometry, Working Group 2, “Techniques for Approximating the ITS-90”, Chapter 5, Bureau International des Poids et Mesures, Sevres, France (1990).
62. Elmquist, R. E., Jarrett, D. G., Jones, G. R., Kraft, M. E., Shields, S. H., Dziuba, R. F., “NIST Measurement Service for DC standard Resistors”, NIST Technical Note 1458, (US Government Printing Office, Washington, DC, 2004).
63. Tinsley Precision Instruments, Models 5187U and 5187W (no longer in production, but widely used).
64. R. L. Rusby, NPL, Private Communication, 2005.
65. F. London, “Superfluids, Vol. 2 Macroscopic Theory of Superfluid Helium”,Wiley 1954.
66. Yu. P. Filippov, V. V. Golikov, E. N. Kulagin, and V. G. Shabratov, in: *Advances in Cryogenic Engineering*, 43a, 773-780 (1998).
67. L. Peng and L. M. Besley, *Meas. Sci. Technol*. 4 1357 (1993).
68. Dimitrov, in: *Advances in Cryogenic Engineering*, 1996.
69. B.W.A. Ricketson and R.E.J. Watkins, *Cryogenics*, 49, 320-325 (2009).
70. L. M. Besley, *J. Phys. E*., 17, 778-781, (1984).
71. T. Shiratori and K. Mitsui, *Jap. J. Appl. Phys*. 17, 1289-1290 (1978).
72. T. Shiratori, K. Mitsui, K. Yanagisawa and S. Kobayashi, “Platinum-cobalt Alloy Resistance Thermometer for Wide Range Cryogenic Thermometry”, in: *Temperature, Its Measurement and Control in Science and Industry,* Vol. 5, 839-844. (American Institute of Physics, New York, 1982).
73. Chino Corporation of Japan, dba Chino Works America, Inc., Model R800-4.
74. Sakurai and Besley, *Rev. Sci. Instr*. 56, 1232-1235 (1985).

75. J. S. Blakemore, *Rev. Sci. Instr*. 33, 106-112 (1962).
76. J. S. Blakemore, in: "*Temperature: Its Measurement and Control in Science and Industry*", Vol. 4, 827-833, H. H.. Plumb, ed., Instrument Society of America, Pittsburgh (1972).
77. G. Haverson and D. A. Johns, in: "*Temperature: Its Measurement and Control in Science and Industry*", Vol. 4, 803-813, H. H.. Plumb, ed., Instrument Society of America, Pittsburgh (1972).
78. P. R. Swinehart, in: *Temperature, Its Measurement and Control in Science and Industry*, Vol. 5, 835-838. (American Institute of Physics, New York, 1982).
79. L.I. Zarubin, I.Y. Nemisha and A. Szmyrka-Grzebyk, *Cryogenics*, 30, 533-537 (1990).
80. Lakeshore Cryotronics, Inc., Models GR-200A and GR-200B, "Germanium RTDs", www.lakeshore.com .
81. V. F. Mitin, *et. al*., *Cryogenics*, 47, 474-482 (2007).
82. Consultative Committee on Thermometry, Working Group 2, "Techniques for Approximating the ITS-90", Chapter 4, Bureau International des Poids et Mesures, Sevres, France (1990).
83. C. A. Swenson and P. C. F. Wolfendale, *Rev. Sci. Instr*. 44, 339-341 (1973).
84. C. G. M. Kirby and M. J. Laubitz, *Metrologia*, **9**, 103-106, (1973).
85. M. S. Anderson and C. A. Swenson, *Rev. Sci. Instr*. 49, 1027-1033, (1978).
86. L. M. Besley, *Rev. Sci. Instr*. 51, 972-976 (1980).
87. L. M. Besley and A. Szmyrka-Grzebyk, *Rev. Sci. Instr*. 61, 1303-1307 (1990).
88. S. S. Courts and C. J. Yeager, in: *Temperature: Its Measurement and Control in Science and Industry* vol 7, D C Ripple Ed., Melville, New York: AIP Conf. Proc., 405-410 (2003).
89. S. S. Courts and P. R. Swinehart, in: *Temperature: Its Measurement and Control in Science and Industry* vol 7, D C Ripple Ed., Melville, New York: AIP Conf. Proc., 393-398 (2003).
90. Ch. Balle, J. Casas, J.M. Rieubland, A. Suraci, F. Togny and N. Vauthier, in: *Adv. Cryo. Eng*., 45B, Quan-Shan Shu, Ed., 1817–1824 (Kluwer, New York 2000).
91. S. S. Courts and P. R Swinehart, in: *Adv. Cryo. Eng*., 45B, Quan-Shan Shu, Ed., 1841-1848 (Kluwer, New York 2000).
92. Lakeshore Cryotronics, Inc., Models CX-1010, -1030, -1050, 1070, -1080 , "CernoxTM RTDs", www.lakeshore.com .
93. R. W. Vest, "Material Aspects of Think Film Technology" Chapter 8, in: Ceramic Materials for Electronics, R. C. Buchanan, Ed., Marcel-Decker, Inc., 532 pp., New York, 1991.
94. N. Koppetzki, *Cryogenics*, 23, 559-561 (1983).
95. A. Briggs, *Cryogenics*, 31, 932-935 (1991).
96. R.G. Goodrich, D. Hall, E. Palm and T. Murphy, *Cryogenics*, 38, 221-225 (1998).
97. Lakeshore Cryotronics, Inc., Models RX-102, -103, -202, "Ruthenium Oxide Rox™ RTDs", www.lakeshore.com ; and Scientific Instruments, Inc., Models RO-600 and RO-105, www.scientificinstruments.com ; and Cryogenic Control Systems, Inc., Model R400, www.cryocon.com .
98. B. W. Mangum and G. A. Evans, "Stability of Some Epoxy-Encapsulated Diode Thermometers", NBSIR 86-3337 (NASA), US Dept. of Commerce, Gaithersburg, MD, February 1986.
99. B. W. Mangum and G. T. Furukawa, "Guidelines for Realizing The International Temperature Scale of 1990 (ITS-90)", *NIST Technical Note 1265*, (US Government Printing Office, Washington, DC, 1990).

100. G. F. Strouse, “NIST implementation and realization of ITS-90 over the range 83 K to 1235 K”, in: *Temperature: Its Measurement and Control in Science and Industry*, Vol. 6, p169, J.F. Schooley, ed., American Institute of Physics, New York (1992).
101. W. L. Tew, G. F. Strouse, C. W. Meyer, and G. T. Furukawa, “Recent Advances in the Realization and Dissemination of the ITS-90 below 83.8058 K at NIST”, *Advances in Cryogenic Engineering*, Vol. 43B, P. Kittel, editor, (Plenum Press, New York, 1998).
102. W. L. Tew and B. W. Mangum, “New Procedures and Capabilities for the Calibration of Cryogenic Resistance Thermometers at NIST”, in *Advances in Cryogenic Engineering*, Vol. 39B, p. 1019, P. Kittel, editor, (Plenum Press, New York, 1994).
103. C. W. Meyer and M. L. Reilly, “Realization of the ITS-90 at the National Institute of Standards and Technology in the range 3.0 K to 24.5561 K using an Interpolating Constant Volume Gas Thermometer”, *Proceedings of TEMPMEKO ’96*, P. Marcarino, editor, pp. 39-44, Levrotto and Bella, Torino, Italy (1997).
104. B. W. Mangum, G T Furukawa, C W Meyer, G F Strouse, W L Tew , “Realization of the ITS-90 at the NIST” *Proceedings of TEMPMEKO ’96*, P. Marcarino, editor, pp. 33-38, Levrotto and Bella, Torino, Italy (1997).
105. C. W. Meyer and M. L. Reilly, “Realization of the ITS-90 at the National Institute of Standards and Technology in the range 0.65 K to 5.0 K using ^{3}He and ^{4}He vapor pressure thermometry”, *Metrologia*, Vol. 33, pp. 383-390, (1996).
106. G. T. Furukawa, B. W. Mangum, and G. F. Strouse, “Effects of different methods of preparation of ice mantles of triple point of water cells…”, *Metrologia*, Vol. 34, pp.215-233, (1997).
107. G.T. Furukawa, “Realization of the mercury triple point”, *in*: "Temperature: Its Measurement and Control in Science and Industry", Vol. 6, p.281, J.F. Schooley, ed., American Institute of Physics, New York (1992).
108. Strouse, G.F. and Lippiatt, J., “New NIST Mercury Triple-Point Cells”, in *Proc. TEMPMEKO 2001*, Vol. 2, p. 783-788, 2002..
109. G. T. Furukawa, J. L. Riddle, W. R. Bigge, E. R. Pfeiffer, “Application of Some Metal SRM’s as Thermometric Fixed Points”, National Bureau of Standards Special Publication 260-77, pp. 87-102, U.S. Government Printing Office, Washington, D.C. (1982).
110. G.T. Furukawa, “Reproducibility of the triple point of argon in sealed transportable cells”, *in*: “Temperature: Its Measurement and Control in Science and Industry”, Vol. 5, p.239, J.F. Schooley, ed., American Institute of Physics, New York (1982).
111. F. Pavese and G. Molinar, “Modern Gas-Based Temperature and Pressure Measurements”, Plenum Press, New York (1992). and F. Pavese, “International Intercomparison of Fixed Points by Means of Sealed Cells*”, BIPM Monographie 84/4*, (1984).
112. G. F. Strouse, B. W. Mangum, C. D. Vaughn, and E. Y. Xu, “A New NIST Automated Calibration System for Industrial-Grade Platinum Resistance Thermometers”, *NISTIR 6225*, National Institute of Standards and Technology, Gaitherburg, MD (2000).
113. G.T. Furukawa, “Argon triple point apparatus with multiple thermometer wells”, in: *Temperature: Its Measurement and Control in Science and Industry*, Vol. 6, p.265, J.F. Schooley, ed., American Institute of Physics, New York (1992).
114. C. W. Meyer and M. L. Reilly, “Realization of the ITS-90 Triple Points From 13,80 K to 83,8 K at NIST”, *Proceedings of the IMEKO International Seminar on Low Temperature Thermometry and Dynamic Temperature Measurement*, pp. L-110 – L-115, IMEKO, Wroclaw, Poland, (September, 1997).

115. G.T. Furukawa, " The triple point of oxygen in sealed transportable cells", *J. Res. Nat. Bur. Stand.* (U.S.), 91, 255 (1986).
116. W. L. Tew, "Sealed-cell devices for the realization of the triple point of neon at the National Institute of Standards and Technology", *Proceedings of TEMPMEKO '96*, P. Marcarino, editor, p. 81, Levrotto and Bella, Torino, Italy (1997).
117. Meyer C W and Tew W L , "The NIST Low Temperature ITS-90 Realization and Calibration Facilities", in *Temperature: Its Measurement and Control in Science and Industry* vol 7, ed D C Ripple et al (Melville, New York: AIP Conf. Proc.) 137-142 (2003).
118. Tew W L and Meyer C W , "Recent Results of NIST Realizations of the ITS-90 below 83.8 K" in *Temperature: Its Measurement and Control in Science and Industry* vol 7, ed D C Ripple et al (Melville, New York: AIP Conf. Proc.) 143-148 (2003).
119. C. W. Meyer, G. F. Strouse, and W. L. Tew, "Non-Uniqueness of the ITS-90 from 13.8033 K to 24.5561 K" , *Proceedings of TEMPMEKO '99*, Delft, Netherlands, June 1999.
120. Fellmuth B., Wolber L., Hermier Y., Pavese F., Steur P.P.M., Peroni I., Szmyrka-Grzebyk A., Lipinski L., Tew W.L., Nakano T., Sakurai H., Tamura O., Head D., Hill K.D., Steele A.G., "Isotopic and other influences on the realization of the triple point of hydrogen" *Metrologia*, 2005, 42, 171-193.
121. S. D. Ward and J. P. Compton, "Intercomparison of Platinum Resistance Thermometers and T_{68} Calibrations", *Metrologia*, Vol. 15, pp. 31-46, (1979).
122. Furukawa, G. T., "Vapor Pressures of Natural Neon and of the Isotopes ^{20}Ne and ^{22}Ne from the triple Point to the Normal Boiling Point., *Metrologia*, Vol. 8, pp.11-27, 1972.
123. W. L. Tew, G. F. Strouse, and C. W. Meyer, "A Revised Assessment of Calibration Uncertainties for Capsule Type Standard Platinum and Rhodium-Iron Resistance Thermometers", *NISTIR 6138*, (US Government Printing Office, Washington DC, April 1998).
124. G. F. Strouse and W. L. Tew, "Assessment of Uncertainties of Calibration of Resistance Thermometers at the National Institute of Standards and Technology", *NISTIR 5319*, (US Government Printing Office, Washington DC, January 1994).
125. B.N. Taylor and C.E. Kuyatt, "Guidelines for Evaluating and Expressing the Uncertainty of NIST Measurement Results", *NIST Technical Note 1297*, 1994 Edition., 20 pp. (Sept. 1994).
126. ISO, "Guide to the Expression of Uncertainty in Measurement", International Organization for Standards, Geneva, Switzerland (1993).
127. H. Preston-Thomas, T. J. Quinn, and P. Bloembergen, "Supplementary Information for the ITS-90", p. 55, BIPM, (December, 1990).
128. E. R. Pfeiffer, "Realization of the ITS-90 below 83.8058 K at the NIST", in *Temperature: Its Measurement and Control in Science and Industry*, edited by J. F. Schooley, Vol. 6, AIP, New York, 1992. pp. 155-160.
129. J. V. Nicholas, *et. al*. "Effects of Heavy Hydrogen and Oxygen on the Triple Point Temperature of Water", *Proceedings of TEMPMEKO '99*, Delft, Netherlands, pp. 95-99., June 1999. We assume the same factor as used by Nicholas: 0.6 μK/ppm ^{2}H.
130. Zhao, M. and Strouse, G.F., "VSMOW Triple Point of Water Cells: Borosilicate versus Fused-Quartz", *Int. J. Thermophysics*, 28, 1928-1930 (2007).
131. Strouse, G.F. and Zhao, M., "The Impact of Isotopic Concentration, Impurities, and Cell Aging on the Water Triple Point Temperature", *Int. J. Thermophysics*, 28, 1913-1922 (2007).

132. W. L. Tew and C. W. Meyer, "Adjustment to the NIST Realization of the ITS-90 from 5 K to 24.5561 K", *Report to the CCT*, CCT/2008-09, 2008, Bureau International des Poids et Mesures, Sevres, France.
133. Working Group 1, Consultative Committee on Thermometery, "Mise en pratique for the definition of the kelvin", Section 2. Technical annex for the International Temperature Scale of 1990 (ITS-90), BIPM, 2007.
134. Steele, A., et. al., *Metrologia*, 39, 2002, 551-571.
135. R. Rusby, D. Head, C. W. Meyer, W. L. Tew, O. Tamura, K. D. Hill, M. de Groot, A. Storm, A. Peruzzi, B. Fellmuth J. Engert, D. Astrov, Y. Dedikov and G. Kytin, "Final Report on CCT-K1: Realizations of the ITS-90, 0.65 K to 24.5561 K, using rhodium–iron resistance thermometers", *Metrologia* 43, Tech. Supp. 03002, (2006).
136. B. Fellmuth, D. Berger, L. Wolber, M. de Groot, D. Head, Y. Hermier, Y. Z. Mao, T. Nakano, F. Pavese, V. Shkraba, A. G. Steele, P. P. M. Steur, A. Szmyrka-Grzebyk, W. L. Tew, L. Wang, and D. R. White, "An International Star Intercomparison of Low-Temperature Fixed Points Using Sealed Triple-Point Cells",in *Temperature: Its Measurement and Control in Science and Industry* vol 7, ed D C Ripple *et. al.* (Melville, New York: AIP Conf. Proc. #684) 885-890 (2003).
137. Apiezon Products, Apiezon N , M&I Materials Ltd., Manchester, M32 0ZD, UK.
138. Automatic Systems Laboratories, Model F18 AC Resistance Bridge, New Addington, CR0 0AE, UK.
139. Tinsley Precision Instruments, Model 5685A AC/DC Standard ("Wilkins") Resistors, New Addington, CR0 0AE, UK.
140. D. R. White, K. Jones, J. M. Williams, I. E. Ramsey, *IEEE Trans. Instrum. Meas*., 46, 1068-1074 (1997).
141. G. F. Strouse and K. D. Hill, "Performance Assessment of Resistance Ratio Bridges Used in the Calibration of SPRTs" in *Temperature: Its Measurement and Control in Science and Industry* vol 7, ed D C Ripple et al (Melville, New York: AIP Conf. Proc.) 327-332 (2003).
142. Agilent Technologies, Model 3458A Auto-calibrating Digital Multi-Meter, Santa Clara , CA 95051 USA.
143. M. E. Cage, D. Yu, B. M. Jeckelmann, R. L. Steiner, and R. V. Duncan, *IEEE Trans. Instrum. Meas*., 40, 262-266 1991.
144. R. J. Corruccini, *Rev. Sci. Instrum*., 31, 637-640 (1960).
145. Committee on Conformity Assessment, International Standards Organization, "General requirements for the competence of testing and calibration laboratories", ISO/IEC 17025:2005, Technical Corrigendum 1, ISO, Geneva, 2005.
146. C. W. Meyer and D. C. Ripple, *Metrologia*, 43 327–340 (2006).
147. D.R. White, M. Ballico, V. Chimenti, S. Duris, E. Filipe, A. Ivanova, A. Kartal Dogan, E. Mendez-Lango, C. Meyer, F. Pavese, A. Peruzzi,E. Renaot, S. Rudtsch, K. Yamazawa, *Int. J. Thermophys*., 28, 1868-1881 (2007). See expanded report: "Uncertainties in the Realisation of the SPRT Subranges of the ITS-90" Consultative Committee on Thermometry, CCT/08-19, Bureau International de Poids et Mesures, Sevres, France, November 2008.
148. Pavese, et. al., *Int. J. Thermophys*., 29, 57-66 (2008).
149. Tew, W. L., *Int. J. Thermophys*., 29, 67-81 (2008).

150. F. Pavese, W. L. Tew, and A. G. Steele, in: *Proceedings of the 8th International Symposium on Temperature and Thermal Measurements in Industry and Science, TEMPMEKO 2001*; Ed. B Fellmuth, (2002).
151. B. W. Mangum, P. Bloembergen, M. V. Chattle, B. Fellmuth, P. Marcarino, and A. I. Pokhodun, Metrologia, 34, 427-429 (1997).
152. C. W. Meyer and W. L. Tew, *Metrologia*, 43 341–352 (2006).
153. K. D. Hill and A. G. Steele, "The Non-Uniqueness of the ITS-90: 13.8 K to 273.16 K" in *Temperature: Its Measurement and Control in Science and Industry* vol 7, ed D C Ripple et al (Melville, New York: AIP Conf. Proc.) 53-58 (2003).

Appendix A. Sample Calibration Reports

A1 SPRT, 13.8 K to 273.16 K
A2 RIRT, 0.65 K to 24.556 K
A3 GeRT, 0.65 K to 27.1 K

UNITED STATES DEPARTMENT OF COMMERCE
NATIONAL INSTITUTE OF STANDARDS AND TECHNOLOGY
GAITHERSBURG, MARYLAND 20899

REPORT OF CALIBRATION

International Temperature Scale of 1990

Standard Platinum Resistance Thermometer
Serial Number 1234567

Submitted by
Anybody, Inc.
Anywhere, XX USA

This standard platinum resistance thermometer (SPRT) was calibrated with an AC bridge operating at a frequency of 30 Hz and with continuous measuring currents of I_1 and I_2 as given below. In accordance with the International Temperature Scale of 1990 (ITS-90) that was officially adopted by the Comité International des Poids et Mesures (CIPM) in September 1989, the combined subranges from 13.8 K to 273.16 K and 273.15 K to 429.7485 K were used to calibrate the thermometer. The calibration points of Hg, H_20, and In were measured in fixed point cells with expanded uncertainties (EU) as given below for the particular cells used in conjunction with this type of SPRT. The calibration points at the Ar, O_2, Ne, H_2 triple points (TP) and H_2 vapor pressure (VP) points were measured by comparison to a reference SPRT, s/n 1842385, that has been calibrated using recent realizations of these fixed points at NIST. The comparison measurements were performed under isothermal conditions, in vacuum, and the expanded uncertainties given here were combined from uncertainties due to the comparison measurements and the fixed point realizations. For a description of the uncertainties, see *NIST Internal Report 6138*, 36 pp. (1998).

Fixed Point	**Temperature**		**Currents**		**EU, (k = 2)**
	T_{90} (K)	t_{90} (°C)	I_1(mA)	I_2 (mA)	(mK)
H_2 TP	13.8033	-259.3467	2.828	5.0	0.63
H_2 VP	17.0357	-256.1143	2.828	5.0	0.26
H_2 VP	20.2712	-252.8799	2.0	2.828	0.26
Ne TP	24.5561	-248.5939	2.0	2.828	0.32
O_2 TP	54.3584	-218.7916	1.0	2.0	0.38
Ar TP	83.8058	-189.3442	1.0	2.0	0.51
Hg TP	234.3156	-38.8344	1.0	1.414	0.3
H_2O TP	273.16	0.01	1.0	1.414	0.05
In FP	429.7485	156.5985	1.0	1.414	0.5

The most recent measurement (11 Apr 2009) of the resistance of this thermometer at 273.16 K was calculated to be: 25.576550 ohms at 0 mA; 25.576600 ohms at 1.0 mA, and 25.576750 ohms at 2.0 mA. During calibration, the resistance at 273.16 K changed by the equivalent of 0.45 mK at 0 mA and 0.55 mK at 1.0 mA.

This thermometer is satisfactory as a defining instrument of the ITS-90 in accordance with the criteria that W(302.9146 K)≥ 1.11807 or W(234.3156 K)≤ 0.844235.

For the Director,
National Institute of Standards and Technology

NIST Service ID No. 33020C
Test No. 685/123456-12
12 Apr 2012
Purchase Order No. 12345-ABC

Gregory Strouse
Leader, Thermodynamic Metrology Group
Sensor Science Division

Standard Platinum Resistance Thermometer
Serial Number 1234567

Submitted by
Anybody, Inc.
Anywhere, XX USA

Coefficients of the ITS-90 Deviation Functions

The following values were determined for the coefficients of the pertinent deviation functions of the ITS-90, as given in the attached material describing the scale. For the convenience of the user, coefficients are given for three different currents, 0 mA, 1.0 mA, and 2.0 mA, as extrapolated from measurements at the two currents I_1 and I_2 given on the cover sheet. The 2 mA case is best used for measurements below about 30 K, while 1 mA is adequate for all other temperatures. The 0 mA case is used for extrapolating to zero power dissipation and elimination of self-heating errors. The attached tables were generated using the 1 mA calibration and 2 mA calibration values only.

0 mA Calibration	**1.0 mA Calibration**	**2.0 mA Calibration**
a_1 = -5.169609557E-04	a_1 = -5.180685293E-04	a_1 = -5.214030680E-04
a_2 = -2.203396593E-04	a_2 = -2.199184135E-04	a_2 = -2.186912471E-04
c_1 = 3.129240516E-06	c_1 = 3.510604101E-06	c_1 = 4.643099836E-06
c_2 = 2.536276863E-08	c_2 = 2.462324196E-07	c_2 = 9.001773889E-07
c_3 = -2.608380512E-07	c_3 = -2.098716209E-07	c_3 = -5.946958735E-08
c_4 = -4.681956260E-08	c_4 = -4.140397051E-08	c_4 = -2.547777041E-08
c_5 = -2.419095387E-09	c_5 = -2.198518148E-09	c_5 = -1.552103277E-09
a_{10} = -5.052981855E-04	a_{10} = –5.048155768E–04	a_{10} = -5.033661122E-04

NIST Service ID No. 33020C
Test No. 685/123456-12
12 Apr 2012
Purchase Order No. 12345-ABC

UNITED STATES DEPARTMENT OF COMMERCE
NATIONAL INSTITUTE OF STANDARDS AND TECHNOLOGY
GAITHERSBURG, MARYLAND 20899

REPORT OF CALIBRATION

International Temperature Scale of 1990

Rhodium-Iron Resistance Thermometer
Serial Number A123

Submitted by
ABC Laboratories,
Anywhere, USA

This Rhodium-Iron Resistance Thermometer (RIRT) was calibrated with an AC resistance bridge at a frequency of 30 Hz using pairs of constant measuring currents between 0.10 mA and 0.50 mA. The thermometer was calibrated under isothermal conditions in vacuum by comparison with various reference thermometers maintained at NIST. From 0.65 K to 24.556 K the reference and check thermometers were RIRT B174 and RIRT B168, respectively. Measurements were made at twenty six (26) temperatures in the range 0.65 K to 24.55.1 K.

The reference and check thermometers have been calibrated at NIST from direct realizations of the ITS-90. Temperatures from 0.65 K to 2.0 K are derived from ^{3}He vapor pressure realizations and temperatures between 2 K and 5 K are derived from ^{4}He vapor pressures realizations. Temperatures between 5 K and 24.56 K are derived from NIST realizations of the ITS-90 via an Interpolating Constant Volume Gas Thermometer.

Table 1 shows data used for the calibration: the resistance, R in ohms; and temperature T in kelvin,. For the purposes of this calibration the resistance values have been corrected to reflect measurement currents of 0.20 mA over the entire calibration range. Table 1 also contains the following results: two polynomial representations of the data, R_{f1} and R_{f2} which are valid in different temperature ranges ; the first derivatives of the fitting functions dR_{fi}/dT; the residuals between the fits and the data, $R_{fi} - R$, expressed in millikelvins; and the Expanded Uncertainty (EU) for the calibration expressed in millikelvins with a coverage factor of $k = 2$. For a description of these uncertainties, see: *NIST Internal Report 6138*, 36 pp., (1998), entitled "A Revised Assessment of Calibration Uncertainties of Capsule type Standard Platinum and Rhodium-Iron Resistance Thermometers".

The resistance data were fitted by two separate functions of temperature, to a 7th (seventh) order polynomial below 7.2 K and a separate 7th (seventh) order polynomial between 5.1 K and 24.56 K. The fits are based on calculated resistances for a fixed measuring current of 0.20 mA for this thermometer. The two functions agree to within 0.025 mK between 5.1 K and 7.2 K, and the first derivatives are continuous to within 0.3 %. Table 2 lists the power series expansion coefficients used in these fits. An interpolation table, which has been generated by these same fits (Table 3), is also provided.

For the Director,
National Institute of Standards and Technology

Gregory Strouse
Leader, Thermodynamic Metrology Group
Sensor Science Division

NIST Service ID No. 33140C
Test No. 685/123456-12
1 Feb 2012
Purchase Order No. 12345-ABC
Page 1 of 3

Rhodium-Iron Resistance Thermometer
Serial Number A123

Submitted by
ABC Laboratories,
Anywhere, USA

Table 1. Temperatuer and Resistance data for RIRT s/n A-123.

T / K	R(0.2 mA)/Ω	R_{f1} / Ω	R_{f2} / Ω	dR_{f1}/dT / Ω/K	dR_{f2}/dT / Ω/K	(R_{f1} - R) / mK	(R_{f2} - R) / mK	EU / mK
0.6580	3.067170	3.067176		0.37133		0.018		0.24
0.8510	3.138713	3.138696		0.36979		-0.045		0.15
1.1792	3.259319	3.259336		0.36504		0.045		0.13
1.6492	3.428681	3.428672		0.35490		-0.026		0.13
2.1995	3.619976	3.619982		0.34010		0.018		0.13
2.7997	3.818843	3.818831		0.32234		-0.036		0.13
3.0999	3.914212	3.914218		0.31328		0.021		0.13
3.4140	4.011132	4.011137		0.30382		0.017		0.12
4.2211	4.246770	4.246765		0.28028		-0.018		0.13
5.0997	4.482467	4.482469	4.482465	0.25670	0.25682	0.008	-0.006	0.19
6.0997	4.727124	4.727123	4.727125	0.23321	0.23310	-0.002	0.005	0.19
7.1993	4.970829	4.970829	4.970824	0.21015	0.21075	0.000	-0.025	0.20
8.3001	5.192048		5.192047		0.19165		-0.006	0.20
9.4003	5.393675		5.393676		0.17529		0.009	0.21
10.5998	5.594520		5.594522		0.16001		0.015	0.22
11.7987	5.778332		5.778332		0.14695		0.001	0.22
12.7975	5.920282		5.920273		0.13748		-0.063	0.23
13.8031	6.054201		6.054196		0.12905		-0.041	0.35
15.3972	6.250522		6.250530		0.11764		0.066	0.61
17.0395	6.435535		6.435540		0.10800		0.047	0.26
18.6928	6.607381		6.607374		0.10015		-0.064	0.29
20.2754	6.760978		6.760972		0.09420		-0.055	0.27
21.5046	6.874426		6.874429		0.09054		0.030	0.28
22.6046	6.972535		6.972542		0.08794		0.076	0.27
23.6052	7.059564		7.059571		0.08609		0.076	0.31
24.5602	7.141132		7.141123		0.08477		-0.105	0.34

A polynomial fit of the resistance as a function of temperature of
Rhodium-Iron Resistance Thermometer
Serial Number A123

Submitted by
ABC Laboratories
Anywhere, USA

For the range of temperatures 0.65 K < T< 7.2 K , the polynomial fit of resistance R_{f1} as a function of temperature T is given by,

$$R_{f1}(T) = \sum_{n=0}^{7} a_n T^n$$

where the coefficients $\boldsymbol{a_n}$ are given in Table 2 below.

For the range of temperatures 5.1 K < T< 24.6 K, the polynomial fit of resistance R_{f2} as a function of temperature T is given by,

$$R_{f2}(T) = \sum_{n=0}^{7} b_n T^n$$

where the coefficients $\boldsymbol{b_n}$ are given in Table 2 below. In both cases, temperatures are in kelvins and resistances are in ohms. The resistances are fitted for measurement currents of 0.20 mA over the entire calibration range.

Table 2.

	coefficient		**coefficient**
$\boldsymbol{a_0}$	2.82347457E+00	$\boldsymbol{b_0}$	2.73538372E+00
$\boldsymbol{a_1}$	3.66282671E-01	$\boldsymbol{b_1}$	4.53717315E-01
$\boldsymbol{a_2}$	1.15867781E-02	$\boldsymbol{b_2}$	-2.78182531E-02
$\boldsymbol{a_3}$	-9.38891280E-03	$\boldsymbol{b_3}$	1.41638709E-03
$\boldsymbol{a_4}$	1.93693564E-03	$\boldsymbol{b_4}$	-5.19275944E-05
$\boldsymbol{a_5}$	-2.42399637E-04	$\boldsymbol{b_5}$	1.24300813E-06
$\boldsymbol{a_6}$	1.77663850E-05	$\boldsymbol{b_6}$	-1.67187154E-08
$\boldsymbol{a_7}$	-5.74397305E-07	$\boldsymbol{b_7}$	9.54409371E-11

Table 3. ITS-90 Interpolation table for the RIRT A-123. Resistance in Ohms.

T/K	0	0.1	0.2	0.3	0.4	0.5	0.6	0.7	0.8	0.9
0								3.082 756	3.119 828	3.156 807
1	3.193 667	3.230 385	3.266 939	3.303 310	3.339 482	3.375 439	3.411 167	3.446 654	3.481 890	3.516 866
2	3.551 573	3.586 005	3.620 156	3.654 020	3.687 594	3.720 873	3.753 856	3.786 541	3.818 924	3.851 007
3	3.882 787	3.914 265	3.945 441	3.976 316	4.006 890	4.037 165	4.067 141	4.096 821	4.126 206	4.155 299
4	4.184 102	4.212 616	4.240 845	4.268 792	4.296 458	4.323 848	4.350 964	4.377 809	4.404 387	4.430 701
5	4.456 754	4.482 551	4.508 095	4.533 389	4.558 437	4.583 243	4.607 811	4.632 144	4.656 247	4.680 122
6	4.703 772	4.727 202	4.750 415	4.773 412	4.796 197	4.818 772	4.841 139	4.863 298	4.885 251	4.906 997
7	4.928 537	4.949 867	4.970 987	4.991 963	5.012 758	5.033 372	5.053 806	5.074 063	5.094 146	5.114 056
8	5.133 797	5.153 371	5.172 780	5.192 026	5.211 111	5.230 039	5.248 811	5.267 428	5.285 895	5.304 211
9	5.322 380	5.340 404	5.358 283	5.376 022	5.393 620	5.411 081	5.428 405	5.445 595	5.462 653	5.479 581
10	5.496 379	5.513 050	5.529 596	5.546 018	5.562 317	5.578 496	5.594 556	5.610 498	5.626 324	5.642 036
11	5.657 634	5.673 121	5.688 498	5.703 766	5.718 926	5.733 980	5.748 930	5.763 776	5.778 520	5.793 164
12	5.807 708	5.822 153	5.836 501	5.850 754	5.864 912	5.878 976	5.892 948	5.906 828	5.920 619	5.934 320
13	5.947 933	5.961 460	5.974 901	5.988 257	6.001 529	6.014 719	6.027 827	6.040 854	6.053 801	6.066 670
14	6.079 460	6.092 174	6.104 812	6.117 375	6.129 864	6.142 279	6.154 622	6.166 894	6.179 095	6.191 226
15	6.203 288	6.215 282	6.227 209	6.239 069	6.250 864	6.262 594	6.274 260	6.285 862	6.297 402	6.308 880
16	6.320 297	6.331 654	6.342 952	6.354 190	6.365 371	6.376 494	6.387 561	6.398 572	6.409 527	6.420 429
17	6.431 276	6.442 070	6.452 812	6.463 502	6.474 141	6.484 729	6.495 268	6.505 758	6.516 199	6.526 592
18	6.536 938	6.547 238	6.557 492	6.567 700	6.577 864	6.587 984	6.598 060	6.608 093	6.618 085	6.628 034
19	6.637 943	6.647 811	6.657 639	6.667 429	6.677 179	6.686 892	6.696 567	6.706 205	6.715 806	6.725 372
20	6.734 903	6.744 399	6.753 861	6.763 290	6.772 685	6.782 048	6.791 380	6.800 680	6.809 949	6.819 188
21	6.828 397	6.837 577	6.846 729	6.855 852	6.864 948	6.874 017	6.883 059	6.892 075	6.901 066	6.910 032
22	6.918 973	6.927 891	6.936 785	6.945 656	6.954 505	6.963 332	6.972 137	6.980 921	6.989 686	6.998 430
23	7.007 154	7.015 860	7.024 547	7.033 217	7.041 869	7.050 503	7.059 122	7.067 724	7.076 310	7.084 882
24	7.093 438	7.101 981	7.110 510	7.119 025	7.127 528	7.136 018	7.144 496			

REPORT OF CALIBRATION

International Temperature Scale of 1990

Germanium Resistance Thermometer
Serial Number 12345

Submitted by
Anybody, Inc.
Anywhere, XX, USA

This Germanium Resistance Thermometer (GeRT) was calibrated using a bi-polar dc resistance ratio measurement system in the range T<13.8 K and an AC resistance bridge at a frequency of 30 Hz in the range T≥13.8 K. Measurements were made using pairs of constant excitation currents I, from 0.1 μA to 500 μA. The thermometer was calibrated under isothermal conditions in vacuum by comparison with various reference thermometers maintained at NIST. From 0.65 K to 13.8 K the reference and check thermometers were RIRT B174 and RIRT B168, respectively. For temperatures above 13.8 K the reference and check thermometers were SPRT 1842385 and SPRT 1774092, respectively. Measurements were made at 35 temperatures in the range 0.65 K to 27.1 K.

The reference and check thermometers have been calibrated at NIST from direct realizations of the ITS-90. Temperatures from 0.65 K to 2.0 K are derived from ^{3}He vapor pressure realizations and temperatures between 2 K and 5 K are derived from ^{4}He vapor pressure realizations. Temperatures between 5 K and 24.556 K are derived from NIST realizations of the ITS-90 via an Interpolating Constant Volume Gas Thermometer. Temperatures above 24.556 K are derived from NIST realizations of the ITS-90 fixed points of e-H_2, and the triple points of Ne, O_2, Ar, Hg, and H_2O, in conjunction with Standard Platinum Resistance Thermometers according to ITS-90 definitions.

Table 1 shows the as-measured calibration data: the temperature T in kelvin; resistance, R in ohms; the standard uncertainty in R, $u[R]$, in ohms; and the piecewise constant measurement currents, I in microamperes. Table 2 contains additional derived quantities for a constant excitation voltage of V_c=2.0 mV: the resistance, $R(V_c)$ in ohms; the standard uncertainty in $R(V_c)$, $u[R(V_c)]$, in ohms ; polynomial fits of this resistance R_{f1} and R_{f2}, in ohms; the residual difference $\Delta T_f \equiv [R_{fi} - R(V_c)]/\alpha$ in millikelvin; the temperature coefficient of resistance α in ohms per kelvin; the estimated self-heating ΔT_{sh} in millikelvin; the observed self-heating coefficient κ in millikelvin per microwatt; and the Expanded Uncertainty U_T for the calibration expressed in millikelvins with a coverage factor of $k = 2$. For a description of these uncertainties, see: *NIST Internal Report 6138*, 36 pp., (1998), entitled "A Revised Assessment of Calibration Uncertainties of Capsule Type Standard Platinum and Rhodium-Iron Resistance Thermometers". Table 3 provides the coefficients for the polynomial representation R_f. An interpolation table, which has been generated by these same functions (Table 4), is also provided.

No statistically significant difference between AC and DC resistance was observed within the range 13.8 K to 27.1 K. All measurements and analysis were performed by W. L. Tew.

For the Director,
National Institute of Standards and Technology

NIST Service ID No. 33355S
Test No. 685/123456-12
23 Nov 2012
Purchase Order No. 123-ABC

Gregory Strouse
Leader, Thermodynamic Metrology Group
Sensor Science Division

Germanium Resistance Thermometer
Serial Number 12345

Submitted by
Anybody, Inc.
Anywhere, XX, USA

Table 1. As-measured calibration data at excitation currents I_1 and I_2.

T / K	$R(I_1)$ / Ω	$u(R(I_1))$ / Ω	I_1 / μA	$R(I_2)$ / Ω	$u(R(I_2))$ / Ω	I_2 / μA
0.6507	53673	33	0.100	53622	31	0.140
0.7503	29456	6	0.140	29437	5	0.200
0.8520	17836	5	0.200	17826	3	0.285
1.0008	9874.6	1.2	0.285	9871.7	1.0	0.400
1.1798	5656.3	0.5	0.400	5653.9	0.5	0.705
1.4003	3318.0	0.2	1.000	3313.8	0.2	2.000
1.6499	2075.1	0.1	1.415	2073.0	0.1	2.830
1.8999	1426.42	0.04	2.000	1425.09	0.04	4.000
2.2001	991.27	0.02	2.830	990.45	0.02	5.655
2.5000	735.77	0.02	2.830	735.45	0.01	5.655
2.8004	571.738	0.009	4.00	571.453	0.009	8.00
3.1005	459.916	0.008	4.00	459.771	0.007	8.00
3.4147	376.263	0.006	5.655	376.156	0.004	10.00
3.8004	302.576	0.005	7.07	302.457	0.005	14.14
4.2222	244.715	0.003	10.00	244.595	0.002	20.00
4.6129	204.687	0.002	10.00	204.617	0.002	20.00
5.1042	166.404	0.001	20.00	166.315	0.001	33.30
6.1046	113.994	0.001	20.00	113.964	0.001	33.30
7.2049	78.8739	0.0010	20.00	78.8562	0.0007	40.00
8.3062	56.8718	0.0010	20.00	56.8650	0.0006	40.00
9.4069	42.6372	0.0006	33.30	42.6337	0.0004	50.00
10.6071	32.4539	0.0006	40.00	32.4486	0.0003	80.00
11.8067	25.6685	0.0004	56.55	25.6650	0.0003	100.0
12.8044	21.6558	0.0003	70.70	21.6514	0.0001	141.4
13.8034	18.62224	0.00002	100.0	18.62045	0.00002	141.4
15.4017	15.11741	0.00002	100.0	15.11650	0.00002	141.4
17.0350	12.61675	0.00002	100.0	12.61625	0.00001	141.4
18.6500	10.80766	0.00002	100.0	10.80677	0.00001	200.0
20.2698	9.42246	0.00001	141.4	9.42131	0.00001	282.8
21.5099	8.56503	0.00001	141.4	8.56419	0.00001	282.8
22.6048	7.917872	0.000008	141.4	7.917218	0.000007	282.8
23.6054	7.398692	0.000008	200.0	7.396816	0.000007	500.0
24.5562	6.958804	0.000009	200.0	6.957246	0.000006	500.0
26.0005	6.372760	0.000005	200.0	6.371563	0.000005	500.0
27.1089	5.979021	0.000004	200.0	5.978030	0.000006	500.0

Submitted by
Anybody, Inc.
Anywhere, XX, USA

Table 2. Derived quantities at fixed calibration voltage V_c=2.0 mV.

T / K	$R(V_c)$ / Ω	$u(R(V_c))$ / Ω	$R_f(V_c)$ / Ω	ΔT_f / mK	α / Ω·K^{-1}	$\Delta T_{sh}(V_c)$ / mK	κ / mK·μW^{-1}	U_T / mK
0.6507	53718	68	53633	0.24	-3.6E+05	<0.05	3.E+02	0.30
0.7503	29470	11	29481	-0.07	-1.60E+05	<0.05	2.E+02	0.20
0.8520	17842	9	17842	0.00	-8.02E+04	<0.05	1.6E+02	0.19
1.0008	9876.1	1.9	9874.5	0.05	-3.48E+04	<0.05	1.1E+02	0.19
1.1798	5656.5	0.5	5656.6	-0.01	-1.56E+04	0.06	8.0E+01	0.17
1.4003	3318.9	0.3	3319.0	-0.01	-7.06E+03	0.07	5.9E+01	0.17
1.6499	2075.5	0.1	2075.3	0.04	-3.46E+03	0.09	4.9E+01	0.14
1.8999	1426.64	0.05	1426.68	-0.02	-1.93E+03	0.11	4.0E+01	0.14
2.2001	991.41	0.03	991.41	0.00	-1.08E+03	0.13	3.2E+01	0.14
2.5000	735.77	0.02	735.80	-0.03	-6.69E+02	0.15	2.7E+01	0.14
2.8004	571.761	0.009	571.763	-0.01	-4.44E+02	0.16	2.3E+01	0.14
3.1005	459.907	0.007	459.889	0.06	-3.12E+02	0.18	2.1E+01	0.14
3.4147	376.269	0.006	376.259	0.05	-2.26E+02	0.20	1.9E+01	0.14
3.8004	302.581	0.005	302.583	-0.01	-1.61E+02	0.21	1.6E+01	0.14
4.2222	244.728	0.003	244.734	-0.05	-1.17E+02	0.23	1.4E+01	0.14
4.6129	204.688	0.003	204.685	0.04	-9.00E+01	0.25	1.3E+01	0.14
5.1042	166.436	0.002	166.431	0.07	-6.73E+01	0.27	1.1E+01	0.17
6.1046	113.998	0.002	113.996	0.03	-4.05E+01	0.32	9.0E+00	0.17
7.2049	78.8703	0.0008	78.8720	-0.07	-2.49E+01	0.38	7.5E+00	0.18
8.3062	56.8670	0.0005	56.8672	-0.01	-1.59E+01	0.44	6.3E+00	0.19
9.4069	42.6345	0.0003	42.6332	0.12	-1.04E+01	0.53	5.6E+00	0.21
10.6071	32.4515	0.0004	32.4518	-0.04	-6.84E+00	0.61	5.0E+00	0.22
11.8067	25.6670	0.0003	25.6685	-0.32	-4.65E+00	0.68	4.3E+00	0.24
12.8044	21.6548	0.0002	21.6544	0.12	-3.47E+00	0.73	4.0E+00	0.25
13.8034	18.62196	0.00002	18.62197	0.00	-2.65E+00	0.78	3.63E+00	0.25
12.8044	21.6548	0.0002	21.6544	-0.05	-3.47E+00	0.73	4.0E+00	0.25
13.8034	18.62196	0.00002	18.62197	-0.01	-2.65E+00	0.78	3.63E+00	0.25
15.4017	15.11673	0.00002	15.11659	0.08	-1.81E+00	0.87	3.31E+00	0.49
17.0350	12.61600	0.00002	12.61634	-0.26	-1.29E+00	0.96	3.03E+00	0.22
18.6500	10.80694	0.00001	10.80699	-0.05	-9.70E-01	1.05	2.83E+00	0.21
20.2698	9.42198	0.00001	9.42188	0.13	-7.54E-01	1.14	2.69E+00	0.19
21.5099	8.56455	0.00001	8.56451	0.05	-6.34E-01	1.21	2.59E+00	0.18
22.6048	7.917394	0.000006	7.91743	-0.07	-5.51E-01	1.26	2.50E+00	0.21
23.6054	7.398397	0.000007	7.39846	-0.12	-4.88E-01	1.34	2.47E+00	0.25
24.5562	6.958488	0.000007	6.95852	-0.07	-4.38E-01	1.40	2.43E+00	0.29
26.0005	6.372426	0.000005	6.37238	0.12	-3.76E-01	1.49	2.38E+00	0.32
27.1089	5.978682	0.000004	5.97870	-0.04	-3.36E-01	1.57	2.35E+00	0.34

Germanium Resistance Thermometer
Serial Number 12345

Submitted by
Anybody, Inc.
Anywhere, XX, USA

For the range of temperatures 0.65 K < T< 13.8 K , a 12th order polynomial fit of resistance R_{f1} as a function of temperature T is given by,

$$\log[R_{f1}(T)] = \sum_{n=0}^{12} a_n (\log(T))^n$$

where the coefficients $\boldsymbol{a_n}$ are given in Table 3 below.

For the range of temperatures 12.8 K < T< 27.1 K, a 6th order polynomial fit of resistance R_{f2} as a function of temperature T is given by,

$$\log[R_{f2}(T)] = \sum_{n=0}^{6} b_n (\log(T))^n$$

where the coefficients $\boldsymbol{b_n}$ are given in Table 3 below. In both cases temperatures are in kelvins and resistances are in ohms. The resistances are fit for a measurement voltage of 2.0 mV over the entire calibration range.

Table 3. Coefficients for the lower and upper polynomial fits R_{f1} and R_{f2} respectively.

Lower Fit		Upper Fit	
a_0	3.99566237117E+00	b_0	-7.09380343327E+00
a_1	-3.52917429696E+00	b_1	3.91356162132E+01
a_2	2.05688232340E+00	b_2	-5.40895821350E+01
a_3	-8.88361996753E-01	b_3	2.18000007442E+01
a_4	5.06701993760E-02	b_4	1.01294756445E+01
a_5	4.26863349870E+00	b_5	-1.06888412430E+01
a_6	-2.22943184851E+01	b_6	2.37749113750E+00
a_7	4.95228392876E+01		
a_8	-4.88190028008E+01		
a_9	-1.36447739281E+00		
a_{10}	4.41757623143E+01		
a_{11}	-3.37153497107E+01		
a_{12}	8.10919229975E+00		

Germanium Resistance Thermometer
Serial Number 12345

Submitted by
Anybody, Inc.
Anywhere, XX, USA

Table 4. Interpolated resistance versus temperature for the polynomial fits R_{f1} and R_{f2} in ohms

T/K	0	0.1	0.2	0.3	0.4	0.5	0.6	0.7	0.8	0.9
0								39284	22790	14506
1	9901	7129	5354	4159	3320.9	2713.0	2259.5	1912.7	1641.9	1426.6
2	1252.6	1109.9	991.6	892.2	807.9	735.78	673.52	619.37	571.95	530.15
3	493.09	460.04	430.42	403.74	379.61	357.70	337.717	319.431	302.641	287.174
4	272.884	259.645	247.348	235.897	225.211	215.217	205.851	197.059	188.790	181.002
5	173.655	166.714	160.150	153.934	148.041	142.448	137.136	132.085	127.279	122.703
6	118.343	114.185	110.217	106.430	102.813	99.356	96.051	92.889	89.864	86.968
7	84.195	81.539	78.993	76.553	74.214	71.970	69.817	67.751	65.767	63.863
8	62.034	60.277	58.589	56.966	55.406	53.906	52.464	51.076	49.740	48.454
9	47.217	46.025	44.877	43.771	42.705	41.678	40.688	39.733	38.811	37.922
10	37.064	36.236	35.437	34.664	33.918	33.197	32.500	31.827	31.175	30.545
11	29.935	29.344	28.773	28.219	27.683	27.164	26.661	26.173	25.700	25.241
12	24.796	24.364	23.944	23.537	23.142	22.758	22.385	22.022	21.670	21.327
13	20.994	20.669	20.354	20.047	19.749	19.458	19.175	18.899	18.6309	18.3690
14	18.1136	17.8646	17.6218	17.3849	17.1537	16.9281	16.7079	16.4929	16.2828	16.0777
15	15.8772	15.6814	15.4899	15.3027	15.1196	14.9405	14.7654	14.5939	14.4262	14.2620
16	14.1012	13.9438	13.7896	13.6385	13.4905	13.3454	13.2032	13.0639	12.9272	12.7932
17	12.6617	12.5327	12.4062	12.2820	12.1601	12.0404	11.9229	11.8076	11.6943	11.5829
18	11.4736	11.3661	11.2605	11.1567	11.0547	10.9544	10.8557	10.7587	10.6633	10.5694
19	10.4771	10.3862	10.2968	10.2088	10.1221	10.0368	9.9528	9.8701	9.7886	9.7084
20	9.6294	9.5515	9.4748	9.3992	9.3247	9.2512	9.1788	9.1075	9.0371	8.9677
21	8.8993	8.8318	8.7652	8.6995	8.6347	8.5708	8.5077	8.4455	8.3841	8.3234
22	8.2636	8.2045	8.1462	8.0886	8.0317	7.9756	7.9201	7.8653	7.8112	7.7578
23	7.7050	7.6528	7.6012	7.5503	7.5000	7.4503	7.4011	7.3525	7.3045	7.2570
24	7.2101	7.1637	7.1178	7.0724	7.0276	6.9832	6.9394	6.8960	6.8531	6.8106
25	6.7686	6.7271	6.6860	6.6454	6.6052	6.5654	6.5260	6.4870	6.4485	6.4103
26	6.3726	6.3352	6.2982	6.2616	6.2254	6.1895	6.1540	6.1188	6.0840	6.0496
27	6.0155	5.9817								

Appendix B. Glossary of Acronyms

ITS-90	International Temperature Scale of 1990
NIST	National Institute of Standards and Technology
CCT	Consultative Committee for Thermometry
RT	Resistance Thermometer
TCR	Temperature Coefficient of Resistance
PTC	Positive Temperature Coefficient
NTC	Negative Temperature Coefficient
AC	Alternating Current
DC	Direct Current
ADC	Analog-to-Digital Converter
DCC	Direct Current Comparator
PRT	Platinum Resistance Thermometer
DUT	Device Under Test
SPRT	Standard Platinum Resistance Thermometer
MPRT	Miniature Platinum Resistance Thermometer
RIRT	Rhodium-Iron Resistance Thermometer
CE-RIRT	Ceramic-Encapsulated Rhodium-Iron Resistance Thermometer
PCRT	Platinum-Cobalt Resistance Thermometer
GeRT	Germanium Resistance Thermometer
ZNRT	Zirconium oxy-Nitride Resistance Thermometer
RORT	Ruthenium-Oxide Resistance Thermometer
IVD	Inductive Voltage Divider
ICVGT	Interpolating Constant Volume Gas Thermometer
LTCF	Low Temperature Calibration Facility
LTRF	Low Temperature Realization Facility
SPRTCL	Standard Platinum Resistance Thermometer Calibration Laboratory
WTP	Water Triple Point
e-H_2	equilibrium Hydrogen
STPC	Sealed Triple Point Cell
OTPC	Open Triple Point Cell
VPPC	Vapor Pressure Point Cell
IC	Immersion Cell